Use of recycled gypsum in road foundation construction

Ganjian, E. , Claisse, P.A. and Sadeghi-Pouya, H.

Published version deposited in CURVE April 2014

Original citation & hyperlink:
Ganjian, E. , Claisse, P.A. and Sadeghi-Pouya, H. (2007) Use of recycled gypsum in road foundation construction. Banbury, Oxon:Waste and Resources Action Programme (WRAP).
http://www.wrap.org.uk/

Copyright © and Moral Rights are retained by the author(s) and/ or other copyright owners. A copy can be downloaded for personal non-commercial research or study, without prior permission or charge. This item cannot be reproduced or quoted extensively from without first obtaining permission in writing from the copyright holder(s). The content must not be changed in any way or sold commercially in any format or medium without the formal permission of the copyright holders.

CURVE is the Institutional Repository for Coventry University
http://curve.coventry.ac.uk/open

wrap Material change for a better environment

Plasterboard technical report

Use of recycled gypsum in road foundation construction

Research into the feasibility of using waste plasterboard gypsum in combination with a range of mineral wastes (blast furnace slag, cement kiln dust, cement bypass dust and power station run-of-station ash) in road bases, sub-bases and stabilised sub-grades

Project code: PBD5-002
Research date: Dec 2005 – Feb 2007

ISBN: 1-84405-368-7
Date: November 2007

Front cover photograph: Placing the concrete binder over the sub-grade layer using the truck mixer chute.

WRAP and Coventry University believe the content of this report to be correct as at the date of writing. However, factors such as prices, levels of recycled content and regulatory requirements are subject to change and users of the report should check with their suppliers to confirm the current situation. In addition, care should be taken in using any of the cost information provided as it is based upon numerous project-specific assumptions (such as scale, location, tender context, etc.).

The report does not claim to be exhaustive, nor does it claim to cover all relevant products and specifications available on the market. While steps have been taken to ensure accuracy, WRAP cannot accept responsibility or be held liable to any person for any loss or damage arising out of or in connection with this information being inaccurate, incomplete or misleading. It is the responsibility of the potential user of a material or product to consult with the supplier or manufacturer and ascertain whether a particular product will satisfy their specific requirements.

The listing or featuring of a particular product or company does not constitute an endorsement by WRAP and WRAP cannot guarantee the performance of individual products or materials. For more detail, please refer to WRAP's Terms & Conditions on its web site: www.wrap.org.uk

Published by
Waste & Resources Action Programme

The Old Academy
21 Horse Fair
Banbury, Oxon
OX16 0AH

Tel: 01295 819 900
Fax: 01295 819 911
E-mail: info@wrap.org.uk

Helpline freephone
0808 100 2040

Context

WRAP

WRAP (Waste & Resources Action Programme) works in partnership to encourage and enable businesses and consumers to be more efficient in their use of materials and recycle more things more often. This helps to minimise landfill, reduce carbon emissions and improve our environment.

Established as a not-for-profit company in 2000, WRAP is backed by Government funding from Defra and the devolved administrations in Scotland, Wales and Northern Ireland.

WRAP and plasterboard

Through its Construction Programme, WRAP is helping the construction industry cut costs and increase efficiency through the better use of materials.

Plasterboard is used extensively in the construction and refurbishment of buildings as a lining for walls and ceilings, and for forming structures such as partitions.

Plasterboard waste can arise on construction sites for a number of reasons, including wasteful design, off-cuts from its installation, damaged boards, and over-ordering. It is estimated that over 300,000 tonnes per year of waste plasterboard is produced on construction sites. It can also arise from strip-out activities during refurbishment and demolition projects; the waste arisings from this source are significantly higher. In total it is estimated that over one million tonnes of waste plasterboard are produced each year from construction and demolition activities.

Most of this waste is currently disposed to landfill, even though it can be easily recycled. WRAP receives funding from Defra through the Business Resource Efficiency and Waste (BREW) programme to divert plasterboard waste from landfill by working to overcome the barriers to plasterboard recycling. Additional funding is also received from the devolved administrations in Scotland, Wales and Northern Ireland.

WRAP is working to overcome these barriers through the following key areas:

- plasterboard waste minimisation;
- site waste management;
- segregation and collection of plasterboard waste;
- development of infrastructure, including waste logistics and recycling capacity;
- market development for materials from plasterboard recycling – recycled gypsum and reclaimed paper;
- education, awareness and behavioural change; and
- informing and influencing legislation, regulations and policy.

More information on WRAP's work can be found at www.wrap.org.uk/construction

Executive summary

Interest in finding alternatives to landfill for plasterboard and other waste gypsum products has increased with the escalating costs of disposal and their reclassification as non-hazardous non-inert waste. WRAP is working to divert plasterboard waste from landfill by seeking to overcome the barriers to plasterboard recycling. One area of its work is to develop markets for the materials from plasterboard recycling (recycled gypsum and reclaimed paper). This project examined the feasibility of using plasterboard gypsum in combination with a range of mineral wastes in road bases, sub-bases and stabilised sub-grades.

The project investigated the use of plasterboard gypsum (PG) combined in mixtures with blast furnace slag, cement kiln dust (CKD), cement bypass dust (BPD) and power station run-of-station ash (ROSA) to form a novel blended binder with pozzolanic properties. This novel binder had potential use to stabilise soils and to produce roller-compacted concrete (RCC) for road foundation construction. The plasterboard gypsum acts as a source of sulphate in the blended binder. The blast furnace slag used in the project was basic oxygen slag (BOS).

Project phases

The project involved the preparation of a large number of paste specimens (cementitious powder and water with no aggregate) in the laboratory to optimise the mix proportions to obtain a cementitious binder that achieved the required properties. Possible candidate blends were then used to optimise the proportions in the concrete mix designs. The stabilisation of two soil types was tested using two novel binders, before one binder – referred to as 'Coventry Binder' – was selected for use in site trials.

The project consisted of five phases:

- characterisation of the materials used (particle size analysis, chemical composition);
- design and optimisation of the paste mix (mix proportions, water requirement, setting time, workability, compressive strength);
- design of the concrete mix (effect of different aggregates, workability, compressive strength);
- characterisation of mixes made with the novel blended powder (hydrogen sulphide release, long-term stability, potential for leaching, hydration mechanism, length change); and
- comparative trials at two construction sites:
  - a car park at Lowdham Grange prison in Nottingham where the novel binder was used to prepare roller-compacted concrete (RCC) in a sub-base layer; and
  - part of an access road at the King's Mill Hospital site in Nottinghamshire where soil stabilised with the novel binder and a semi-dry paste (grout) containing the novel binder was used as the sub-base and base course respectively.

Results

Optimisation of the proportions in the ternary and four-component combinations was not a linear task and fine tuning was required to obtain the proportions of materials for maximum compressive strength.

The mix with 15% PG, 5% BPD and 80% BOS (Coventry Binder) was identified as the optimum combination of these three waste materials. This mix with 13% water achieved the highest compressive strength at 28 days of all the mixes tested. After 360 days standard curing, the compressive strength of paste mixtures made with the Coventry Binder was up to four times higher than at 28 days.

ROSA showed satisfactory pozzolanic potential for use with slag and plasterboard gypsum. However, the slow-reacting nature of this material was illustrated by the slower development of compressive strength of ROSA-containing mixes. Although the ultimate compressive strength of a 15% PG, 5% BPD, 30% BOS and 50% ROSA mix was excellent, the 15% PG, 5% BPD and 80% BOS mix was preferred because it demonstrated high early compressive strength and involved fewer different materials.

Increasing the content of BPD in ternary combinations of PG, BOS and BPD resulted in a lower compressive strength. Replacement of the BPD with commercial hydrated lime or Maerz kiln dust (MKD) resulted in up to 50% less compressive strength at 28 days. The performance of MKD was less than that of hydrated lime.

Concrete mixes incorporating slag and gypsum developed strength at a slower rate than ordinary Portland cement (OPC) mixes. It is therefore important to allow sufficient time for the setting and curing of such mixes.

The novel blended binder developed in this project can be used to stabilise soil containing clay and/or sand. Using 50% binder resulted in an acceptable compressive strength according to standard recommendations (the higher the binder content, the higher the compressive strength). XRD analysis also indicated the formation of hydration products such as ettringite after 28 days standard curing.

No heavy metal or any other hazardous elements leached from the paste made with Coventry Binder. However, the amounts of sulphate and calcium that leached were more than from OPC paste.

Incorporating up to 50% extra paper in the paste mixtures had no adverse effect on the release of hydrogen sulphide from paste or concrete made with the Coventry Binder. No traces of hydrogen sulphide were found using a range of analytical techniques with any of the mixtures developed during the project.

As expected, the permeability of roller-compacted concrete made with Coventry Binder was lower than OPC paste due to the presence of aggregates. Semi-dry paste in the site trial showed higher permeability compared with the same laboratory paste mixture.

Investigations on the length change of paste and mortar samples indicated that semi-dry Coventry Binder paste showed the largest progressive expansion at 28 days age at 20° C. Incorporation of aggregates resulted in less expansion in mortar samples. Increasing the storage temperature to 40° C also resulted in less expansion in all paste and mortar mixes.

Satisfactory performance of the semi-dry paste and roller-compacted concrete made with the novel blended binder (Coventry Binder) was observed in the site trials at 28, 90 and 180 days. The compressive strength of the sub-bases made with Coventry Binder was similar to that found in the laboratory for the designed mix.

Conclusions

Crushed plasterboard gypsum can be used as a source of sulphate together with slag (BOS) and cement kiln dust/bypass dust to form a sulphate-activated pozzolan. The optimum proportions of gypsum depend on the chemical properties of the slag and cement kiln dust/bypass dust. Laboratory experiments showed that a ternary combination of PG-BPD-BOS containing 15% crushed plasterboard gypsum resulted in the highest compressive strength. The long-term compressive strength results of paste mixtures containing 15% crushed plasterboard gypsum showed an increase of up to four-fold after 360 days standard curing compared with the strength at 28 days.

Road foundations prepared using the novel developed binder (Coventry Binder) performed as well as conventional materials in site trials involving a car park and access road at two construction sites in Nottinghamshire. The foundation of the access road was built with a mix with no cement and it is carrying heavy traffic as a haul road of a construction site.

Further extended site trials could help to promote uptake of this application for waste plasterboard gypsum.

Further work

Analysis of the project results using artificial neural networks will enable the compressive strengths of similar cementitious mixtures to be predicted without the need for further extensive experimental work.

The mechanism of the hydration reactions of the binary and ternary blended binders will be investigated further using scanning electron microscopy (SEM) to develop a more accurate model of the interactions of the chemical components and admixtures.

Contents

1.0 Introduction

The pressure to reutilise waste materials is increasing with the escalating cost of disposal to landfill. The majority of plasterboard waste has traditionally been landfilled, having been classified as a non-hazardous inert waste able to be co-disposed of with other wastes. But from July 2005, the EU Landfill Directive required plasterboard and other waste gypsum products to be reclassified as non-hazardous non-inert wastes [1, 2]. This has boosted demand for alternatives to disposal for these wastes.

This project examined the use of plasterboard and gypsum waste in road bases, sub-bases and stabilised sub-grades.

1.1 Project Team

The Construction Materials Applied Research Group at Coventry University undertakes the majority of its funded research projects in finding ways to reduce the amount of cement in concrete.

Professor Peter Claisse is a professor in Construction Materials and a chartered Civil Engineer with many years' experience in construction and in research into construction materials. He leads the Applied Research Group and has interests in using secondary aggregates and novel cementitious binders as construction materials.

Dr. Essie Ganjian is a senior lecturer in highway and pavement Engineering and Civil Engineering construction techniques. Dr Essie Ganjian is a Civil Engineer who has worked on major projects on the production of concrete using waste materials. He has been involved in research into measuring and modelling the thermal conductivity of concrete, uses of by-products such as sulphur, natural pozzolans and silica fume in concrete and analysis of damage to concrete structures.

Dr. Homayoon Sadeghi Pouya, who has a PhD from The University of Sheffield, is a Research Fellow. He has been working as a structural engineer and concrete technologist since 1998. His speciality is in Civil Engineering materials and concrete technology.

This project involved two industrial collaborators – Lafarge Plasterboard Limited (www.lafargeplasterboard.co.uk) and Skanska UK (www.skanska.co.uk). Since its establishment in Bristol in 1987, Lafarge Plasterboard has become a major player in the drywall industry in UK. Skanska UK is part of Skanska, the third largest construction services group in Europe. It offers design, building, civil engineering and building services in the UK and is a leading private finance initiative/public–private partnership (PFI/PPP) service provider. Skanska is committed to waste reduction and recycling, and was keen to assist in site trials for the project.

1.2 Sulphate-activated pozzolans

Blast furnace slag is a glassy granular material formed when molten blast-furnace slag is cooled rapidly, usually by immersion in water. It has been used as pozzolanic admixture in various construction works [3, 4].

Blast furnace slag cement in concrete is typically hydrated after mixing with Portland cement to provide a source of alkalinity with which the slag reacts to form cement hydration products [5]. Cement made from granulated blast furnace slag activated by means of calcium sulphate is known in the UK as supersulphated cement (SSC) [6]. The cement is made by grinding a mixture of 80–85% granulated slag, 10–15% anhydrite or hard-burned gypsum, and about 5% Portland cement. Hydration, initial setting and hardening of supersulphated cement are associated with the formation of calcium sulphoaluminate. The final setting and strength gain of these kinds of cements are attributed to ettringite – hydrated alumina together with a hydrated calcium silicate [7].

Alternative sources of alkalis such as alkaline solutions, slaked lime or cement kiln dust can be used to activate the slag. Cement kiln dust (CKD) and bypass dust (BPD) are generated during cement manufacturing and may, therefore, be considered an industrial waste [8, 9].

Such waste ashes pose a major waste disposal problem. They can be used with slag, gypsum and alkalis to form a binder which can be used in blended cements or for various applications to:

- reduce greenhouse gas emissions;
- reduce the cost of concrete; and
- improve the strength, durability and other properties of construction materials [10].

1.3 Project aims and objectives

The aim of this project was to investigate gypsum waste-slag-ash binders combined with fine aggregate such as recycled aggregate or metallurgical slags for use as road foundation. To achieve this aim, the project objectives were to:

- develop cost-effective, novel cementitious mixes using plasterboard and gypsum waste and a range of mineral wastes;
- construct a trial road using stabilised sub-based with the novel cementitious binder; and
- construct part of a car park using the developed technology and confirm its satisfactory performance in a site environment.

1.4 Project tasks

This report details the work carried out during the project. The tasks involved:

- determination of particle size, chemical analysis and crystallography of raw materials used;
- preparation of a wide range of laboratory paste mixes to optimise the mix proportions and to develop a new cementitious binder that achieves the required properties (90 mixes);
- mix design and casting of ordinary and roller-compacted concretes (12 mixes);
- laboratory studies on the effectiveness of the new binder to stabilise soils;
- chemical analysis, crystallography and thermal analysis of selected mixes to investigate the hydration mechanism of the new binder;
- investigation of appropriate methods for the determination and quantitative analysis of any possible hydrogen sulphide (H_2S) gas produced;
- laboratory studies on the long-term performance of the paste mixes using the new binder, i.e. length change test and high pressure through-flow test;
- preparation of about 100 tonnes of developed cementitious binder using basic oxygen slag (BOS), plasterboard gypsum (PG) and BPD for site trials;
- three site trials using stabilised soil, roller-compacted concrete (RCC) and high-strength paste (grout) made with the new binder; and
- evaluation of the site trials at 28, 90 and 180 days to investigate the long-term performance of RCC and semi-dry paste layers.

An overview of the project and the laboratory programme is shown in Figure 1.

1.5 Dissemination

The project findings have been disseminated through:

- progress meetings with reports based on the minutes;
- submission of a technical paper to *ACI Materials Journal* on 14 October 2006 titled 'Strength optimisation of novel binder containing plasterboard gypsum waste';
- presentation at the WARMNET conference, Tackling Waste 2006, held in Nottingham on 6 July 2006, titled 'Investigation on utilisation of plasterboard waste gypsum and pozzolanic materials as cementitious binder'; and
- presentation of the research results at the Sustainable Construction Materials conference held in June 2007 titled 'Development of novel cementitious binders using plasterboard waste and pozzolanic materials for road bases'.

Figure 1 Overview of the project

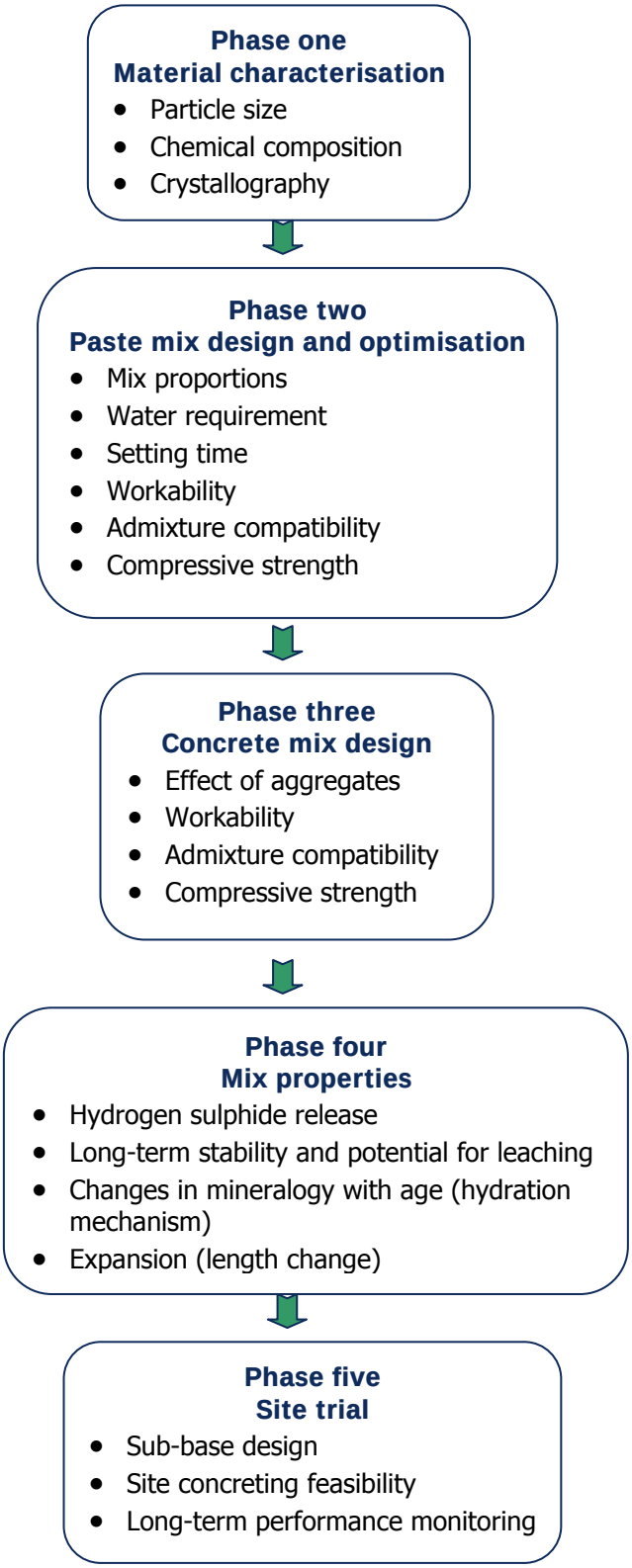

2.0 Concrete and paste mix development

2.1 Materials

The following materials have been used in the investigation:

- plasterboard gypsum (PG);
- two types of basic oxygen slag (BOS) and cement kiln dust (CKD);
- one source of run of station ash (ROSA);
- fine and coarse aggregates;
- superplasticiser.

Details of each material are given below.

2.1.1 Plasterboard gypsum

The plasterboard gypsum used was obtained from Lafarge Plasterboard's recycling plant in Bristol. Because the waste plasterboard gypsum is collected from demolition sites, contaminants such as paper and glass can be found in the gypsum. At this stage, big pieces of paper and other contaminants were separated using a series of sieves before the gypsum was crushed using a metal tamper. The crushed product was sieved through a 600 µm sieve and stored in a sealed bucket.

Another form of waste plasterboard gypsum from the Lafarge plasterboard recycling plant called 'processed PG' was also used. The processed PG contained lower levels of large particles of plasterboard but the size and amount of paper pieces were similar to the 'plasterboard gypsum' from the Lafarge plant. For the site trial, the plasterboard was dried, ground and passed through a 500 µm sieve[1] (see section 4).

Figure 2 shows the waste plasterboard before and after processing, together with other materials used in the project.

Figure 2 Waste plasterboard gypsum and various types of waste materials: (1) basin oxygen slag; (2) run of station ash; (3) lime; (4) cement kiln dust and (5) incinerated ash

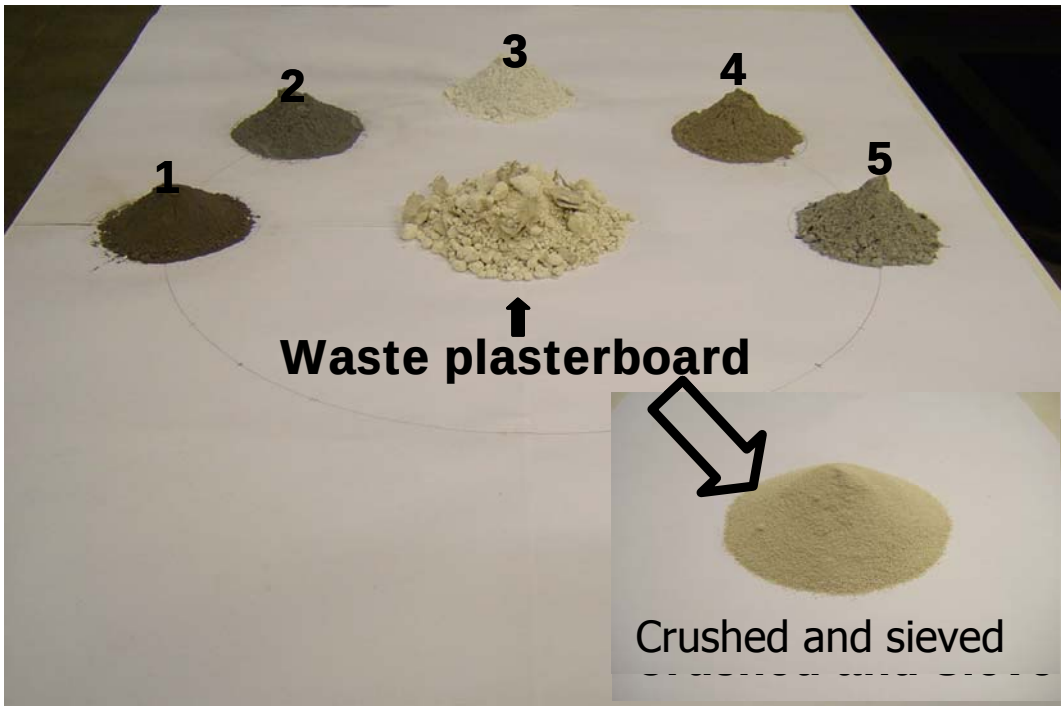

[1] *This was the only size of sieve available to the processing plant for preparation of the material for the site trials.*

Particle size analysis of the gypsum was carried out using a Malvern Mastersize 2000 laser analyser with an accuracy of ±1%. As shown in Figure 3, the particles are between 1 µm and 1 mm in diameter, and mostly >300 µm.

Figure 3 Particle size analysis of crushed and sieved PG

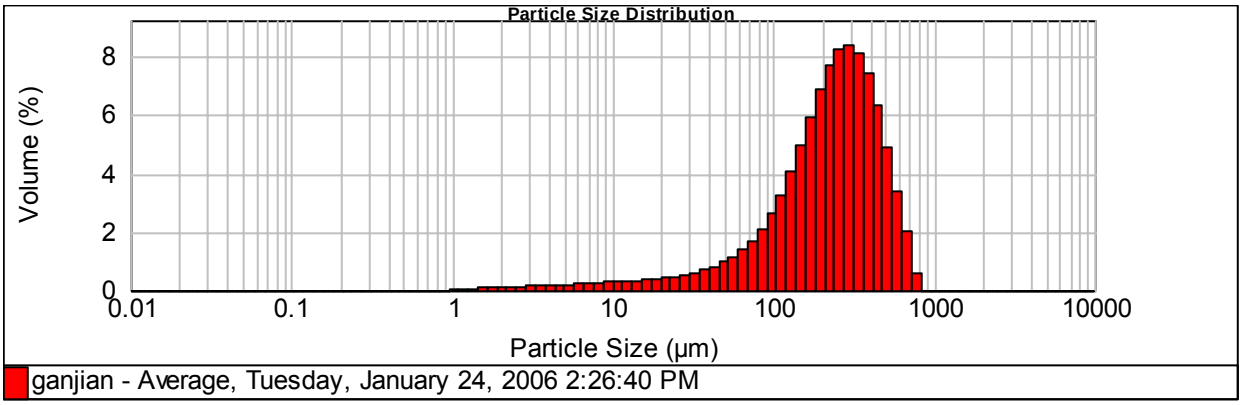

The nature of this source of waste plasterboard means that some degree of impurities and contaminants is inevitable. Thermogravimetric analysis (TGA) of materials was carried out using a PerkinElmer Pyris 1 thermogravimetric analyser. The thermograph (Figure 4) confirms the presence of impurities in the PG. The loss of mass at ≥200° C implies the presence of a number of impurities and contaminants in the gypsum.

Figure 4 TGA results for plasterboard gypsum

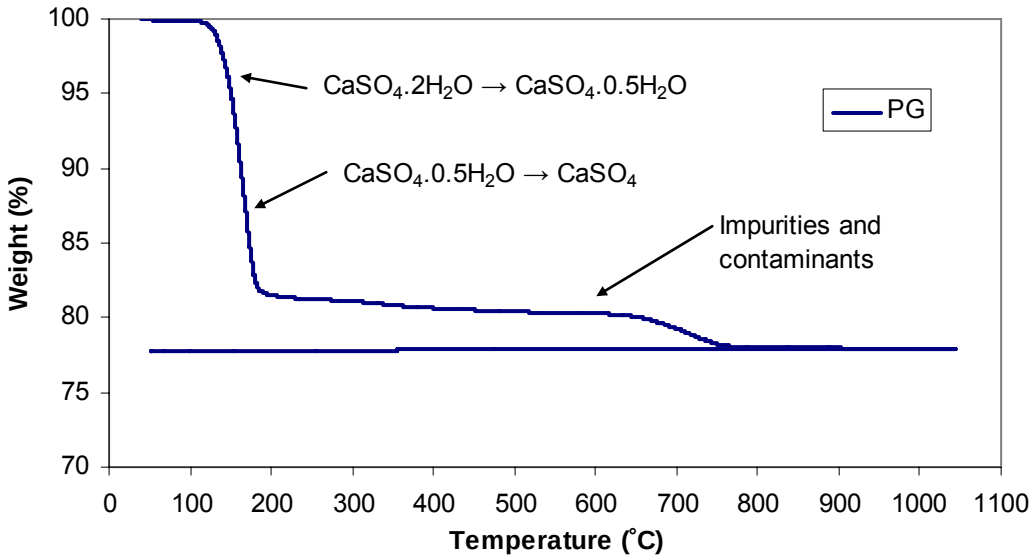

2.1.2 Basic oxygen slag

The blast furnace slag used was obtained from Tarmac UK (i.e. from the Corus plant at Scunthorpe). The slag was ground using a laboratory ball mill and passed through a 600 µm sieve before being added to the mixes. Figure 5 shows that the average particle size is 40–60 µm, indicating that the efficiency of the ball mill is acceptable.

Figure 5 Particle size analysis of ground BOS

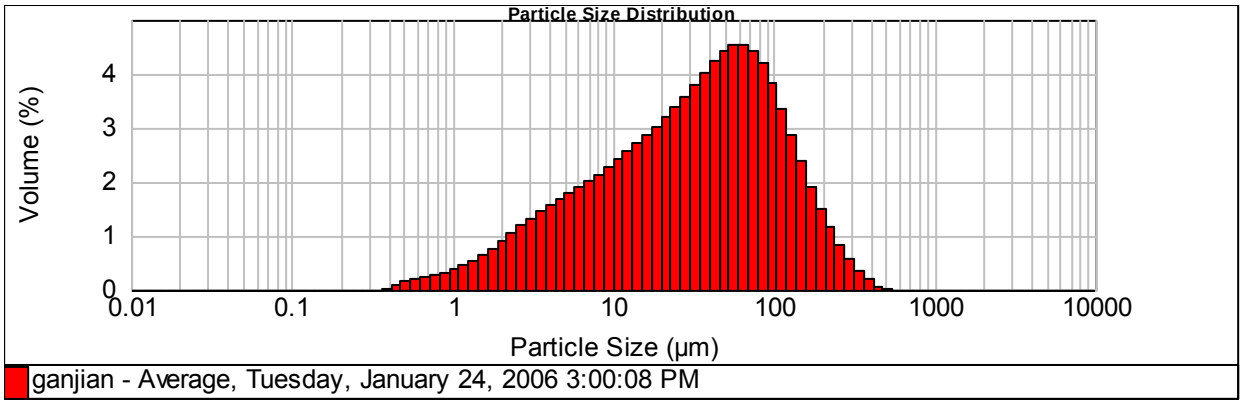

Fresh slag left exposed to air for period of over one month is described as 'weathered' BOS (W-BOS). Further TGA studies confirmed a considerable difference between fresh slag (UW-BOS) and samples that had been affected by carbonation under atmospheric carbon dioxide (CO_2), i.e. weathered BOS (Figure 6.). The chemical composition of the unweathered and weathered BOS is given in Table 1 (section 2.3).

Figure 6 TGA results for unweathered and weathered BOS

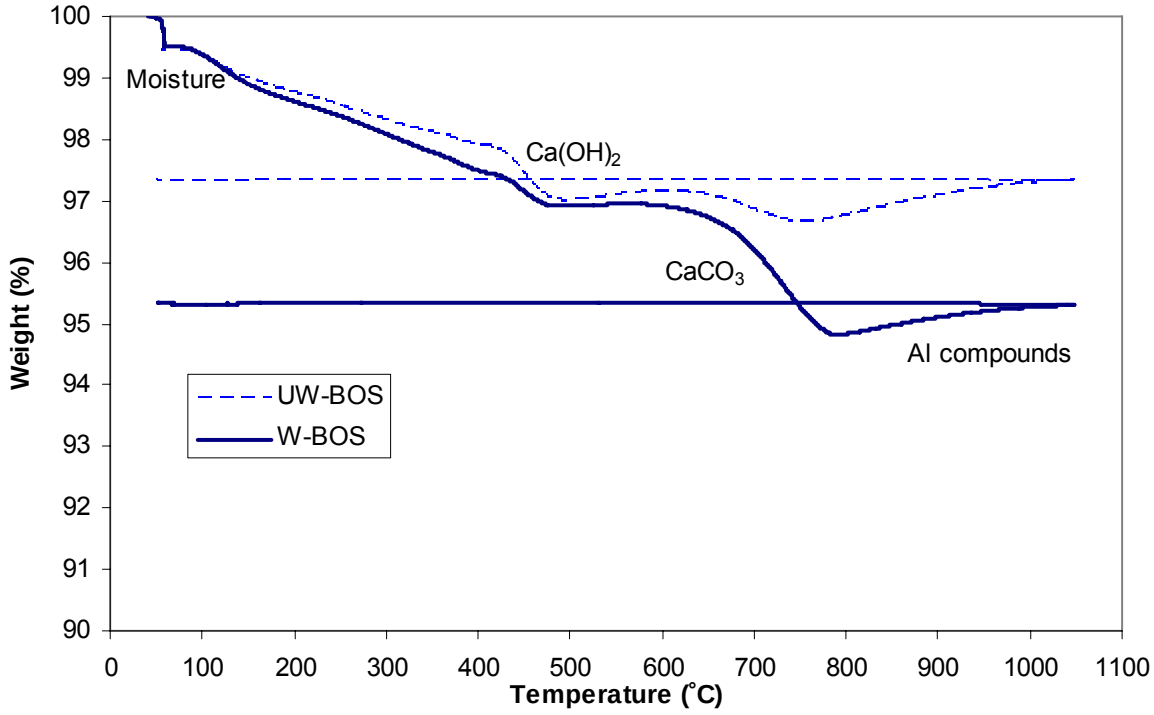

2.1.3 Cement kiln dust and bypass dust

Two different sources of cement kiln dust were used; one was obtained from Rugby Cement Barrington and the other from Castle Cement. As expected, the two dusts had a different composition (see Table 1 in section 2.3 for their relative oxide content).

The material supplied by Rugby Cement, called CKD, was obtained from electrostatic precipitators in the chimney stack. If the kiln has a bypass fitted, this material is usually recycled back into the kiln feed.

The material supplied by Castle Cement, called bypass dust (BPD), is obtained from the kiln bypass. The bypass is used to bleed off volatile materials that would otherwise recirculate around the kiln and pre-heater system (condensing in cooler parts of the kiln causing blockages) or eventually end up in the cement clinker.

The main difference between CKD and BPD is related to the temperature at which these materials are produced. CKD is taken out of the kiln during its initial length where the temperature is about 300° C, while BPD is from part of the kiln where the temperature is about 1000° C. As a result, BPD contains more cementitious phases compared with CKD, which contains a higher amount of calcium carbonate (limestone).

The CKD and BPD were supplied in powder form. The results of particle size analysis are shown in Figures 7 and 8 respectively. The CKD contains some type of coarser particles, which may be due to clustering and the moisture present in the sample. However, the average size of fine particles is nearly the same (about 10 µm) for the CKD and BPD.

Figure 7 Particle size analysis of CKD

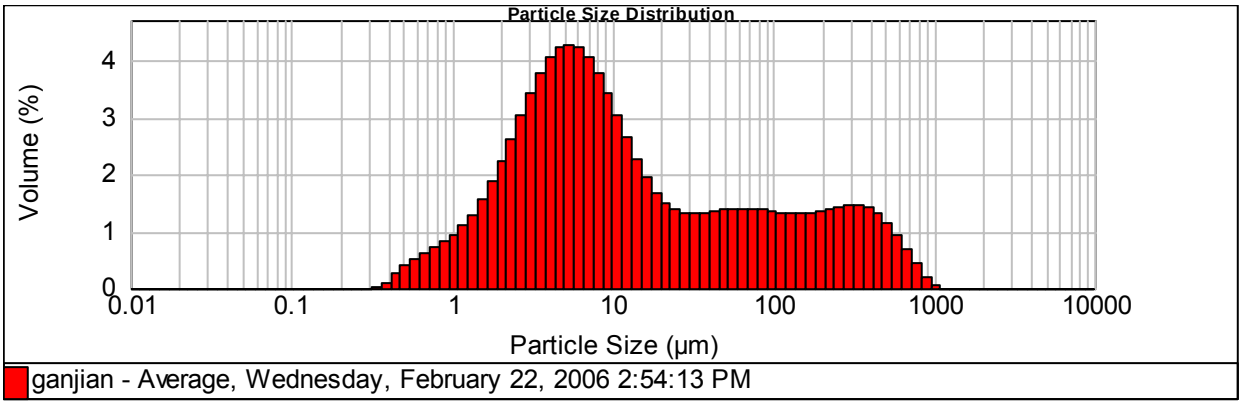

Figure 8 Particle size analysis of BPD

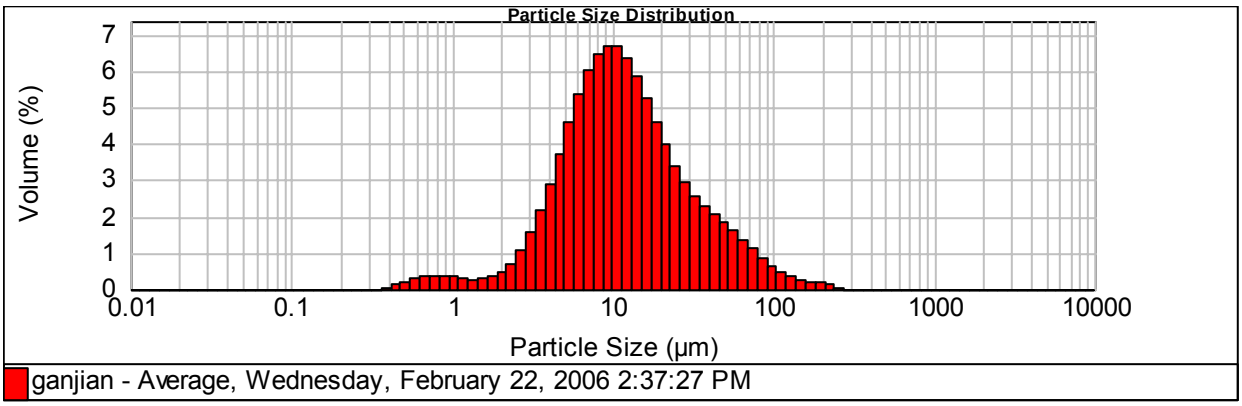

The TGA results (Figure 9) confirmed there were significant differences between the CKD and BPD samples. TGA showed that the CKD contained about 25% $CaCO_3$, which might reduce the activity of the powder and pH of the pore solution in the mix. In addition, the chemical composition of these kinds of materials will differ with time and will not be consistent due to changes in the raw materials supplied to the kiln as well as variations in temperature and duration in the kiln.

Figure 9 TGA results for BPD and CKD

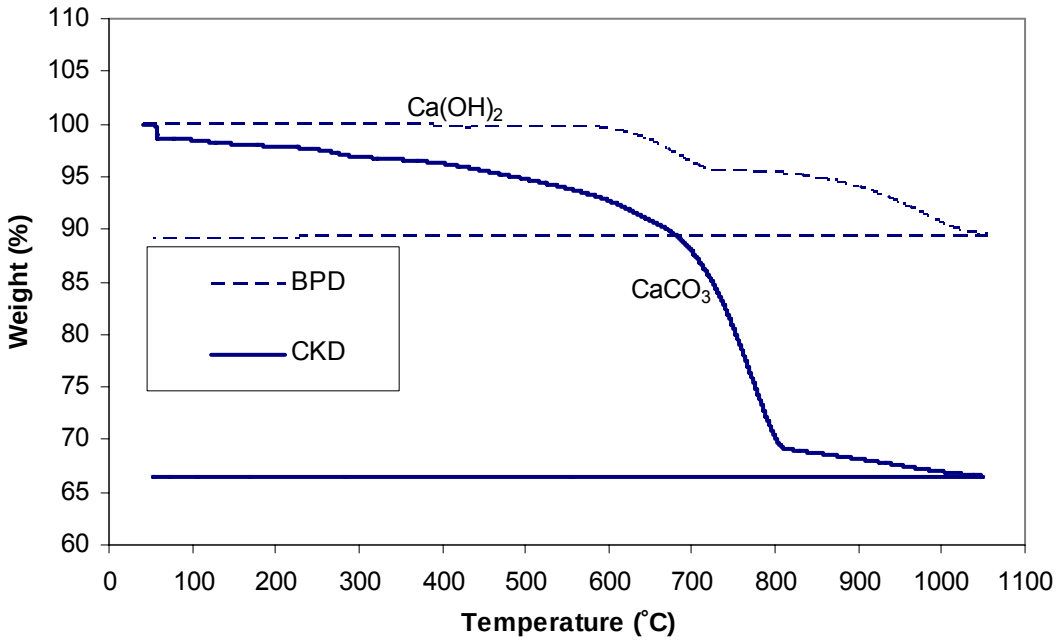

2.1.4 Run-of-station ash

Dry run-of-station ash (ROSA) supplied by Rugby Ash was also used in the concrete and paste mixes. ROSA is unclassified PFA (i.e. the rejects from PFA grading) and was supplied as a fine powder as shown by the particle size analysis (Figure 10). TGA indicated the presence of ~7% carbon content at around 600–800° C (Figure 11).

Figure 10 Particle size analysis of ROSA

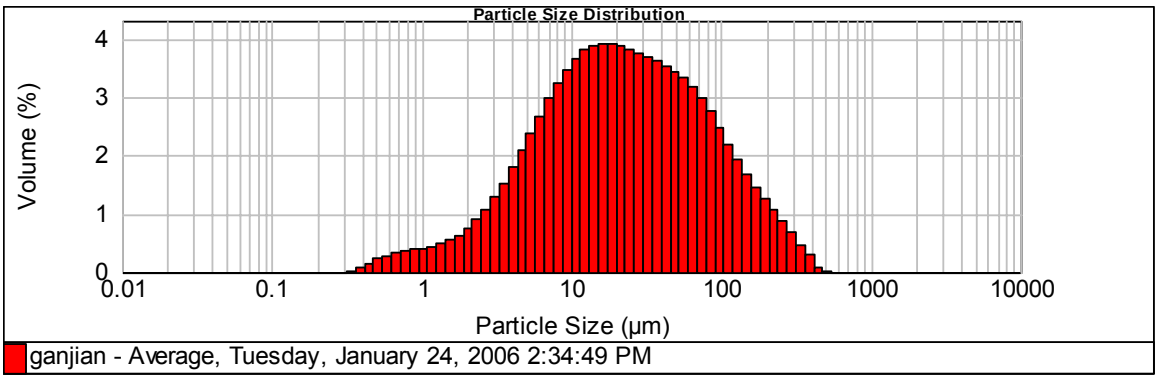

Figure 11 TGA results for ROSA

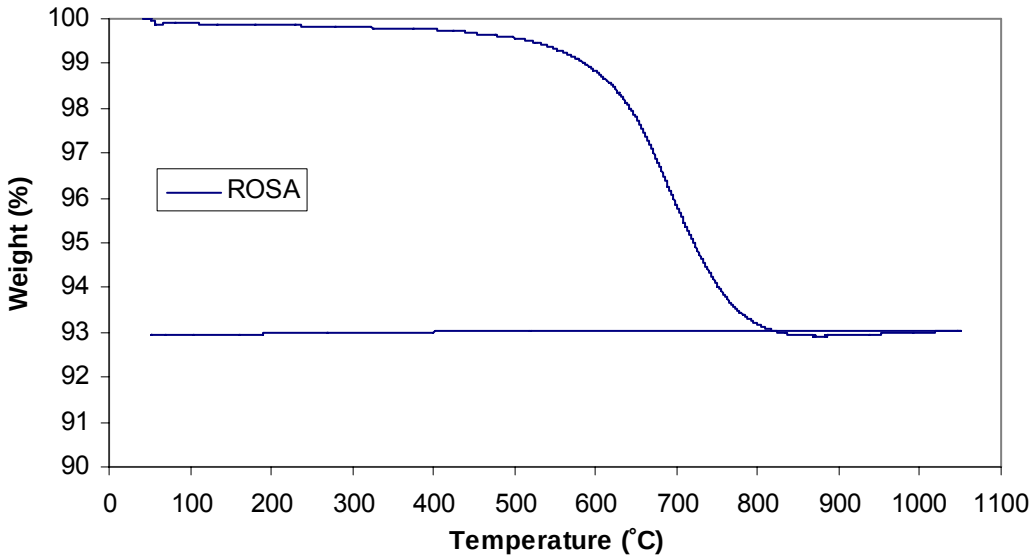

2.1.5 Hydrated lime and Maerz kiln dust

Lime used in construction works is made from limestone (calcium carbonate) burned in a lime kiln to form quicklime. The quicklime is added to water in a process known as slaking. The term 'hydrated' simply refers to any type of lime that has been slaked. After mixing with water, the mixture is hardened by a chemical process called carbonation as water evaporates and the lime reacts with carbon dioxide in the air. During each of these processes, the lime undergoes a chemical change but the final stage (carbonation) converts it back to calcium carbonate which is chemically and physically similar to the original limestone.

In this project, two sources of lime – commercial hydrated lime and Maerz kiln dust (MKD) lime – supplied by Buxton Lime Industries were used as a source of alkali in the paste mixtures.

The commercial hydrated lime was mainly calcium hydroxide complying with the requirements of BS EN 459-1: 2001 [11].

MKD is a by-product of lime manufacture and is collected from the chimney of lime kilns. It is a blend of calcium carbonate and calcium hydroxide. The MKD used in this project was supplied in a form of white powder. Its bulk density was 1000 kg/m^3 and the grading was 95% passing through 500 µm sieve. The typical chemical analysis of the MKD used is given in Table 1 (section 2.3).

2.1.6 Aggregates

Two sources of natural aggregates were used in the project:

- medium grade natural sand; and
- 10 mm uncrushed gravel complying with BS 882:1992 and BS EN 12620: 2002 [12].

The relative density of the sand and gravel was 2.6 g/cm^3.

A Type 1 recycled aggregate supplied by J.C. Balls & Sons (www.jcballs.co.uk/recycling.htm) was used to make concrete mixes. This recycled aggregate (Figure 12) contained crushed rocks, crushed concrete and masonry blocks, asphalt and fine materials such as silt and clay. The maximum size of recycled aggregates used was 75 mm and the average density was measured at about 2.5 g/cm^3.

Figure 13 shows the sieve analyses of the natural and recycled aggregates used in the project.

Figure 12 Recycled aggregate used

Figure 13 Sieve analysis of natural and recycled aggregates used in the project

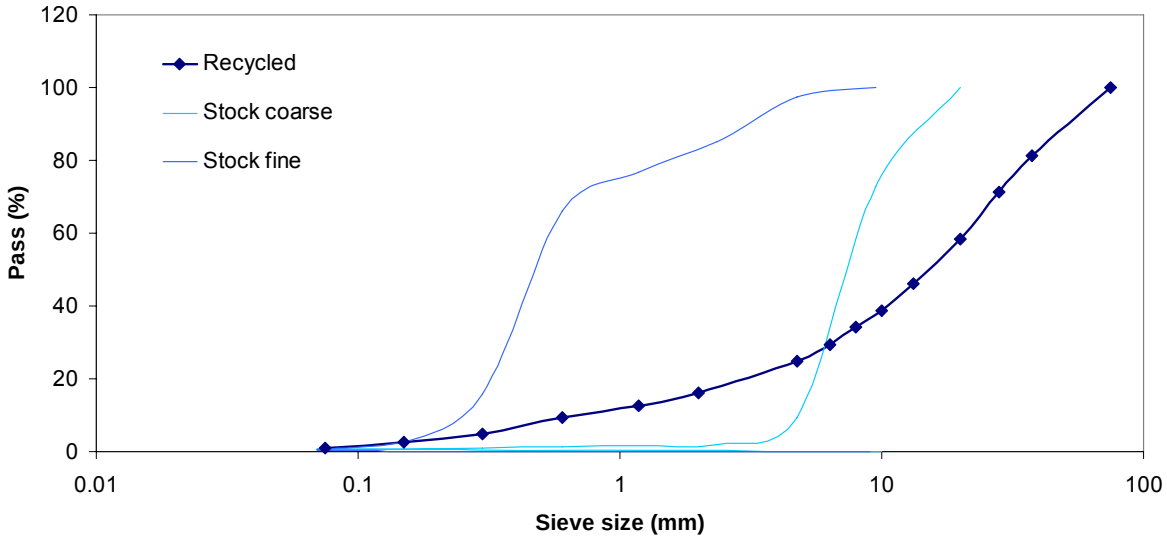

As shown in Figure 14, the calculated coarse and fine fractions of the recycled aggregate complied with the requirements of BS-EN 12620-2002.

Figure 14 BS limits compared with coarse and fine fractions of recycled aggregates used

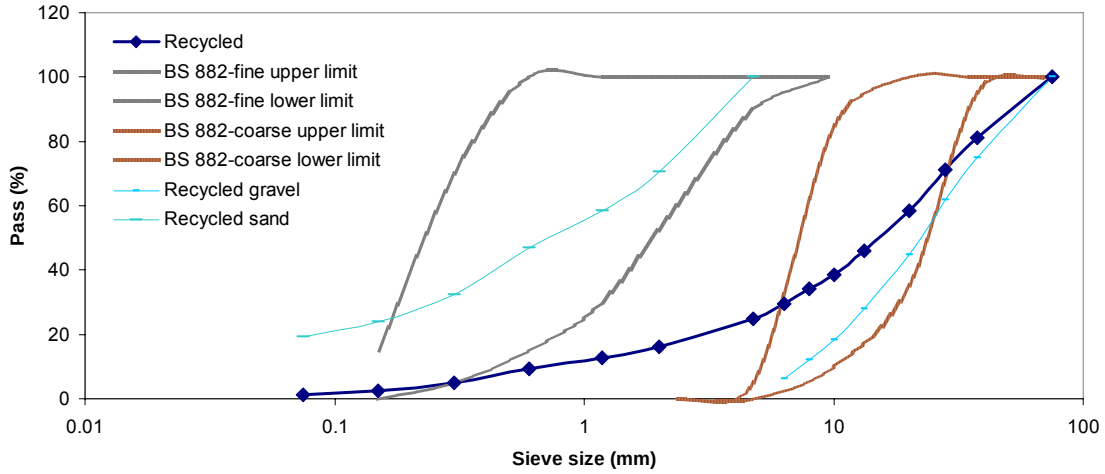

2.1.7 Superplasticiser

Two types of high-range water-reducing agents, Sika ViscoCrete-10 and Sika ViscoCrete-premium, were used in the project to increase the workability of the paste and concrete mixtures. The former is sulphonate based and less effective compared with the latter, which is based on an acrylic polymer and has a high efficiency at low doses. It was used to complete the laboratory test series at the same liquid to binder (L/B) ratio.

2.1.8 Water

Potable tap water (i.e. drinking water quality) was used to make the paste and concrete mixes.

2.2 Particle size comparison of raw materials

Figure 15 shows the particle size distribution of the raw materials used in this project.

Figure 15 Particle size distribution of raw materials used in the project

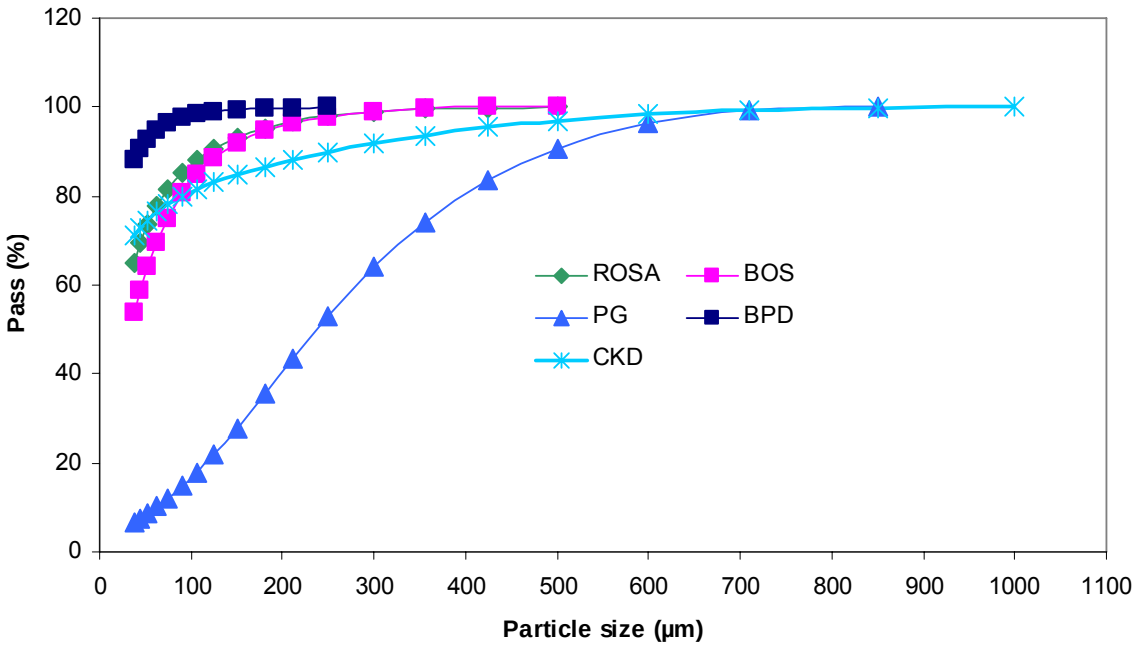

The crushed PG contains more particles in the range 200–400 µm compared with the other materials. The ground BOS has a maximum particle size of about 300 µm – an indication that the grinding process worked properly.

It is generally accepted that pozzolanic materials with a finer particle size results in faster hydration and reduced setting time of the binder. This is due to the higher surface area and electric charges induced on the surface of particles during the grinding process.

2.3 Chemical analysis of raw materials

The chemical composition of the materials used was determined using X-ray fluorescence (XRF) techniques. The proportion of different oxides present is shown in Table 1. Although there are variations in the chemical composition of different batches of BPD supplied, it was concluded that the effect of these variations would not be detrimental when using a low proportion of BPD in the mixture.

Table 1 Relative oxide content and loss on ignition (LOI) of the raw materials used in the project

Oxides	Percentage								
	PG	W-BOS	UW-BOS	ROSA	CKD	BPD I	BPD II	BPD (Coventry binder)*	MKD
SiO_2	2.43	11.45	11.43	45.91	9.89	12.86	21.86	13.90	2.00
TiO_2	0.03	0.37	0.39	1.41	0.14	0.12	0.29	0.12	–
Al_2O3	0.81	2.32	1.60	26.51	3.72	3.50	3.85	2.59	1.00
Fe_2O_3	0.36	27.32	28.24	5.23	1.24	2.12	2.57	1.51	0.40
MnO	0.00	3.65	4.35	0.08	0.02	0.02	0.02	0.01	–
MgO	0.40	9.32	8.27	2.13	0.94	2.46	1.13	0.69	0.30
CaO	37.30	37.44	41.29	6.88	40.42	58.28	53.40	51.61	10.00
Na_2O	0.03	0.03	0.02	0.61	0.43	0.29	0.41	0.74	–
K_2O	0.24	0.01	0.02	1.35	6.36	1.71	3.64	10.41	–
P_2O_5	0.02	1.26	1.48	0.98	0.08	0.06	0.08	0.05	–
SO_3	53.07	0.28	0.44	1.37	5.59	6.75	7.10	5.01	0.20
LOI	4.09	3.12	1.12	7.11	30.99	10.23	5.02	4.40	85.00

* See section 3.1.5.

The typical chemical composition of pozzolanic materials such as pulverised fuel ash (PFA) and ground granulated blast furnace slag (GGBS) is well understood and their use as cement replacements is well-established in construction and concrete technology. Figure 16 compares the chemical composition of the waste materials used in this project and commonly used cementitious materials (OPC, GGBS and PFA).

Figure 16 The comparative CaO-Al_2O_3-SiO_2 content of conventional and waste pozzolanic materials

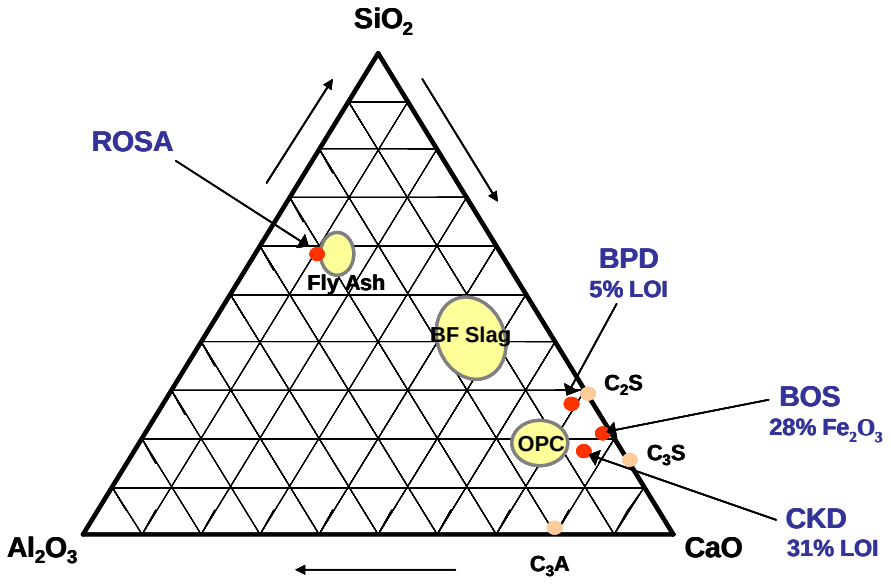

The composition of BOS is quite different from that of BF slag (GGBS). This is due to the nature of the process from which these materials are derived. GGBS is produced during the production of steel in the blast furnace while BOS is obtained from basic oxygen furnace process. Figure 17 presents a general schematic that depicts the blast furnace feedstocks and the production of blast furnace co-products (iron and slag).

Figure 17 General schematic of blast furnace operation and blast furnace slag production

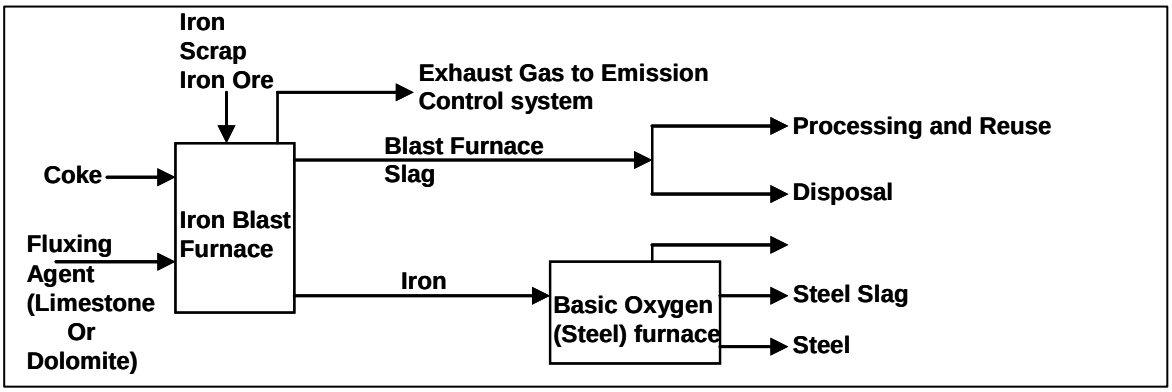

2.4 Mix proportions

2.4.1 Paste and concrete mixtures

A large number of paste specimens were made during the investigation. This report uses the word 'paste' to mean a mixture of cementitious powder and water with no aggregate. 'Semi-dry' paste refers to a paste containing a low proportion of water.

The proportions used in the pastes in this study were designed to optimise the mixture ingredients to achieve the highest compressive strength. A considerable number of initial 'cup' mixes and trial mixes were made using various materials and proportions to identify suitable mix ingredients (Appendix A).

A systematic laboratory study was designed to determine the effects of:

- different replacement levels of PG, BOS, ROSA, CKD, BPD, hydrated lime and MKD;
- slag weathering; and
- water content.

Based on the optimum proportions obtained from the paste mixes, various concrete mixes were designed using 380 kg/m^3 binder and different L/B (liquid to binder) ratios. Tables 2–17 show the mixture proportions used to make pastes and concretes, their liquid-to-solid (L/S) ratios and flow as measured on a flow table (see section 2.6).

Table 2 Mix proportions for PG-CKD-BOS paste mixtures

Mix code	PG (%)	CKD (%)	UW-BOS (%)	L/S	Flow (mm)
PG 20/UW-BOS80	20	–	80	0.30	150
PG40/UW-BOS60	40	–	60	0.30	136
PG60/UW-BOS40	60	–	40	0.30	110
CKD60/PG8-UW-BOS32	8	60	32	0.30	161
CKD40/PG12-UW-BOS48	12	40	48	0.30	120
CKD20/PG16-UW-BOS64	16	20	64	0.30	92

Table 3 Mix proportions for PG-BPD-BOS paste mixtures

Mix code	PG (%)	BPD (%)	BOS (%)	L/S	Flow (mm)
BPD10/BOS90	–	10	90	0.30	146
BPD20/BOS80	–	20	80	0.30	104
BPD40/BOS60	–	40	60	0.30	108
BPD60/BOS40	–	60	40	0.30	91
BPD90/BOS10	–	90	10	0.30	88
PG5/BPD38-BOS57	5	38	57	0.30	178
PG10/BPD36-BOS54	10	36	54	0.30	176
PG15/BPD34-BOS51	15	34	51	0.30	158
PG20/BPD32-BOS48	20	32	48	0.30	157
PG30/BPD28-BOS42	30	28	42	0.30	115

Table 4 Mix proportions for BPD-PG-BOS paste mixtures

Mix code	PG (%)	BPD (%)	BOS (%)	L/S	Flow (mm)
PG10/BOS90	10	–	90	0.30	170
PG20/BOS80	20	–	80	0.30	158
PG40/BOS60	40	–	60	0.30	110
PG60/BOS40	60	–	40	0.30	90
BPD5/PG19/BOS76	19	5	76	0.30	175
BPD10/PG18/BOS72	18	10	72	0.30	177
BPD20/PG16/BOS64	16	20	64	0.30	160
BPD30/PG14/BOS56	14	30	56	0.30	185
BPD50/PG10/BOS40	10	50	40	0.30	171

Table 5 Mix proportions for PG-BPD paste mixtures

Mix code	PG (%)	BPD (%)	BOS (%)	L/S	Flow (mm)
PG10/BPD90	10	90	–	0.30	103
PG20/BPD80	20	80	–	0.30	105
PG40/BPD60	40	60	–	0.30	108
PG60/BPD40	60	40	–	0.30	109

Table 6 Mix proportions for fine tuning of BOS-PG-BPD paste mixtures*

Mix code	PG (%)	BPD (%)	BOS (%)	L/S	Flow (mm)
BOS80/PG15/BPD5	10	5	80	0.30	162
BOS85/PG10/BPD5	10	5	85	0.30	162
BOS77/PG20/BPD3	20	3	77	0.30	158
BOS80/PG5/BPD15	5	15	80	0.30	140
BOS80/PG10/BPD10	10	10	80	0.30	148
BOS80/PG12/BPD8	12	8	80	0.30	154
BOS80/PG2/BPD18	2	18	80	0.30	124

* Primary data prior to fine tuning are given in Tables 3–5

Table 7 Mix proportions for measuring the effect of ROSA on BOS-CKD-PG paste mixtures

Mix code	PG (%)	CKD (%)	W-BOS (%)	ROSA (%)	L/S	Flow (mm)
PG15/CKD5/BOS10/ROSA70	15	5	10	70	0.30	38.5
PG15/CKD5/BOS20/ROSA60	15	5	20	60	0.30	47.2
PG15/CKD5/BOS30/ROSA50	15	5	30	50	0.30	59.1
PG15/CKD5/BOS40/ROSA40	15	5	40	40	0.30	56.8
PG15/CKD5/BOS50/ROSA30	15	5	50	30	0.30	61.5
PG15/CKD5/BOS60/ROSA20	15	5	60	20	0.30	107.7
PG15/CKD5/BOS70/ROSA10	15	5	70	10	0.30	124.0

Table 8 Mix proportions for measuring the effect of L/S ratio and weathering on BOS-CKD-PG paste mixtures

Mix code	PG (%)	CKD (%)	UW-BOS (%)	W-BOS (%)	L/S	Flow (mm)
PG15/CKD5/W-BOS80-0.2	15	5	–	80	0.20	78
PG15/CKD5/W-BOS80-0.25	15	5	–	80	0.25	112
PG15/CKD5/W-BOS80-0.3	15	5	–	80	0.30	152
PG15/CKD5/W-BOS80-0.4	15	5	–	80	0.40	209
PG15/CKD5/UW-BOS80-0.2	15	5	80	–	0.20	78
PG15/CKD5/UW-BOS80-0.25	15	5	80	–	0.25	145
PG15/CKD5/UW-BOS80-0.3	15	5	80	–	0.30	191
PG15/CKD5/UW-BOS80-0.4	15	5	80	–	0.40	>250

Table 9 Mix proportions of semi-dry mixtures of BOS-BPD-PG and PG-BPD-BOS-ROSA

Mix code	PG (%)	BPD (%)	BOS (%)	ROSA (%)	L/S	Flow (mm)
PG15/BPD5/BOS80-0.3	15	5	80	–	0.30	175
PG15/BPD5/BOS80-0.2	15	5	80	–	0.20	0
PG15/BPD5/BOS80-.15	15	5	80	–	0.15	0
PG15/BPD5/BOS80-.13	15	5	80	–	0.13	0
PG15/BPD5/BOS30/ROSA50-0.3	15	5	30	50	0.30	125
PG15/BPD5/BOS30/ROSA50-0.25	15	5	30	50	0.25	0
PG15/BPD5/BOS30/ROSA50-0.23	15	5	30	50	0.23	0
PG15/BPD5/BOS30/ROSA50-0.19	15	5	30	50	0.19	0
PG15/BPD5/BOS30/ROSA50-0.15	15	5	30	50	0.15	0

Table 10 Mix proportions for BPD-BOS-ROSA mixtures

Mix code	BPD (%)	BOS (%)	ROSA (%)	L/S	Flow (mm)
BPD5/BOS76/ROSA19	5	76	19	0.30	>250
BPD5/BOS50/ROSA45	5	50	45	0.30	152
BPD5/BOS27/ROSA68	5	27	68	0.30	123
BPD5/BOS15/ROSA80	5	15	80	0.30	83
BPD10/BOS72/ROSA18	10	72	18	0.30	155
BPD10/BOS35/ROSA55	10	35	55	0.30	132
BPD20/BOS64/ROSA16	20	64	16	0.30	143
BPD40/BOS48/ROSA12	40	48	12	0.30	134
BPD40/BOS30/ROSA30	40	30	30	0.30	130
BPD60/BOS32/ROSA8	60	32	8	0.30	125

Table 11 Mix proportions for ROSA-BOS-BPD mixtures

Mix code	BPD (%)	BOS (%)	ROSA (%)	L/S	Flow (mm)
ROSA32/BOS8/BPD60	60	8	32	0.30	96
ROSA48/BOS12/BPD40	40	12	48	0.30	94
ROSA64/BOS16/BPD20	20	16	64	0.30	86
ROSA72/BOS18/BPD10	10	18	72	0.30	55

Table 12 Mix proportions for BPD-BOS-ROSA mixtures

Mix code	BPD (%)	BOS (%)	ROSA (%)	L/S	Flow (mm)
BOS20/ROSA48/BPD32	32	20	48	0.30	115
BOS40/ROSA36/BPD24	24	40	36	0.30	126
BOS60/ROSA24/BPD16	16	60	24	0.30	150

Table 13 Mix proportions for PG-BOS-ROSA mixtures

Mix code	PG (%)	BOS (%)	ROSA (%)	L/S	Flow (mm)
PG5/BOS15/ROSA80	5	15	80	0.30	90
PG5/BOS76/ROSA19	5	76	19	0.30	>250
PG5/BOS50/ROSA45	5	50	45	0.30	136
PG8/BOS20/ROSA72	8	20	72	0.30	85
PG10/BOS30/ROSA60	10	30	60	0.30	95
PG10/BOS75/ROSA15	10	75	15	0.30	>250
PG12/BOS48/ROSA40	12	48	40	0.30	153
PG16/BOS64/ROSA20	16	64	20	0.30	>250
PG20/BOS35/ROSA45	20	35	45	0.30	130
PG30/BOS40/ROSA30	30	40	30	0.30	119

Table 14 Mix proportions for BOS-Lime and BOS-MKD paste mixtures

Mix code	Hydrated lime (%)	MKD (%)	BOS (%)	L/S	Flow (mm)
Lime10/BOS90	10	–	90	0.30	>250
Lime30/BOS70	30	–	70	0.30	167
Lime50/BOS50	50	–	50	0.30	124
Lime70/BOS30	70	–	30	0.30	89
MKD10/BOS90	–	10	90	0.30	>250
MKD30/BOS70	–	30	70	0.30	172
MKD50/BOS50	–	50	50	0.30	132
MKD70/BOS30	–	70	30	0.30	93

Table 15 Mix proportions for BOS-Lime and BOS-MKD paste mixtures

Mix code	Hydrated lime (%)	MKD (%)	ROSA (%)	L/S	Flow (mm)
Lime10/ROSA90	10	–	90	0.30	130
Lime30/ROSA70	30	–	70	0.30	114
Lime50/ROSA50	50	–	50	0.30	95
Lime70/ROSA30	70	–	30	0.30	87
MKD10/ROSA90	–	10	90	0.30	142
MKD30/ROSA70	–	30	70	0.30	124
MKD50/ROSA50	–	50	50	0.30	98
MKD70/ROSA30	–	70	30	0.30	94

Table 16 Mix proportions for measuring the effect of hydrated lime and MKD on BOS-PG-ROSA paste mixtures

Mix code	Hydrated lime (%)	MKD (%)	PG (%)	BOS (%)	ROSA (%)	L/S	Flow (mm)
BOS80/PG15/Lime5	5	–	15	80	–	0.30	114
BOS80/PG15/MKD5	–	5	15	80	–	0.30	152
BOS50/ROSA30/PG15/Lime5	5	–	15	50	30	0.30	108
BOS50/ROSA30/PG15/MKD5	–	5	15	50	30	0.30	118
ROSA75/PG15/MKD10	–	10	15	–	75	0.30	110
ROSA65/PG15/MKD20	–	20	15	–	65	0.30	94

Table 17 Mix proportions of concrete mixtures

Mix code	Mix proportions (kg/m^3)										L/B	Slump (mm)
	PG	BPD	BOS	ROSA	Water	Water reducer		Sand	Coarse 10 mm	Recycled aggregate		
						Ordinary	Polymeric					
PG15/BPD5/BOS80 (SP)	57	19	304	–	152	7.6 (2%)	–	830	1050	–	0.40	10
PG15/BPD34/BOS51	57	129.2	193.8	–	152	–	–	795	1050	–	0.40	10
PG15/BPD5/BOS80 (PSP)	57	19	304	–	152	–	2.66 (0.7%)	830	1050	–	0.40	180
PG15/BPD5/BOS80 (RA-PSP)	57	19	304	–	152	–	1.9 (0.5%)	–	–	1545	0.40	20
PG15/BPD5/BOS80 (PPG-PSP)	57	19	304	–	152	–	2.66 (0.7%)	830	1050	–	0.40	160
PG15/BPD5/BOS80 (RA-PPG-PSP)	57	19	304	–	152	–	1.9 (0.5%)	–	–	1545	0.40	40
PG15/BPD5/BOS80 (RA-RCC)	57	19	304	–	95	–	–	–	–	1980	0.25	0
PG15/BPD5/BOS60/ROSA20	57	19	228	76	152	–	–	800	1050	–	0.40	0
PG10/BPD5/BOS32/ROSA53 (SP)	38	19	121.6	201.4	152	5.7 (1.5%)	–	770	1050	–	0.40	120
PG15/BPD5/BOS30/ROSA50 (RA-PSP)	57	19	114	190	152	–	2.66 (0.7%)	–	–	1808	0.40	30
PG15/BPD5/BOS30/ROSA50 (RA-RCC)	57	19	114	190	114	–	–	–	–	1910	0.30	0

PPG = processed plasterboard gypsum
PSP = polymer superplasticiser
RA = recycled aggregate
SP = superplasticiser

2.4.2 Soil stabilisation mixtures

Two types of soils – sandy clay (Figure 18) and silty sand (Figure 19) – were mixed with various amounts of two selected binders in order to investigate soil stabilisation.

The quantities of binder chosen were 20, 40, 50 and 60%; Table 18 shows the proportions of soil and binder used. The optimum moisture content (OMC) of each soil was determined according to BS 1377-4: 1990 [13]; the results are presented in Table 19 and Figure 20.

To compensate for the amount of water necessary for hydration of the binder, an extra 0.5% of water by weight was added to the mixture of soil and binder.

Figure 18 Sandy clay soil (Soil A)

Figure 19 Silty sand soil (Soil B)

Table 18 Mix proportions of stabilised soil mixtures

Mix code	Soil (%)	Binder (%)	Moisture content (%)
Soil-A 80/Binder-A 20	80	20	14.2
Soil-A 60/Binder-A 40	60	40	14.2
Soil-A 50/Binder-A 50	50	50	14.2
Soil-A 40/Binder-A 60	40	60	14.2
Soil-A 40/Binder-B 60	40	60	15.2
Soil-B 80/Binder-A 20	80	20	13.9
Soil-B 60/Binder-A 40	60	40	13.9
Soil-B 50/Binder-A 50	50	50	13.9

Table 19 Optimum moisture content of soils used (compatibility test)

Soil type	Optimum moisture content (%)	Peak dry density (g/cm^3)
Soil-A	13.70	1.86
Soil-B	13.40	1.92

Figure 20 Compatibility and optimum moisture content of soils used

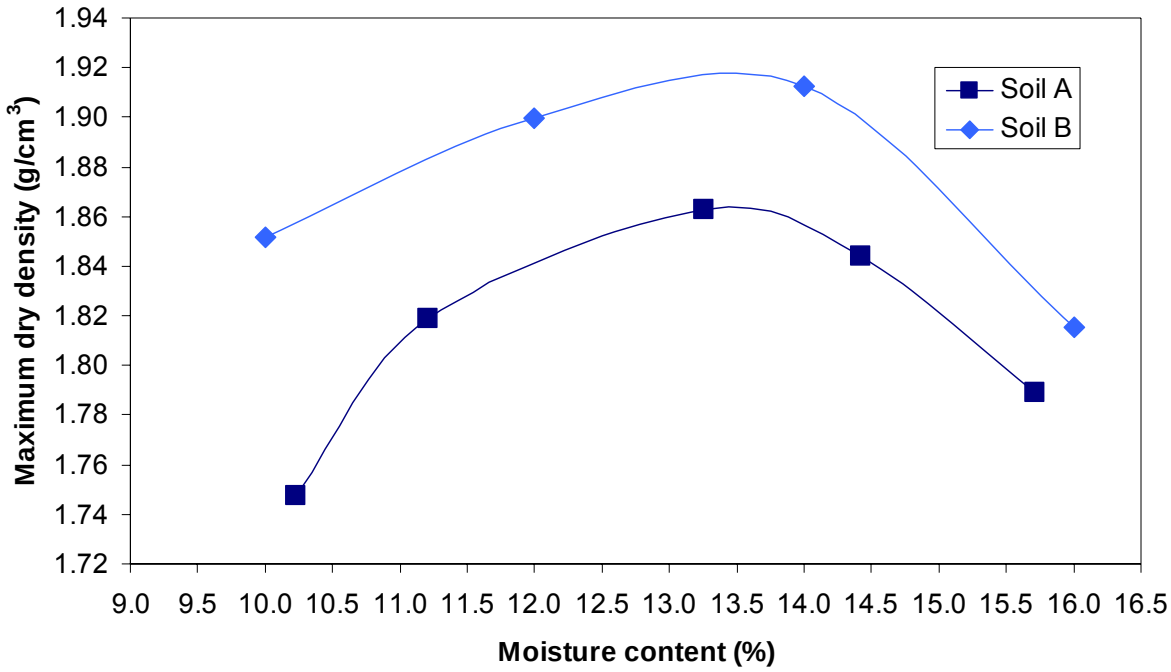

2.5 Mixing and casting

2.5.1 Laboratory facilities

Appendix B describes the equipments used for mixing, casting and curing the paste and concrete mixes. It also shows the testing equipment and machines used to measure the properties of fresh and hardened paste and concrete.

2.5.2 Paste mixtures

The mixing was carried out in a mixer of 2-litre capacity according to the following procedure:

- PG, BOS, BPD and ROSA (as applicable) were mixed dry for 1 minute.
- Half the mixing water (with superplasticiser if applicable) was added during the next 30 seconds of mixing.
- Mixing was continued for a further 30 seconds at medium speed.
- The mixer was stopped and the mixture scraped off the sides of the bowl and blades.
- The remainder of the mixing water was added and mixing was carried out for a further two minutes at high speed.

2.5.3 Concrete mixtures

The fine and coarse aggregates were air-dried before mixing. The water content of the mix was adjusted based on natural moisture content and the measured saturated surface dry (SSD) moisture content of the aggregates. The mixing was performed according to the guidelines set out in BS 1881-125: 1986 [14].

A horizontal pan mixer of 10-litre capacity was used to make the concrete mixes. The mixing method was as follows:

- The fine and coarse aggregate were mixed with about one-third of the water to allow absorption to take place for 30 seconds.
- The PG, BOS and BPD were mixed dry by hand.
- Half the reminder of the water was added with PG, BOS, CKD, BPD and ROSA (as applicable) and mixed for 1 minute.
- The mixer was stopped and the mixture scraped off the sides of the pan and hand mixed.
- The remainder of mixing water was added and mixing continued for another 2 minutes.

2.5.4 Casting and curing

The paste and concrete samples were cast in pre-oiled 50-mm and 100-mm cube moulds respectively. The moulds were covered after casting with wet fabric and a polyethylene sheet until demoulding the next day. After demoulding, specimens were stored in containers kept at 20±2° C and 98% relative humidity (RH).

2.6 Test methods

The flow of the paste and concrete mixes was measured using a flow table (BS EN 12350-5: 2000 [15]) and a slump test.

A mix is considered to be flowable when the spread is 510–620 mm in diameter. This corresponds to 110–210 mm in diameter for the small modified flow table used in this study according BS 4551-1: 1998 [16] and ASTM C230 [17]. For high flowability, a spread of >190 mm in diameter is required.

Compressive strengths of cubes up to the age of 28 days were determined. Concrete specific compliance tests, including high pressure through-flow and hydrogen sulphide tests, were also carried out. The results of these tests are given in section 4.

3.0 Laboratory results

3.1 Paste mixes

3.1.1 PG-BOS mixture with and without CKD

The results of compressive strength tests on PG-BOS-CKD at two stages (i.e. initially without CKD) are presented in Table 20. Figure 21 shows the compressive strength development of PG-BOS paste mixes. The mix incorporating 20% PG and 80% BOS achieved the highest compressive strength compared to mixes with a lower slag content.

In the second stage, the ternary mixture of PG-CKD-BOS incorporating various amounts of CKD and the same BOS to PG ratio of 4 was tested for compressive strength as shown in Figure 22. The relationship between the compressive strength of the ternary system and the CKD content is depicted in Figure 23.

Table 20 Compressive strength of PG-BOS-CKD mixes

Mix code	Strength at days (MPa)*			Flow (mm)	Density (kg/m^3)
	3	7	28		
PG20/UW-BOS80	1.80	3.61	7.77	150	1910
PG40/UW-BOS60	1.65	3.37	4.18	136	1760
PG60/UW-BOS40	1.30	2.99	3.45	110	1580
CKD60/PG 8-UW-BOS32	1.23	2.10	6.97	161	1990
CKD40/PG12-UW-BOS48	0.91	1.60	7.22	120	1930
CKD20/PG16-UW-BOS64	1.35	2.90	13.10	92	2050

* Highlighted cells indicate the highest or optimum compressive strength achieved in each group.

Increasing the amount of CKD from 20 to 60% in the ternary system resulted in a reduction in the compressive strength of the mixes by nearly 50% at 28 days (Figure 22). The highest compressive strength (13.1 MPa) of the mixes tested was for the mix with 20% CKD, 16% PG and 64% BOS (Table 20). Because insufficient CKD was available, it was not possible to include other combinations of PG-CKD-BOS in these initial investigations. Therefore the mix optimisation focused on using BPD instead (see section 3.1.4).

Figure 21 Compressive strength development of pastes containing PG and BOS

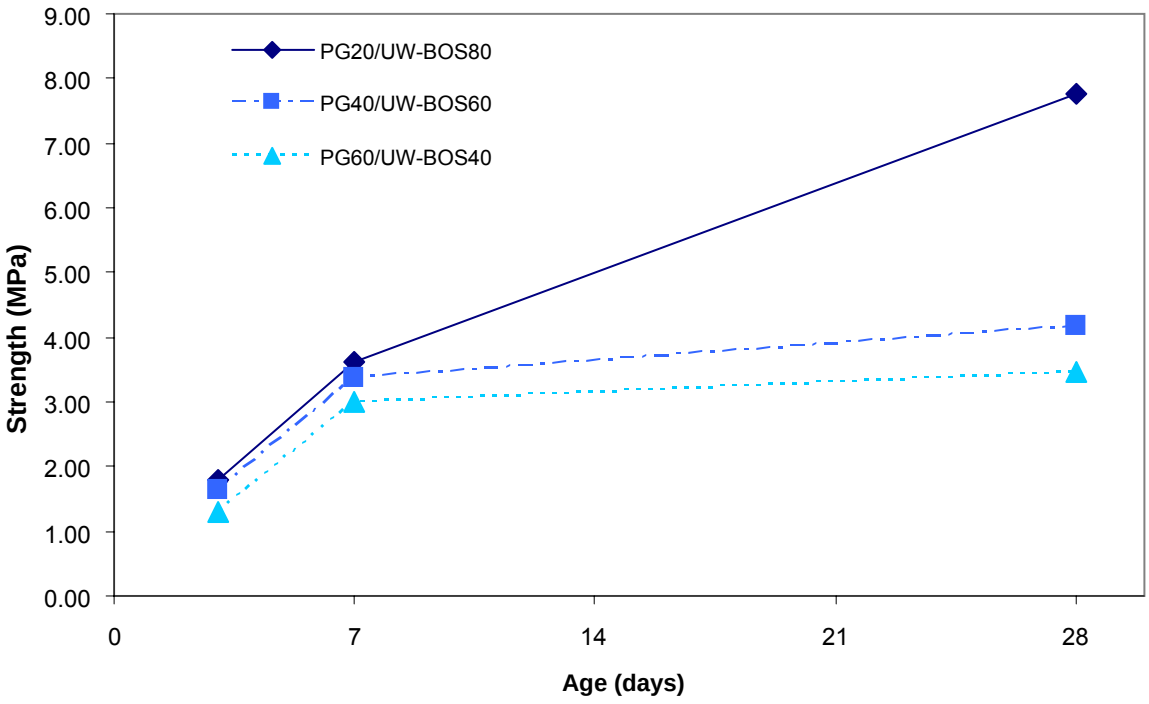

Figure 22 Compressive strength development of pastes containing CKD, PG and BOS

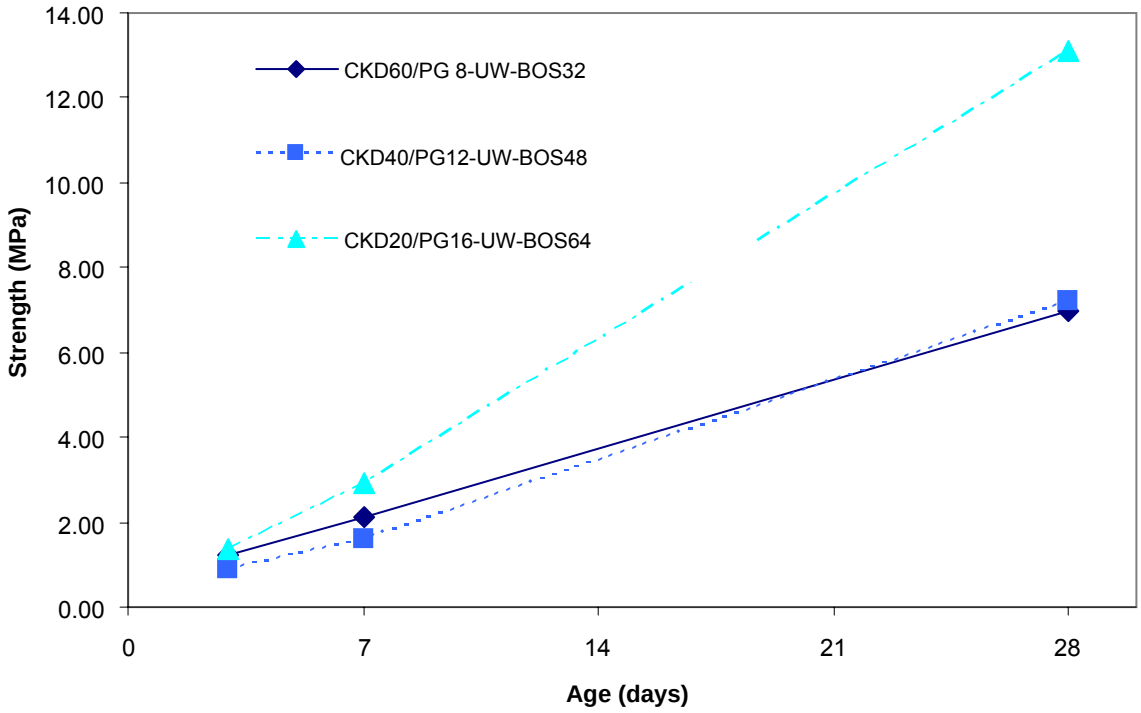

Figure 23 Compressive strength versus CKD content

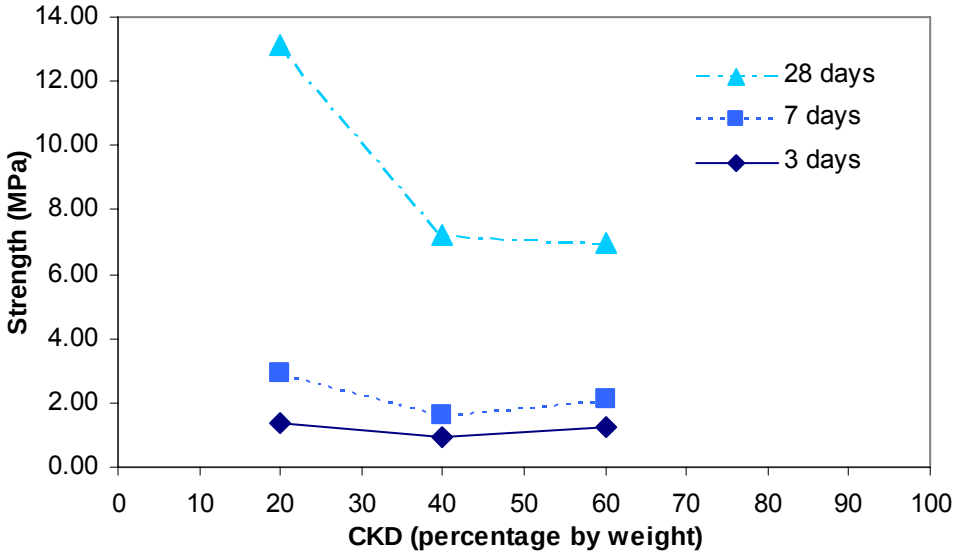

3.1.2 Effect of ROSA on PG-CKD-BOS mixture

The results of compressive strength of mixes incorporating four components (PG, CKD, BOS and ROSA) are presented in Table 21. These tests were carried out using a mixture with 15% CKD rather than the one containing 20% CKD which had shown the highest compressive strength in earlier tests (see section 3.1.1) primarily due to the limited supplies of CKD.

Table 21 Compressive strength of PG, CKD, BOS and ROSA mixtures

Mix code	Strength at days (MPa)*			Flow (mm)	Density (kg/m^3)
	3	7	28		
PG15/CKD5/BOS10/ROSA70	0.46	1.41	10.60	108	1680
PG15/CKD5/BOS20/ROSA60	0.34	1.32	18.90	115	1760
PG15/CKD5/BOS30/ROSA50	0.31	1.33	19.10	124	1780
PG15/CKD5/BOS40/ROSA40	0.37	1.34	8.21	122	1860
PG15/CKD5/BOS50/ROSA30	0.98	1.48	11.45	126	1880
PG15/CKD5/BOS60/ROSA20	0.62	1.83	9.83	162	2080
PG15/CKD5/BOS70/ROSA10	0.50	1.73	6.32	175	2030

* Highlighted cell indicates the highest or optimum compressive strength achieved in the group.

Figure 24 shows the compressive strength development for the mixes containing a range of ROSA-BOS content and same amount of PG and CKD. It shows that the mix incorporating 50% ROSA and 30% BOS achieved the highest 28-day strength.

This result indicates that replacing part of the BOS content with ROSA had a beneficial effect on early and long-term compressive strength up to this stage. This could be due to the activating effect of ROSA on BOS or the intrinsic pozzolanic potential of ROSA. The L/S ratio for all mixes was kept constant at 0.3 (Table 3).

Figure 24 Compressive strength development of pastes containing PG, CKD, BOS and ROSA

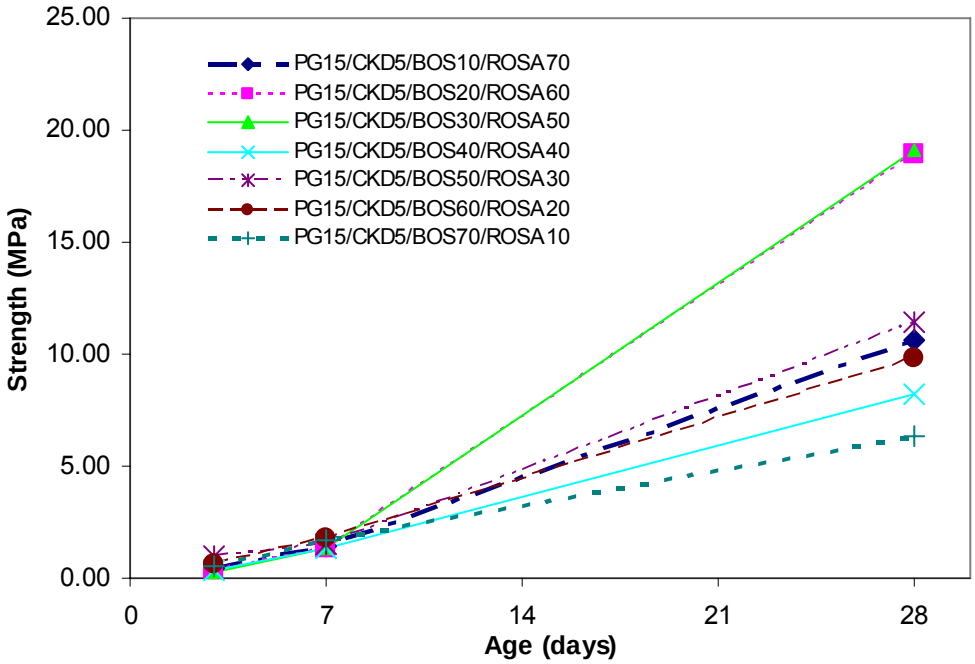

Figure 25 shows the changes in compressive strength with changes in ROSA content at different ages. Although change in ROSA content does not have a significant effect on strength at early ages, it becomes significant at the test age of 28 days. Two peaks of compressive strength at the testing age of 28 days can be observed. The highest strength belongs to the mix incorporating 50% ROSA, showing clearly the superior pozzolanic potential of this ash. At 7 days, the strength of the mix incorporating 20% ROSA is the highest but, in the long term, this trend changes.

The relative high strength of mixes incorporating ROSA is mainly because of the formation of aluminium-bearing products in the hydrated matrix of the paste.

In summary, use of a combination of BOS and ROSA is suggested for the trial mix, providing the four materials can be blended to form a final consistent powder.

Figure 25 Compressive strength of PG-CKD-BOS-ROSA mixes versus ROSA content at different ages

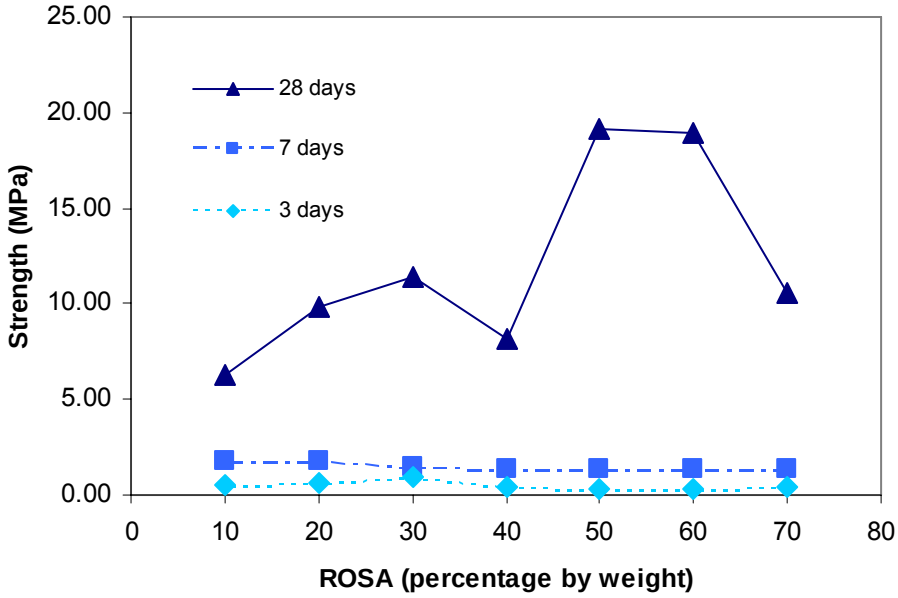

3.1.3 Effect of liquid to solid ratio, superplasticisers and weathering of BOS on PG-CKD-BOS mixtures

Table 22 presents the compressive strength results of PG-CKD-BOS mixtures with various liquid to binder ratios and workabilities.

Table 22 Compressive strength of mixtures of PG-CKD-BOS with various L/S ratios

Mix code	Strength at days (MPa)*			Flow (mm)	Density (kg/m^3)	L/S
	3	7	28			
PG15/CKD5/W-BOS80-0.2	0.26	2.23	6.44	78	2160	0.20
PG15/CKD5/W-BOS80-0.25	1.49	2.55	5.10	112	2090	0.25
PG15/CKD5/W-BOS80-0.3	1.14	1.90	4.70	152	1920	0.30
PG15/CKD5/W-BOS80-0.4	0.34	0.85	1.90	209	1790	0.40
PG15/CKD5/UW-BOS80-0.2	0.43	1.50	7.68	78	1970	0.20
PG15/CKD5/UW-BOS80-0.25	0.37	1.10	5.65	145	2060	0.25
PG15/CKD5/UW-BOS80-0.3	0.22	0.87	4.15	191	1890	0.30
PG15/CKD5/UW-BOS80-0.4	0.15	0.39	2.49	High	1790	0.40
PG15/CKD5/W-BOS80-0.2 superplasticiser	1.94	3.10	9.33	100	2340	nd

* Highlighted cells indicate the highest or optimum compressive strength achieved in each group. nd = not determined

Figure 26 and 27 show that a lower water content of the mix results in a higher compressive strength. This is in accordance with general concepts of cement and concrete technology.

Figure 26 Compressive strength development of pastes containing PG, CKD, W-BOS with various L/S ratios

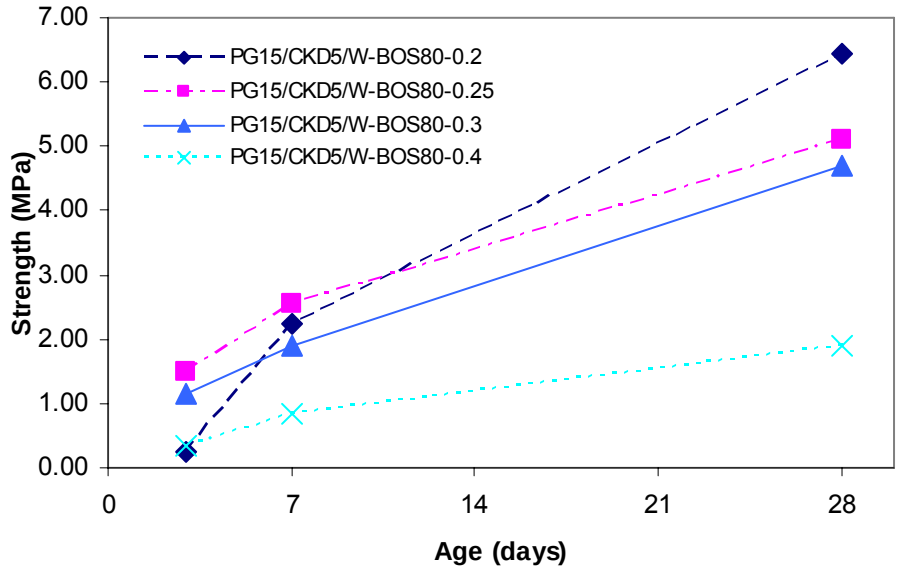

Figure 27 Compressive strength development of pastes containing PG, CKD, UW-BOS with various L/S ratios

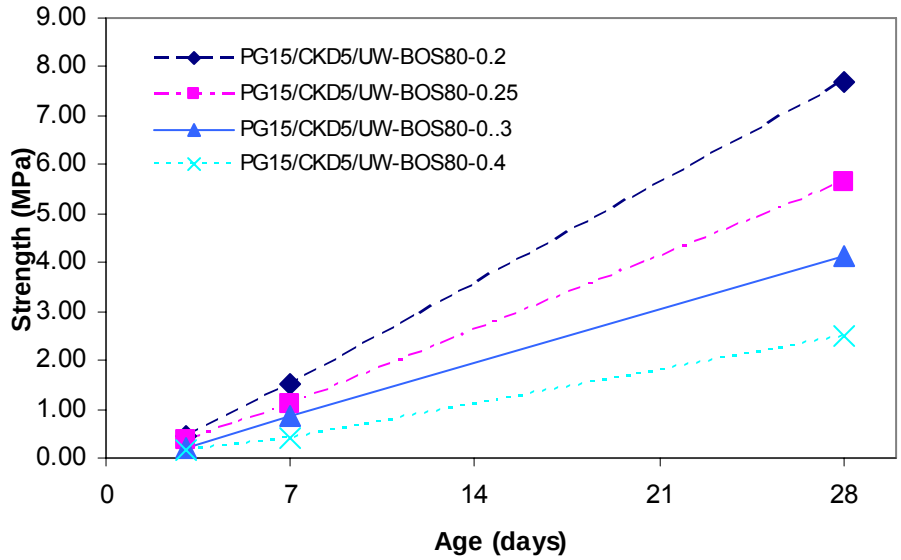

The mix with an L/S ratio of 0.2 achieved the highest strength at a test age of 28 days regardless of the weathering condition of the slag (Figures 26 and 27). The results also indicate that PG15/CKD5/BOS80-0.2 gains strength at a higher rate compared with other mixes.

These results indicate that reducing the water content will improve the long-term strength of the paste even though the flow of the mix might not be high enough to achieve appropriate compaction. A much greater improvement in strength might be achieved by using flow-improving agents and plasticisers, or different compaction methods instead of the vibrating table. Further results from studies on the effect of water content are discussed in section 3.1.6.

Incorporating weathered slag resulted in an increase in compressive strength at early test ages of 3 and 7 days (Figure 28). As the weathered BOS contains more calcium carbonate than the unweathered BOS, the increase in strength could be due to presence of calcium carbonate improving the microstructure of the hardened paste. However, the lack of calcium hydroxide content in the weathered slag adversely affects the strength of these mixes at 28 days.

Figure 28 Compressive strength versus L/S ratio for weathered and unweathered BOS at different ages

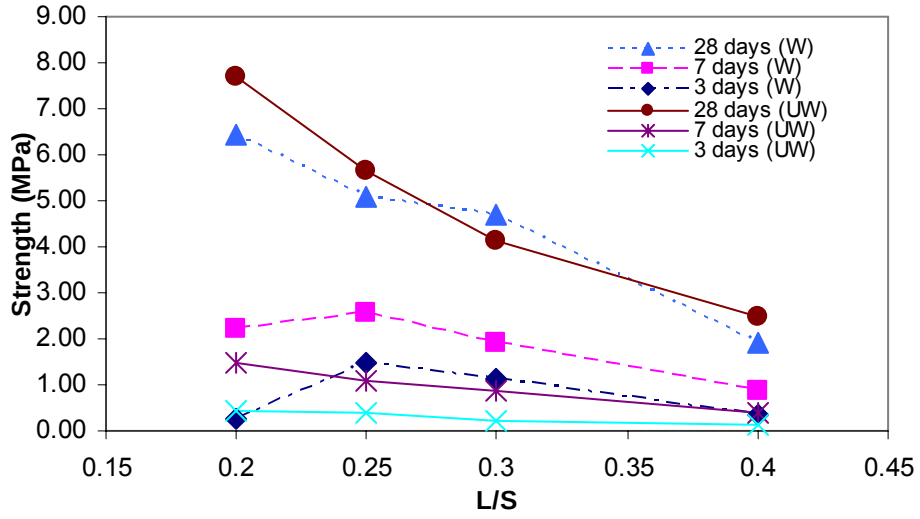

The mix PG15/CKD5/BOS80-0.2-P, which incorporates superplasticiser as a flow-improving agent, showed the highest gain in strength at 3, 7 and 28 days compared with the mix of the same L/S ratio (0.2) but without superplasticiser (Figure 29). Use of superplasticiser improved the flow from 78 to 100 mm (Table 22).

Figure 29 Comparison of the compressive strength development of PG-CKD-BOS pastes with superplasticiser and various L/S ratios

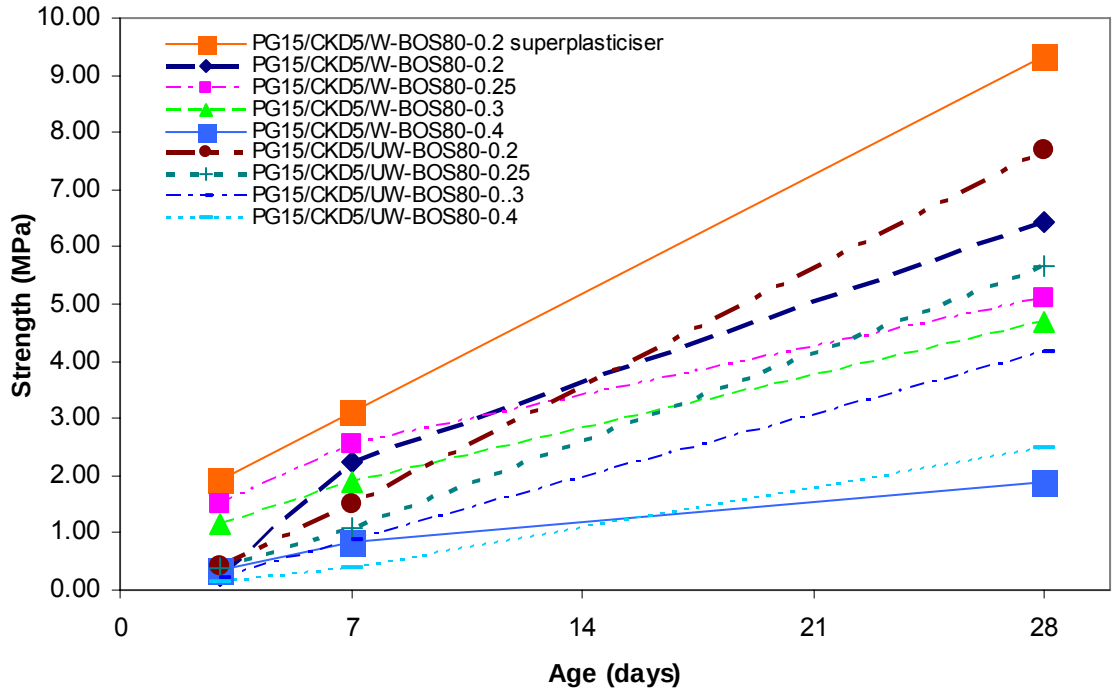

An increase in the flow of the mix will have a beneficial effect on compaction and, as a result, compressive strength will improve. The presence of the water-reducing agent may also improve the early strength by affecting the setting and hardening rate of such mixes.

3.1.4 Optimisation of mixture (PG, BPD, BOS)

The combinations of PG, BPD and BOS were investigated with respect to compressive strength. In order to optimise the ternary mixture of PG, BPD and BOS, a two-stage method was adopted.

- In the first stage, the strength of binary mixtures of each ingredient was determined.
- In the second stage, the third ingredient was added to the binary mix with the highest strength.

To distinguish the order of the components in each mixture, the name of the last component added to the optimum binary mix is given first, e.g. PG-BOS-BPD means PG was added to the optimum binary mixture of BOS and BPD in the second stage.

(a) PG-BPD-BOS mixture

The results for compressive strength of PG-BPD-BOS mixtures are shown in Table 23. The strength development of paste mixes using a range of BPD and BOS with same water content shows that the mix containing 40% BPD and 60% BOS had the highest strength at 7 days (Figure 30). Although Table 23 and Figure 31 show that the optimum amount of BPD for 3-day strength is 60%, this could be due to the rapidly reacting components of the BPD used. At 7 and 28 days, the highest compressive strength was achieved by the mix of BPD40/BOS60.

Table 23 Compressive strength of PG-BPD-BOS mixes*

Mix code	Strength at days (MPa)†			Flow (mm)	Density (kg/m^3)
	3	7	28		
BPD10/BOS90	0.22	0.50	3.58	146	2140
BPD20/BOS80	0.82	1.46	6.50	104	1940
BPD40/BOS60	1.34	2.80	9.50	108	1860
BPD60/BOS40	1.76	2.47	8.90	91	1700
BPD90/BOS10	0.27	0.89	6.40	88	1580
PG5/BPD38/BOS57	0.39	1.10	5.95	178	2030
PG10/BPD36/BOS54	0.73	1.81	8.04	176	1960
PG15/BPD34/BOS51	0.42	1.42	5.01	158	1970
PG20/BPD32/BOS48	0.67	1.19	3.68	157	1900
PG30/BPD28/BOS42	0.77	1.38	3.10	115	1760

* Figures 30-33 are derived from this table.

† Highlighted cells indicate the highest or optimum compressive strength achieved in each group.

Figure 30 Compressive strength development of pastes containing BPD and BOS

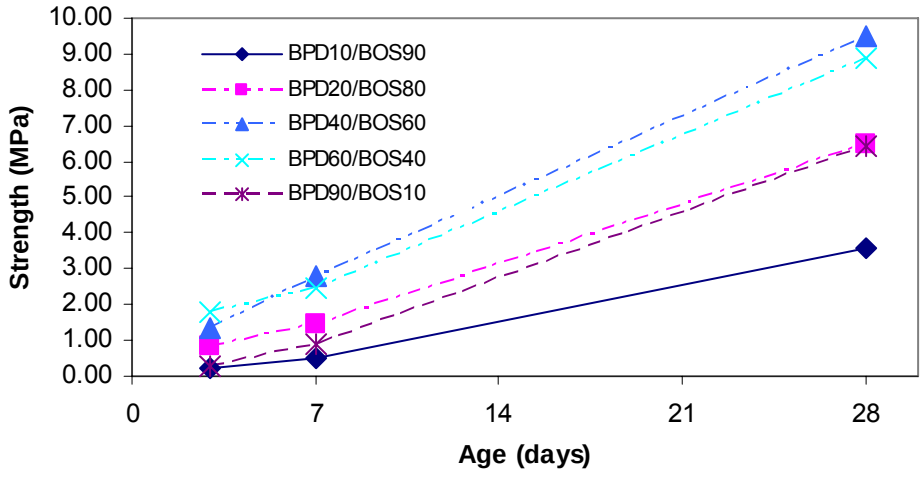

Figure 31 Compressive strength of BPD-BOS mixes versus BPD content at different ages

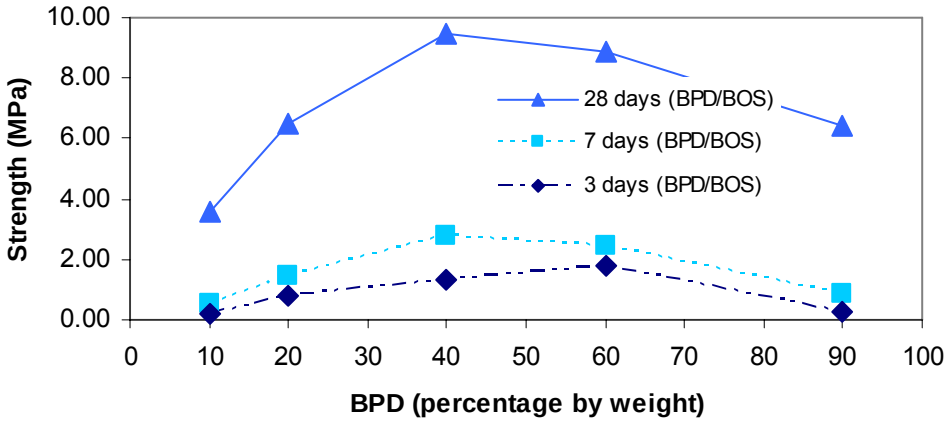

Based on the highest compressive strength achieved at 28 days, the mix design was carried forward and paste mixes containing 5–30% PG and same ratio of BPD to BOS were made. The highest strength at 3, 7 and 28 days was for the mix containing 10% plasterboard gypsum (Figures 32 and 33). Increasing the amount of PG above 10% resulted in a decrease in compressive strength (Figure 33). Therefore, it was initially concluded that the mix PG10/BPD36/BOS54 was the optimum mixture in this combination.

Figure 32 Compressive strength development of pastes containing PG, BPD and BOS

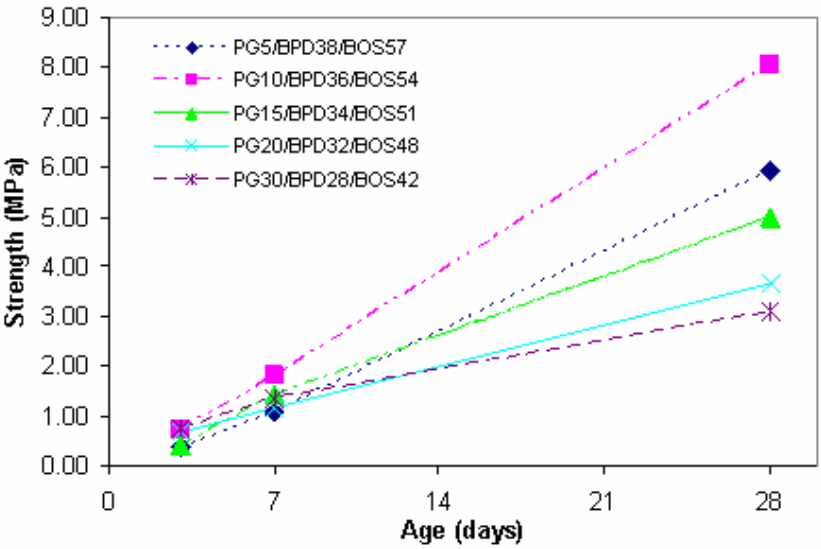

Figure 33 Compressive strength of PG-BPD-BOS mixes versus PG content

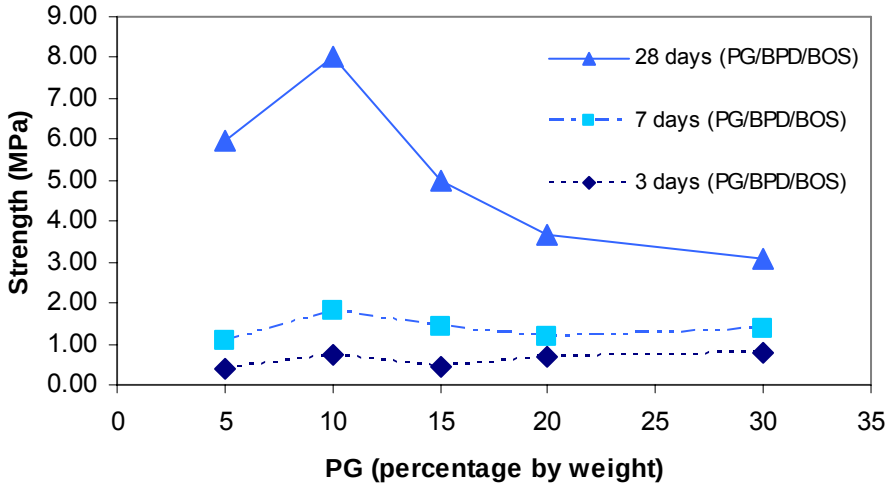

(b) BPD-PG-BOS mixture

The results for compressive strength of another combination of bypass dust, gypsum and slag (BPD-PG-BOS) are presented in Table 24. In this combination, the BPD was added to the optimum initial mixture of PG and BOS.

The strength development of PG-BOS and BPD-PG-BOS mixes is shown in Figures 34 and 35 respectively. In the first stage, the mixture of 20% PG and 80% BOS achieved the highest strength at all test ages. The catalyst effect of PG in the binary combination of PG-BOS was considerable, reducing the amount of BOS from 90% to 80% and combined with a corresponding increase in PG content from 10% to 20%, increasing the PG content by 10% resulted in a 16% increase in strength. In the ternary combination, the mix without BPD gained higher strength at 3 and 7 days, but the mix with 5% BPD achieved the highest strength at 28 days.

Table 24 Compressive strength of BPD-PG-BOS mixes*

Mix code	Strength at days (MPa)†			Flow (mm)	Density (kg/m^3)
	3	7	28		
PG10/BOS90	0.34	1.17	8.80	170	2170
PG20/BOS80	0.95	2.30	10.26	158	2110
PG40/BOS60	0.76	1.63	6.40	110	2020
PG60/BOS40	0.75	1.17	4.04	90	1900
BPD0/PG20/BOS80	0.95	2.30	10.26	158	2110
BPD5/PG19/BOS76	0.31	1.43	10.50	175	2180
BPD10/PG18/BOS72	0.27	1.30	8.70	177	2140
BPD20/PG16/BOS64	0.29	1.25	5.80	160	2110
BPD30/PG14/BOS56	0.45	1.27	6.70	185	2090
BPD50/PG10/BOS40	0.83	2.02	6.90	171	2020

* Figures 34–38 are derived from this table.

† Highlighted cells indicate the highest or optimum compressive strength achieved in each group.

Figure 34 Compressive strength development of PG-BOS mixes

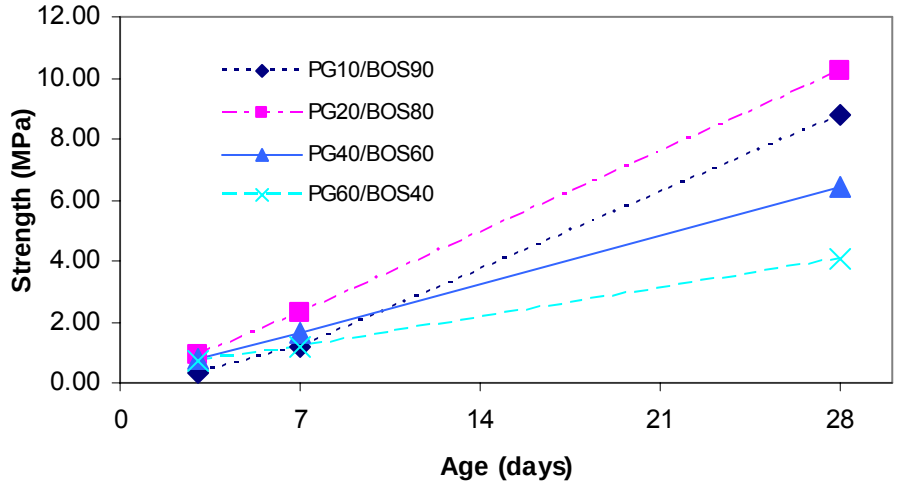

Figure 35 Compressive strength development of BPD-PG-BOS mixes

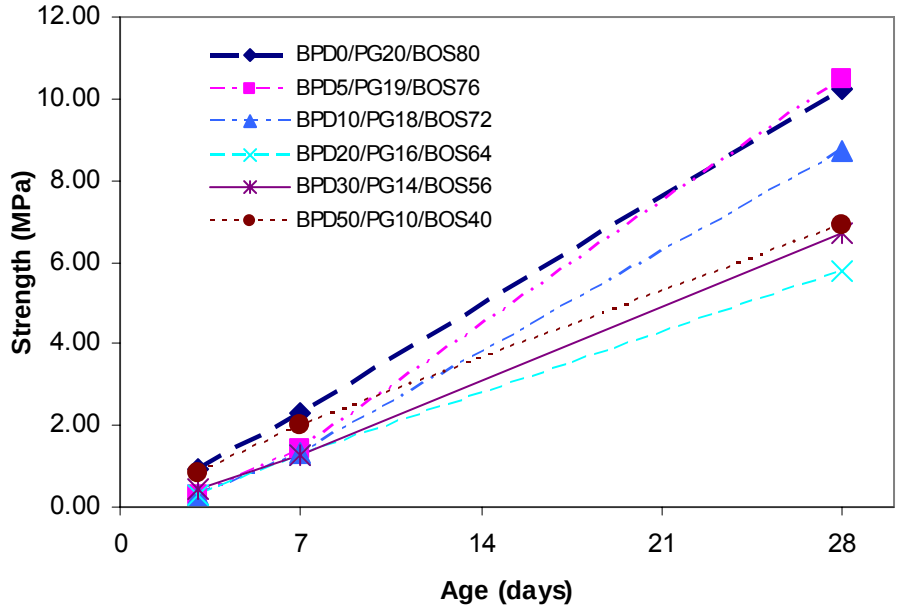

The effect of the amount of PG and BPD on binary and ternary combinations of PG-BOS and BPD-PG-BOS at different ages is shown in Figures 36 and 37 respectively. Figure 35 indicates the optimum percentage for PG in the binary combination is 20% and shows a dramatic decrease in strength when PG is increased from 20% to 60%.

The effect of BPD in the ternary system shown in Figure 37 is quite remarkable: the compressive strength fell by up to 50% as a result of increasing the BPD content from 5 to 20%. The strength improved slightly when the BPD content increased from 20% to 30%, and then remained the same for higher contents of BPD. The effect of BPD on the hydration and strength gain of ternary combinations is discussed in section 3.6.

According to the results for BPD-PG-BOS mixes, the highest compressive strength was for mix BPD5/PG19/BOS76. These results were subsequently modified to achieve the final optimum proportions.

Figure 36 Compressive strength of PG-BOS mixes versus PG content

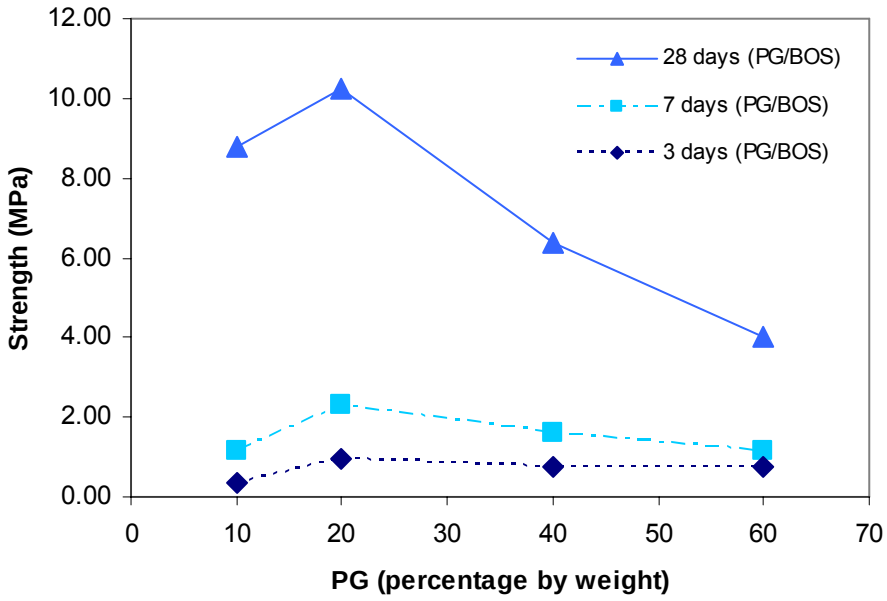

Figure 37 Compressive strength of BPD-PG-BOS mixes versus BPD content

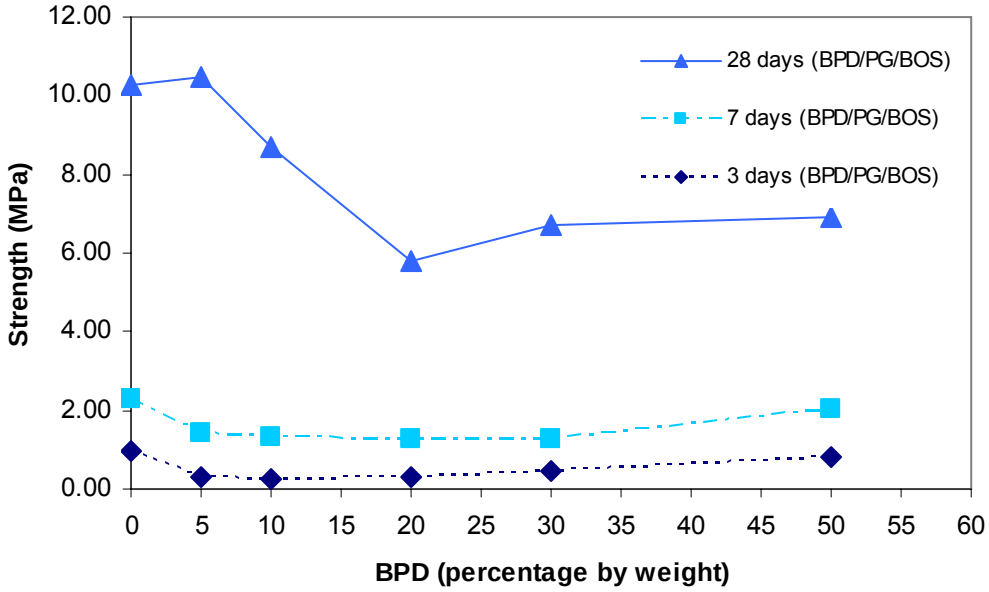

The role of PG in both binary and ternary systems is shown in Figure 38. In the ternary system, increasing the PG content up to 16% in the mix resulted in a reduction in compressive strength. However, a further increase in the amount of PG led to a considerable improvement in strength, with the maximum value of 10.5 MPa as the optimum in this particular combination (Table 24).

Figure 38 Compressive strength of PG-BOS and BPD-PG-BOS mixes versus PG content

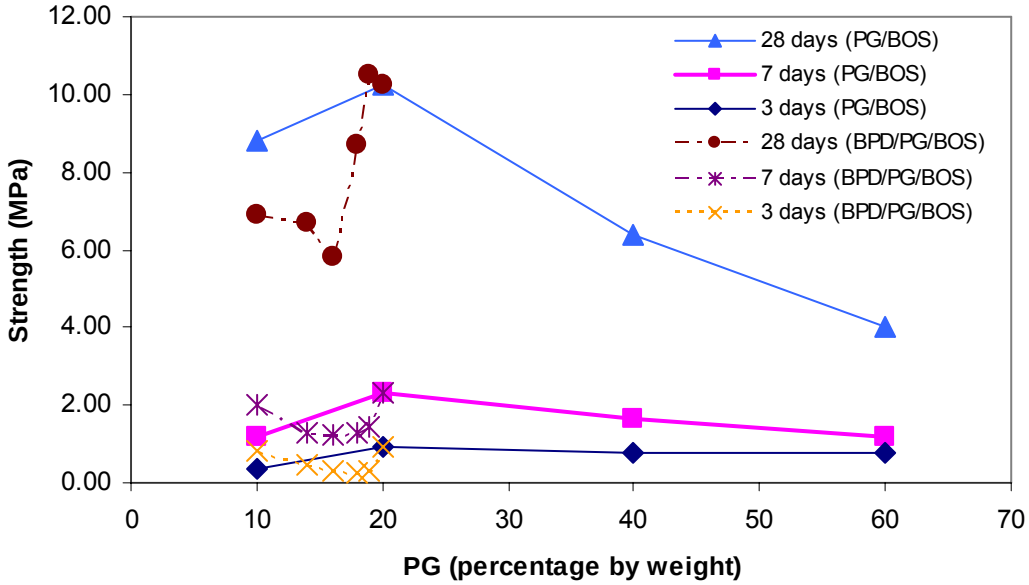

(c) BOS-PG-BPD mixture

In order to investigate all possible combinations of PG, BPD and BOS mixtures, the combination of PG-BPD was also considered. The results for compressive strength testing are shown in Table 25.

Table 25 Compressive strength of PG-BPD mixes*

Mix code	Strength at days (MPa)†			Flow (mm)	Density (kg/m^3)
	3	7	28		
PG10/BPD90	3.10	5.45	12.55	103	1970
PG20/BPD80	2.25	3.65	8.00	105	1930
PG40/BPD60	1.42	2.20	4.69	108	1910
PG60/BPD40	0.94	1.30	2.50	108	1730

* Figures 39 and 40 are derived from this table.

† Highlighted cell indicates the highest or optimum compressive strength achieved in the group.

As shown in Figures 39 and 40, the higher the BPD content, the higher the compressive strength. This is due to the cementitious properties of BPD, which acts as the main binder in this combination. However, as BPD is not considered a pozzolanic material, further reaction between gypsum and BPD will not take place.

Figure 39 Compressive strength development of PG-BPD mixes

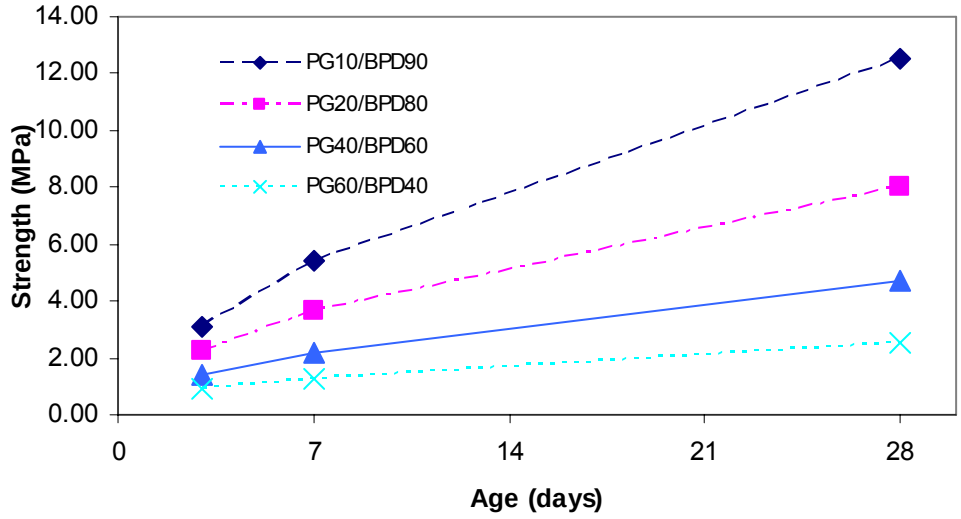

Figure 40 Compressive strength of PG-BPD mixes versus BPD content

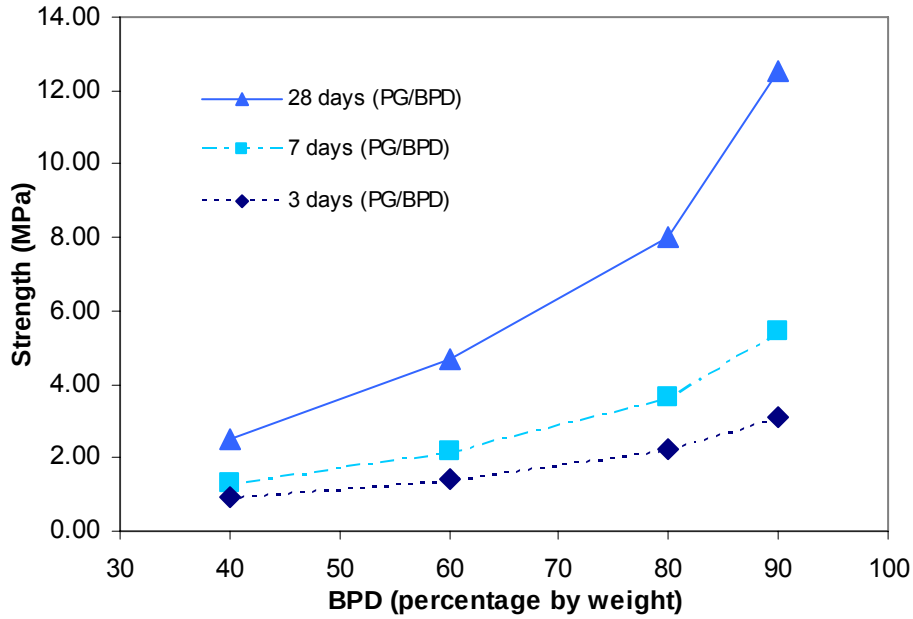

3.1.5 Fine tuning and comparison of combinations

The results of further paste mixes to finalise the optimisation of the ternary system of BOS, PG and BPD are presented in Table 26. Figure 41 shows the strength development of the above mixes.

The mix incorporating 80% BOS, 15% PG and 5% BPD achieved the highest compressive strength. It shows the acceptable potential of BOS as this mix contained a high quantity of BOS. A close look at results reveals the effect of BPD in the mix incorporating 18% BPD, 2% PG and 80% BOS, which resulted in an almost similar strength. This result indicates that the activating effect of BPD and PG on BOS correlates to the ratio of PG to BPD. The mechanism and parameters affecting the hydration of slag in the ternary system are discussed in section 3.6.

It was concluded that the optimum proportions of the ternary combination of PG, BPD and BOS is 15% PG, 5% BPD and 80% BOS. This blended mixture is referred to in this report as 'Coventry Binder'.

Table 26 Fine tuning of mixtures of PG, BPD and BOS – compressive strength*

Mix code	Strength at days (MPa)†			Flow (mm)	Density (kg/m^3)
	3	7	28		
BOS80/PG15/BPD5	0.28	0.59	10.80	162	2540
BOS85/PG10/BPD5	0.21	0.46	10.10	162	2550
BOS77/PG20/BPD3	0.26	0.54	9.10	158	2370
BOS80/PG5/BPD15	0.35	0.68	9.40	140	2630
BOS80/PG10/BPD10	0.29	0.78	7.00	148	2570
BOS80/PG12/BPD8	0.28	0.76	9.60	154	2580
BOS80/PG2/BPD18	0.41	0.65	10.50	124	2700

* Figure 41 is derived from this table.

† Highlighted cell indicates the highest or optimum compressive strength achieved in each group.

Figure 41 Fine tuning mixture of PG, BPD and BOS strength development – compressive strength

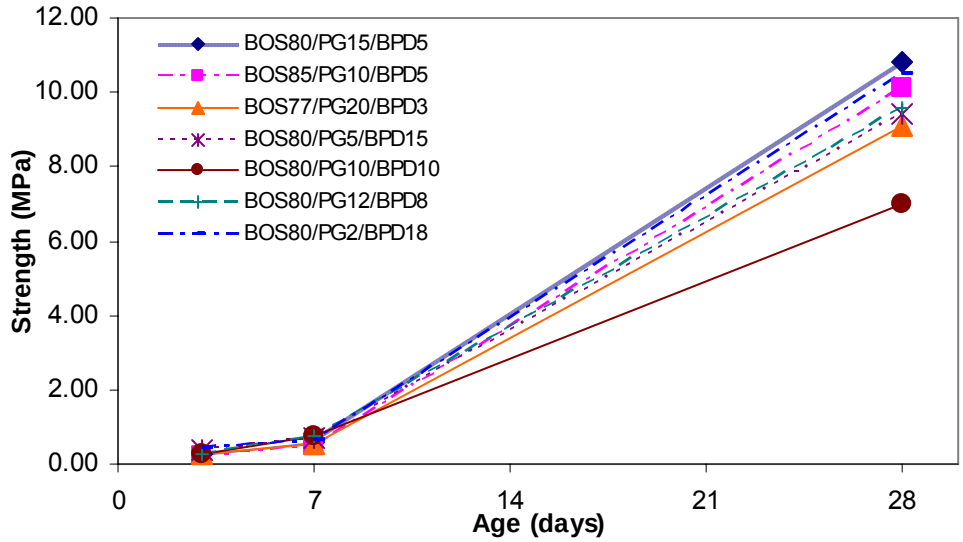

Figure 42 summarises the results for the compressive strength of various combinations of PG, BPD and BOS against PG content. This summary shows that:

- optimisation of the ternary system depends on the alteration of components selected in each step of the optimisation process;
- optimisation is a not a linear task and various combinations of material will not result in the same compressive strength; and
- the results can be improved by slight changes in proportions of materials to include those mixes that are not necessarily considered by following the linear optimisation method.
- the drop in strength for mixes with 10% PG (i.e. the double points for 10% PG, in figure 42) corresponds to mixes with same PG content but different amount of BOS and BPD. (BOS85/PG10/BPD5 and BOS80/PG10/BPD10) as summarised in Table 26. This shows the significant effect of minor changes in the amount of pozzolan and activators on compressive strength of mixes.

Figure 42 Compressive strength of various combinations of PG, BPD and BOS versus content

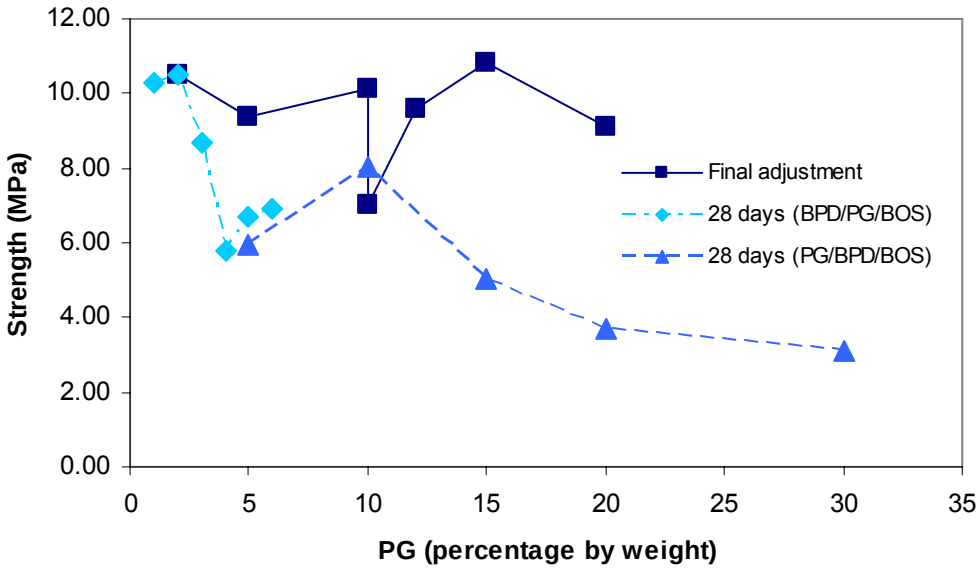

3.1.6 Semi-dry mixture of PG-BPD-BOS and PG-BPD-BOS-ROSA

The effects of water content and compaction on two selected mixtures of materials were then investigated. Mixes were made using various water-to-binder ratios, and compacted using a metal tamper to achieve the maximum possible compaction. Results of compressive strength testing are presented in Table 27.

Table 27 Compressive strength of semi-dry mixtures of PG-BPD-BOS and PG-BPD-BOS-ROSA

Mix code	Strength at days (MPa)*			Flow (mm)	Density (kg/m^3)	L/S
	3	7	28			
PG15/BPD5/BOS80-0.3	0.32	1.50	11.20	175	2030	0.30
PG15/BPD5/BOS80-0.2	1.11	2.83	20.10	0	2380	0.20
PG15/BPD5/BOS80-0.15	2.10	6.50	25.90	0	2490	0.15
PG15/BPD5/BOS80-0.13	5.10	12.80	30.55	0	2540	0.13
PG15/BPD5/BOS30/ROSA50-0.3	0.36	1.10	19.10	125	1100	0.30
PG15/BPD5/BOS30/ROSA50-0.25	0.62	1.18	21.50	0	1920	0.25
PG15/BPD5/BOS30/ROSA50-0.23	0.82	2.58	24.90	0	1920	0.23
PG15/BPD5/BOS30/ROSA50-0.19	0.98	2.60	26.60	0	1830	0.19
PG15/BPD5/BOS30/ROSA50-0.15	0.87	2.49	25.90	0	1880	0.15

* Highlighted cells indicate the highest or optimum compressive strength achieved in each group.

These results highlight the dramatic improvement in compressive strength of mixes which have low water content. It is generally accepted that a reduction in the amount of water will result in less pores and improved paste pore structure. In addition, less water in the system will affect the setting time of the mixture as the hydration product can fill the gaps between unreacted materials more quickly.

The highest achieved strength in this set of mixes was 30.55 MPa (Table 27), which is almost comparable with ordinary Portland cement. Figures 43 and 44 show the strength development of the mixes at different ages.

Figure 43 Compressive strength development of semi-dry PG-BPD-BOS with various L/S ratios

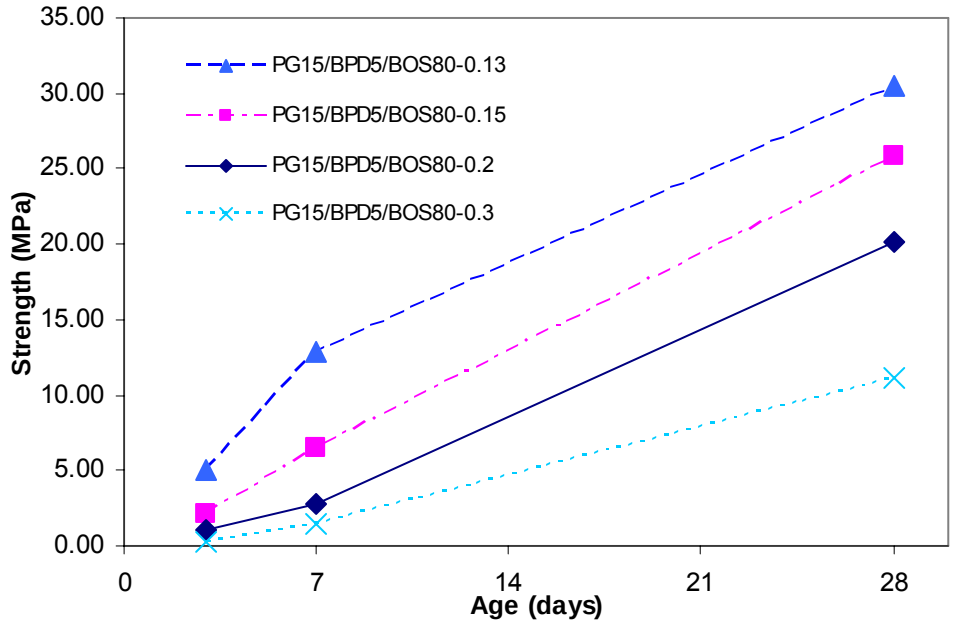

Figure 44 Compressive strength development of semi-dry PG-BPD-BOS-ROSA with various L/S ratios

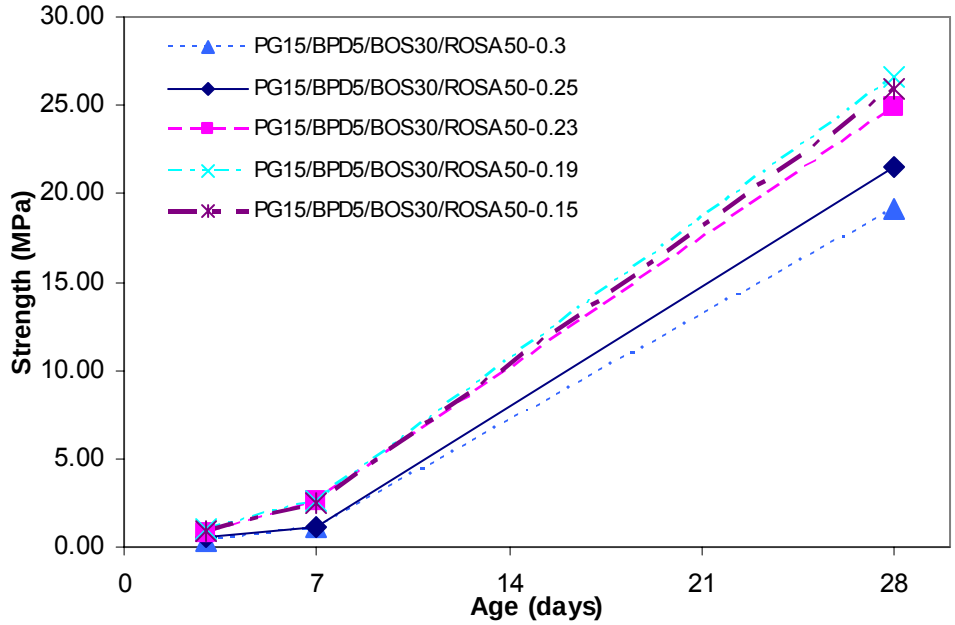

The mixture containing ROSA also showed satisfactory compressive strength (Figure 44). However, the water demand in the mix incorporating ROSA is higher than the mix without it.

The effect of water content on the compaction of semi-dry mixes together with compressive strength is shown in Figure 45.

Figure 45 Effect of L/B ratios on density and compressive strength of semi-dry pastes

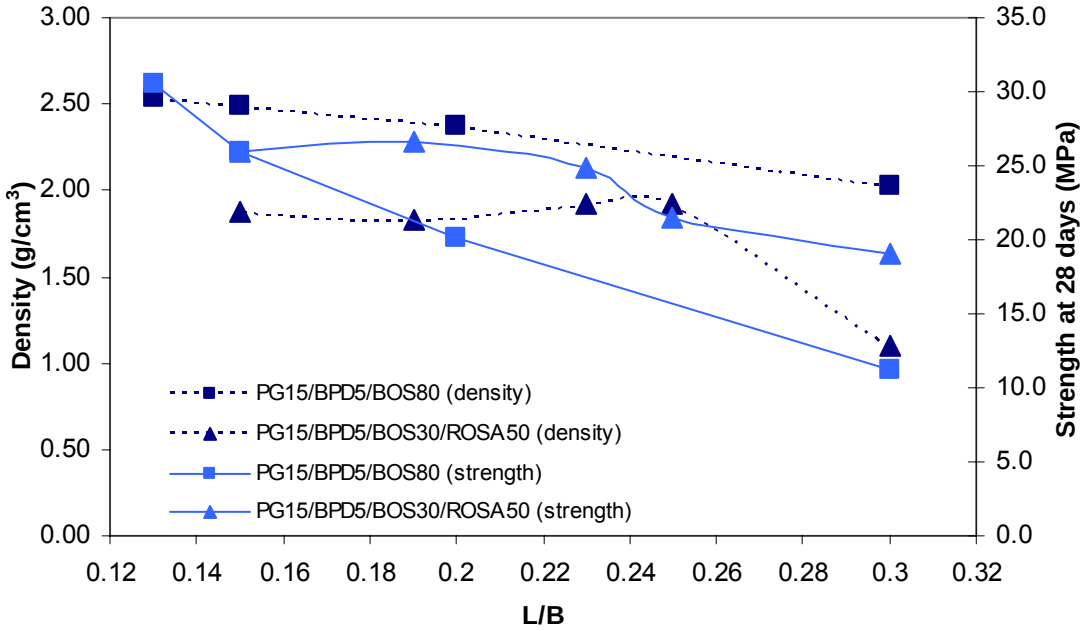

The highest compressive strength was found for the mix with 15%PG, 5% BPD and 80% BOS, and a water/binder (L/B) ratio of 0.13 (Figure 45). The increase in the density of this paste mix from 2 with an L/B ratio of 0.3 to 2.6 at an L/B of 0.13 (i.e. reduced water content) is important and emphasises the direct relationship of compressive strength with the density of the mix; in other words, the higher the compaction of the mix, the higher the compressive strength.

A close look at the results of density and compressive strength of the mix employing ROSA reveals the effect of water content on the compactibility of this mixture. Reducing the L/B ratio from 0.25 to 0.15 resulted in a lower density although the compressive strength rose slightly (Figure 45). From laboratory experience, mixes containing ROSA demand more water. Therefore, compaction of such mixes at very low water to binder ratio will not give a satisfactory finished surface that can be easily disturbed after compaction.

These results suggested that a semi-dry mixture of PG-BPD-BOS would be a strong choice for the site trials. Further combinations were investigated (see section 3.1.7) but these resulted in less compressive strength that this semi-dry mixture. Section 3.2 describes the results of investigations into the use of the blend PG15/BOS80/BPD5 (Coventry Binder) in roller-compacted concrete.

3.1.7 Further combinations of PG, BPD, BOS and ROSA

Various combinations were considered in order to investigate the potential of these pozzolanic and activating materials, and possible mixes with properties required. Tables 28–31 present the results of compressive strength testing at different ages. The strength development of the mixes is shown in Figures 46–49.

Table 28 Compressive strength of BPD-BOS-ROSA mixtures

Mix code	Strength at days (MPa)*			Flow (mm)
	3	7	28	
BPD5/BOS76/ROSA19	0.21	0.98	8.50	>250
BPD5/BOS50/ROSA45	0.48	2.50	11.50	152
BPD5/BOS27/ROSA68	0.56	1.20	8.30	123
BPD5/BOS15/ROSA80	0.78	2.35	7.90	83
BPD10/BOS72/ROSA18	0.24	1.70	8.16	155
BPD10/BOS35/ROSA55	0.87	4.23	14.70	132
BPD20/BOS64/ROSA16	0.21	1.80	6.80	143
BPD40/BOS48/ROSA12	0.26	0.80	5.10	134
BPD40/BOS30/ROSA30	0.25	0.90	10.50	130
BPD60/BOS32/ROSA8	0.31	0.77	4.46	125

* Highlighted cell indicates the highest or optimum compressive strength achieved in the group.

Table 29 Compressive strength of ROSA-BOS-BPD mixtures

Mix code	Strength at days (MPa)*			Flow (mm)
	3	7	28	
ROSA32/BOS8/BPD60	0.58	3.20	18.40	96
ROSA48/BOS12/BPD40	0.66	2.35	12.35	94
ROSA64/BOS16/BPD20	0.60	1.80	8.10	86
ROSA72/BOS18/BPD10	0.58	1.47	6.20	55

* Highlighted cell indicates the highest or optimum compressive strength achieved in the group.

Table 30 Compressive strength of BOS-ROSA-BPD mixtures

Mix code	Strength at days (MPa)*			Flow (mm)
	3	7	28	
BOS20/ROSA48/BPD32	0.25	2.0	13.0	115
BOS40/ROSA36/BPD24	0.37	2.0	14.6	126
BOS60/ROSA24/BPD16	0.28	1.9	13.6	150

* Highlighted cell indicates the highest or optimum compressive strength achieved in the group.

Table 31 Compressive strength of PG-BOS-ROSA mixtures

Mix code	Strength at days (MPa)*			Flow (mm)
	3	7	28	
PG5/BOS15/ROSA80	0.48	3.32	9.10	90
PG5/BOS76/ROSA19	0.22	0.84	8.90	>250
PG5/BOS50/ROSA45	0.45	2.10	13.40	136
PG8/BOS20/ROSA72	0.61	3.84	13.40	85
PG10/BOS30/ROSA60	0.47	2.38	18.60	95
PG10/BOS75/ROSA15	0.22	1.00	5.90	>250
PG12/BOS48/ROSA40	0.37	1.60	7.10	153
PG16/BOS64/ROSA20	0.43	1.10	11.50	>250
PG20/BOS35/ROSA45	0.51	1.70	15.50	130
PG30/BOS40/ROSA30	0.41	1.10	10.60	119

* Highlighted cell indicates the highest or optimum compressive strength achieved in the group.

Figure 46 Compressive strength development of BPD-BOS-ROSA mixtures

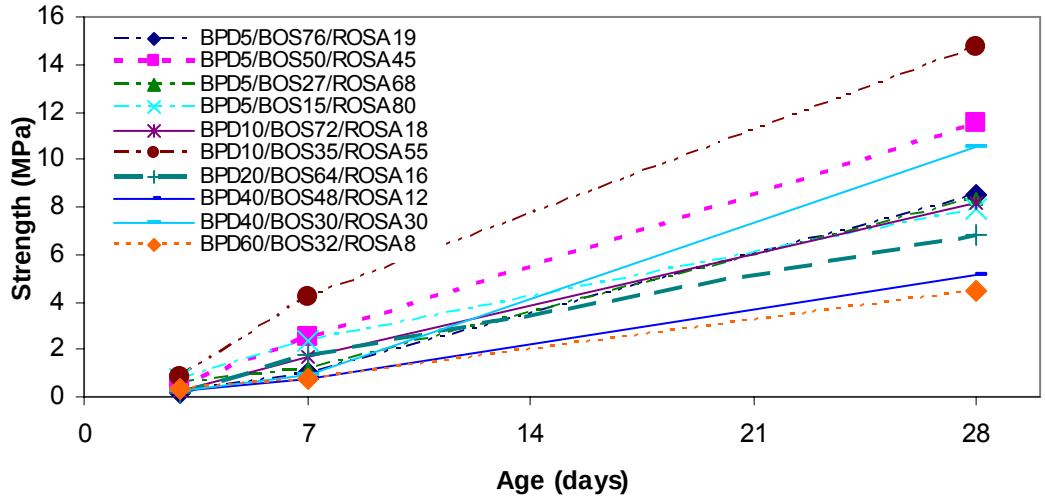

Figure 47 Compressive strength development of ROSA-BOS-BPD mixtures

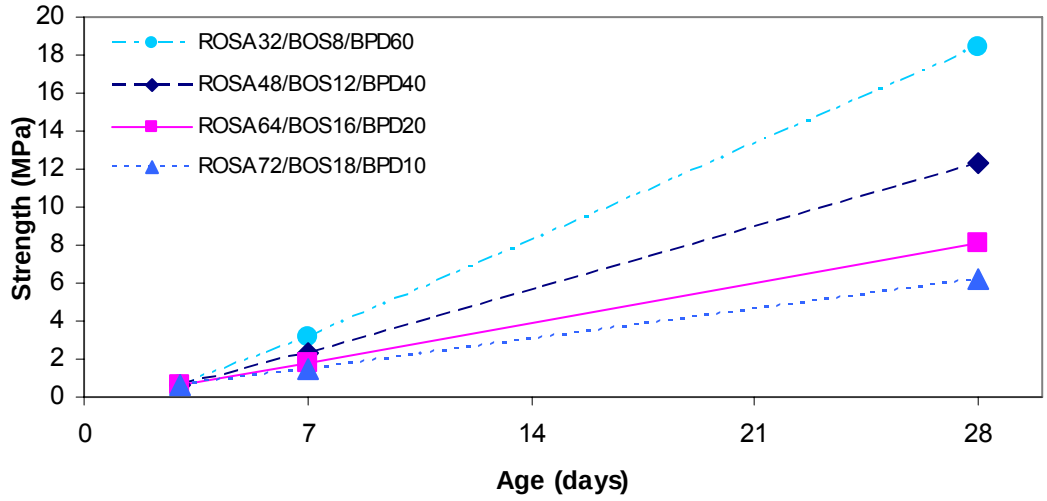

Figure 48 Compressive strength development of BOS-ROSA-BPD mixtures

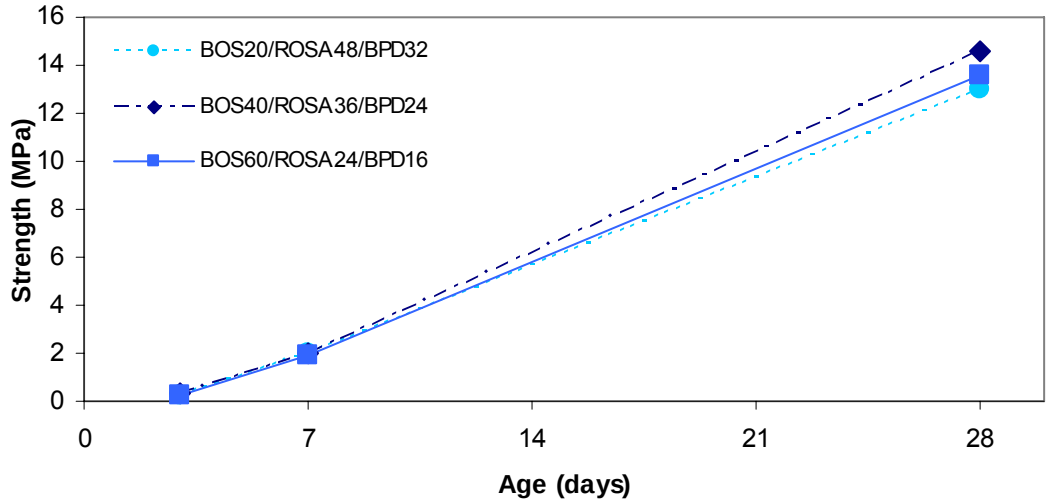

Figure 49 Compressive strength development of PG-BOS-ROSA mixtures

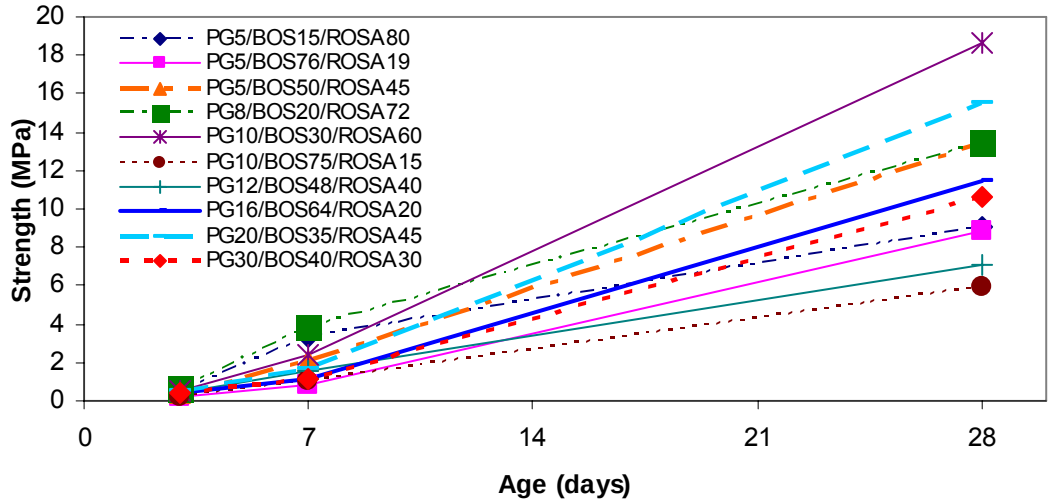

Compressive strength testing showed that combinations of pozzolanic materials such as BOS and ROSA with an activator such as PG or BPD can produce a binder with acceptable compressive strength at 28 days. However, results from mixes with a high BPD content may not be consistent due to variations in the chemical composition of this waste material.

The mixture of PG-BOS-ROSA without BPD still achieved an acceptable compressive strength at 28 days (Table 31). Mixes with a minimum amount of BPD were therefore proposed for the site trial because the variations caused by large quantities of BPD can be significant, affecting the strength and the long-term performance of the binder that develops. In addition, combinations of other sources of waste materials were investigated (see section 3.1.8).

3.1.8 Effect of lime and MKD on BOS, PG and ROSA mixtures

The effect of commercial hydrated lime and waste MKD from a lime kiln on the hydration of BOS and ROSA was investigated in binary and ternary mixtures of lime, BOS, ROSA and PG.

(a) Lime or MKD with BOS

A limited range of binary mixtures of hydrated lime or MKD with BOS were tested for compressive strength (Tables 32 and 33).

Table 32 Compressive strength of lime-BOS mixtures

Mix code	Strength at days (MPa)*			Flow (mm)	Density (kg/m^3)
	3	7	28		
Lime10/BOS90	0.04	0.17	0.49	>250	2120
Lime30/BOS70	0.24	0.33	1.06	167	1936
Lime50/BOS50	0.39	0.60	1.38	124	1832
Lime70/BOS30	0.58	0.76	1.18	89	1712

* Highlighted cell indicates the highest or optimum compressive strength achieved in the group.

Table 33 Compressive strength of MKD-BOS mixtures

Mix code	Strength at days (MPa)*			Flow (mm)	Density (kg/m^3)
	3	7	28		
MKD10/BOS90	0.05	0.17	0.55	>250	2000
MKD30/BOS70	0.07	0.18	0.63	172	2080
MKD50/BOS50	0.16	0.25	0.59	132	1984
MKD70/BOS30	0.22	0.27	0.49	93	1944

* Highlighted cell indicates the highest or optimum compressive strength achieved in the group.

The optimum amount of hydrated lime in the binary mixture of BOS-lime was 50%, resulting in a strength of 1.38 MPa (Table 32). At 28 days, 0.63 MPa was the highest strength for MKD-BOS binary mixtures which corresponded to 30% MKD (Table 33). Commercial hydrated lime, which is mainly calcium hydroxide, was thus more effective at activating the BOS than MKD, which consists primarily of calcium carbonate and calcium hydroxide.

Compressive strength development of lime-BOS and MKD-BOS mixes is shown in Figures 50 and 51. Although the mix incorporating 70% hydrated lime showed the highest strength at 7 days, the mixture of 50% lime and 50% BOS achieved the optimum strength in the binary system at 28 days (Figure 50). The same trend was observed in the binary system of MKD-BOS where the mix incorporating 30% MKD and 70% BOS achieved the highest compressive strength (Figure 51). This is due to the long-term pozzolanic reaction of BOS with calcium hydroxide in MKD and hydrated lime. The higher early strength of these mixes is due to formation of calcium carbonate once the calcium hydroxide present had been exposed to atmospheric carbon dioxide.

Figure 50 Compressive strength development of lime-BOS mixtures

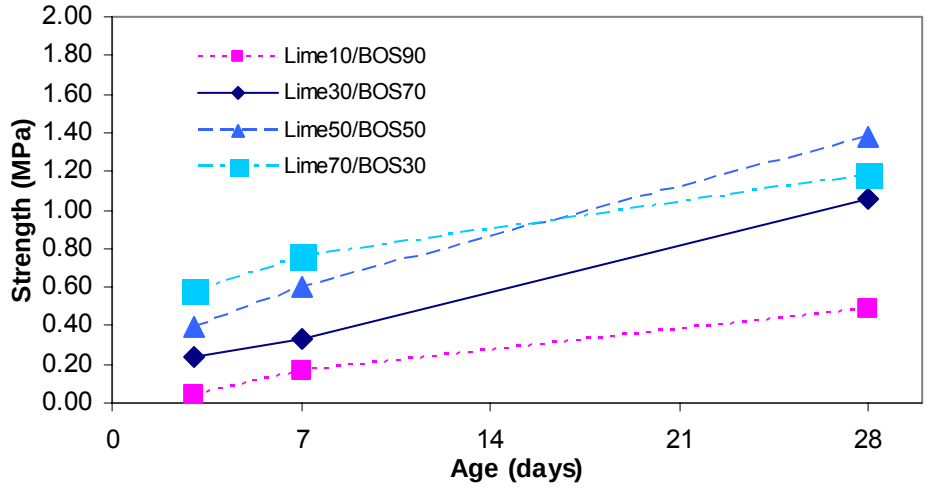

Figure 51 Compressive strength development of MKD-BOS mixtures

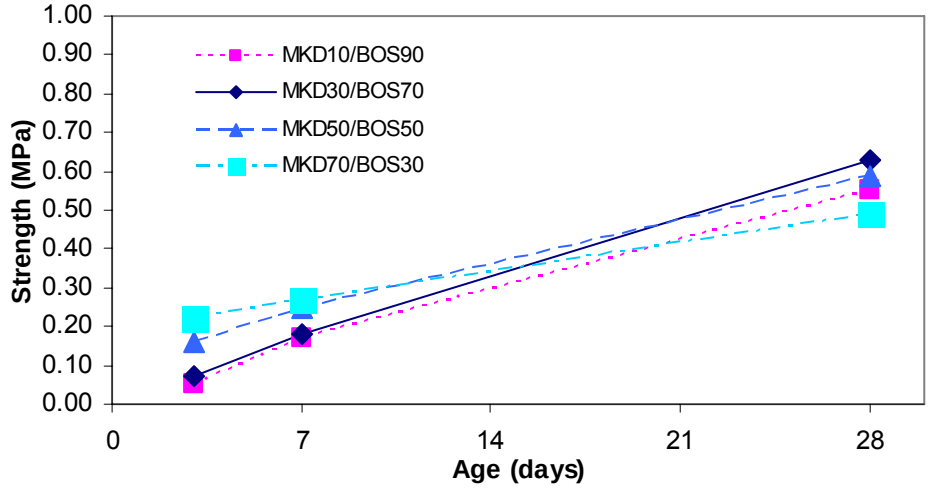

Figure 52 uses data from Tables 32 and 33 to present a comparison of the binary systems BPD-BOS and the lime/MKD-BOS mixes. BPD was more efficient at reacting with BOS to form a cementitious gel. This is partly because of the cementitious properties of BPD itself (phases such as C3S and C2S present in the BPD are mainly responsible for this phenomenon).

Figure 52 Comparison of the compressive strength of lime/MKD/BPD-BOS mixtures versus lime/MKD/BPD content

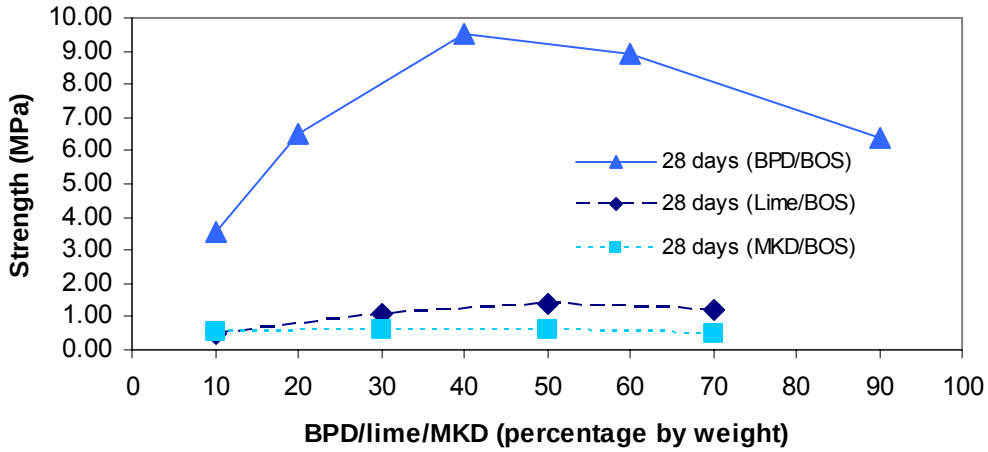

(b) Lime or MKD with ROSA

Tables 34 and 35 present the compressive strength of mixtures incorporating ROSA. The optimum amount of hydrated lime in lime-ROSA and MKD-ROSA mixtures was 50%, corresponding to the strength of 3.23 and 2.84 MPa respectively. Hydrated lime was more efficient in activating ROSA, although the compressive strength in both mixes was almost similar.

Table 34 Compressive strength of lime-ROSA mixtures

Mix code	Strength at days (MPa)*			Flow (mm)	Density (kg/m^3)
	3	7	28		
Lime10/ROSA90	0.21	0.49	1.12	130	1552
Lime30/ROSA70	0.31	0.50	2.68	114	1576
Lime50/ROSA50	0.24	0.45	3.23	95	1592
Lime70/ROSA30	0.48	0.71	2.21	87	1598

* Highlighted cell indicates the highest or optimum compressive strength achieved in the group.

Table 35 Compressive strength of MKD-ROSA mixtures

Mix code	Strength at days (MPa)*			Flow (mm)	Density (kg/m^3)
	3	7	28		
MKD10/ROSA90	0.26	0.46	0.90	142	1512
MKD30/ROSA70	0.21	0.41	1.58	124	1592
MKD50/ROSA50	0.16	0.32	2.84	98	1616
MKD70/ROSA30	0.09	0.21	2.70	94	1620

* Highlighted cell indicates the highest or optimum compressive strength achieved in the group.

Figures 53 and 54 show the strength development of lime-ROSA and MKD-ROSA mixes respectively. In the mix incorporating 90% ROSA and 10% lime, the amount of activator was insufficient to release the pozzolanic potential of ROSA. In contrast, in the mix employing 50% lime, the rate of strength gain increased at 7 days and it showed the highest strength in this binary system (Figure 53).

Figure 53 Compressive strength development of lime-ROSA mixtures

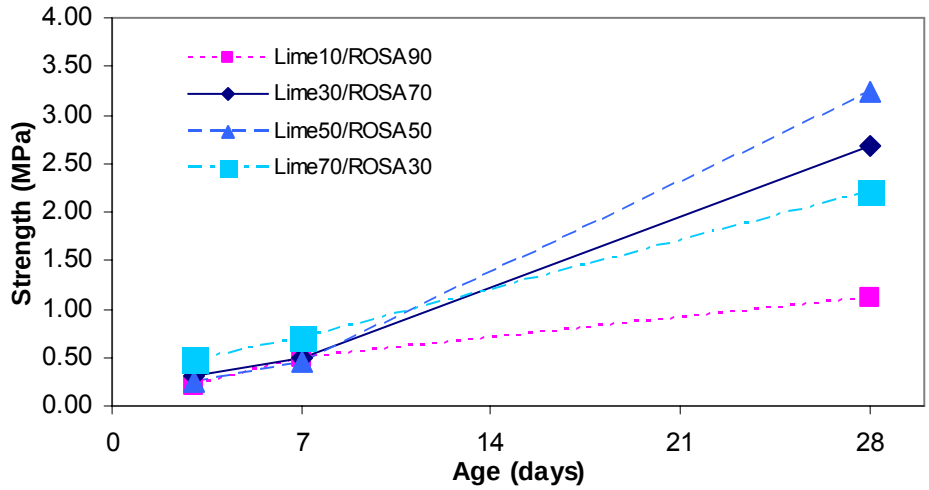

In MKD-ROSA mixtures, the strength of the mixes incorporating 50% and 70% MKD showed almost similar compressive strength (Figure 53). This phenomenon could be because, within an optimum range, the presence of more calcium hydroxide leads to more activation of pozzolanic materials.

Figure 54 Compressive strength development of MKD-ROSA mixtures

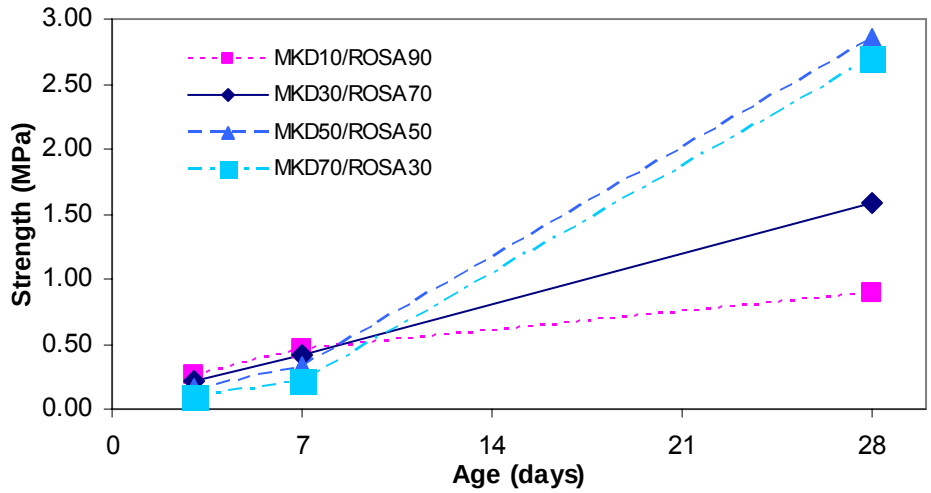

Figure 55 used data from Tables 34 and 35 to present a comparison of binary mixtures of BPD-ROSA with the lime/MKD-ROSA mixtures. The mixture incorporating BPD achieved much a higher compressive strength compared with those made with hydrated lime and MKD. This result is similar to those achieved with binary combinations of BPD-BOS. As mentioned previously, this could be due to cementitious compounds present in BPD resulting in formation of more cementitious matrix within 28 days.

Figure 55 Comparison of the compressive strength of lime/MKD/BPD-ROSA mixtures versus lime/MKD/BPD content

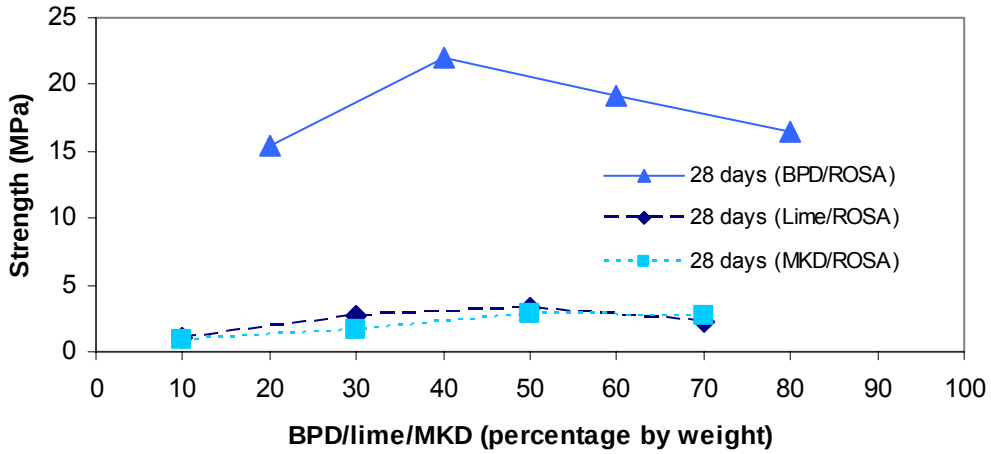

(c) Lime and MKD to replace BPD

In order to compare the effect of hydrated and MKD waste lime in mixtures containing PG using the optimum proportions of PG-BOS-BPD and PG-BOS-ROSA-BPD obtained previously, the BPD content was replaced by commercial hydrated lime and MKD. In addition, two ternary mixes incorporating ROSA, PG and lime/MKD were made to investigate the effect of lime on the activation of ROSA in presence of PG. Table 36 presents the results of compressive strength testing of these mixes.

Table 36 Compressive strength of PG-BOS-ROSA mixture

Mix code	Strength at days (MPa)*			Flow (mm)	Density (kg/m^3)
	3	7	28		
BOS80/PG15/Lime5	0.18	0.52	1.70	114	2168
BOS80/PG15/MKD5	0.12	0.31	1.02	152	1976
BOS30/ROSA50/PG15/Lime5	0.64	2.54	10.56	108	1888
BOS30/ROSA50/PG15/MKD5	0.16	0.22	0.79	118	1832
ROSA75/PG15/MKD10	0.42	0.97	9.51	110	1632
ROSA65/PG15/MKD20	0.68	1.05	12.30	94	1752

* Highlighted cell indicates the highest or optimum compressive strength achieved in the group.

The replacement of BPD with hydrated lime or MKD resulted in very low strength (1.7 MPa) compared with when BPD was used (10.8 MPa) (Table 24). In addition, the mix containing MKD showed less strength than the mix containing hydrated lime. A similar trend was observed in mixes made with ROSA when BPD was replaced by lime or MKD (Figure 56).

Figure 56 Compressive strength development of MKD/lime, BOS, ROSA and PG mixtures

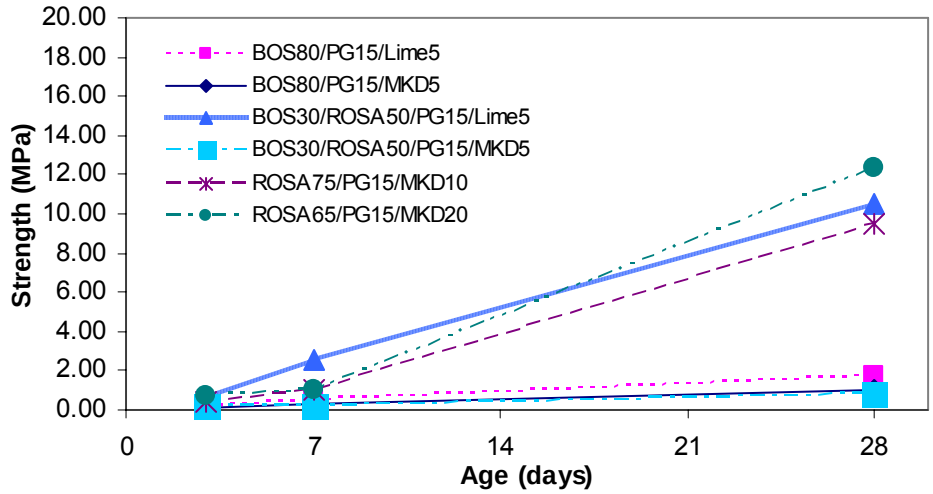

However, the ternary mixture of ROSA-PG-MKD showed that, with the same amount of PG, replacing BOS and lime with ROSA and MKD results in similar compressive strength. In other words, the efficiency of 30% BOS and 5% lime is about the same as 25% ROSA and 5% MKD. This implies that more calcium hydroxide is needed to activate the same amount of BOS compared with ROSA in order to achieve the same compressive strength.

Figures 57 and 58 show the comparison of the replacement of BPD with hydrated lime and MKD in the BOS-PG-BPD and BOS-ROSA-PG-BPD mixtures respectively. Replacement of BPD with hydrated lime or MKD in the ternary system BOS-PG-BPD resulted in less compressive strength (Figure 57). The comparison also revealed that the lime and BKD do not have a similar efficiency in terms of activation of BOS; lime is less efficient than BKD resulting in a lower compressive strength.

The efficiency of hydrated lime in the BOS-ROSA-PG mixture was higher than MKD, but they both suffer from a lack of efficiency compared with BPD. The compressive strength fell by about 50% when BPD was replaced with hydrated lime (Figure 58). The mix incorporating MKD as a replacement for BPD showed the lowest compressive strength of 0.79 MPa after 28 days (Table 36).

Figure 57 Comparison of the replacement of BPD with lime and MKD in BOS-PG-BPD mixtures

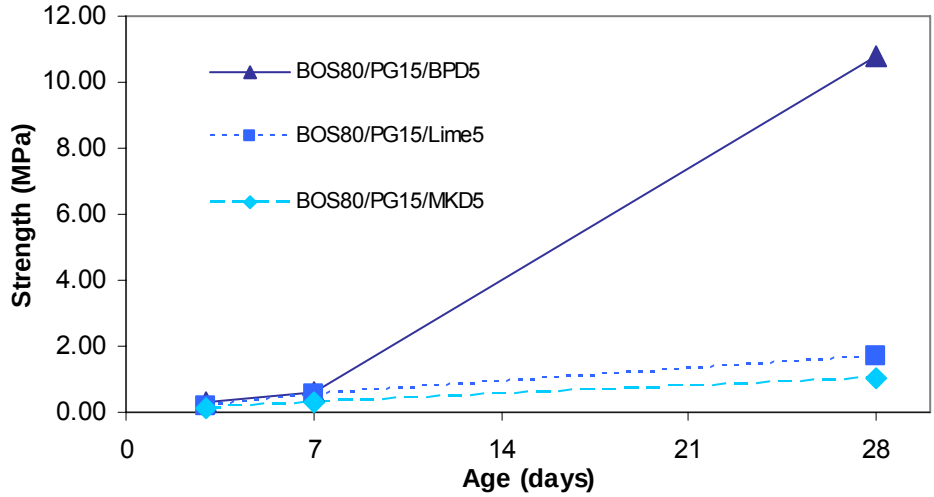

Figure 58 Comparison of the replacement of BPD with lime and MKD in BOS-ROSA-PG-BPD mixtures

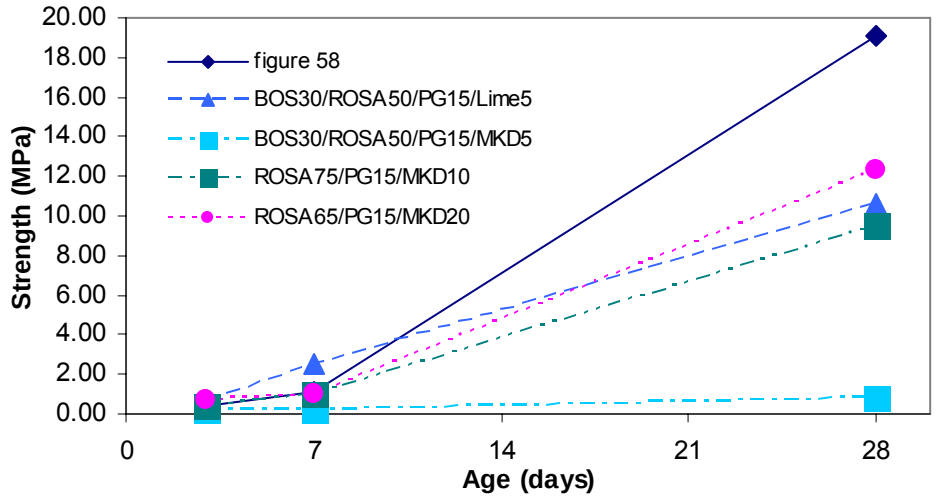

3.1.9 Long-term compressive strength of BOS, PG, BPD and ROSA mixtures

Table 37 presents the results of compressive strength of paste mixtures containing PG, BOS, ROSA and BPD up to 90 days. The strength results of this group of paste mixtures up to 28 days are discussed in section 3.1.5. In some mixtures, the compressive strength increased by up to 60% after 90 days moist curing. This demonstrates the intrinsic potential of BOS and ROSA to form a hydrated cementitious matrix in presence of sufficient alkali.

Table 37 Long-term compressive strength of PG, BOS, ROSA and BPD paste mixtures

Mix code	L/S	Strength at days (MPa)				Flow (mm)	Density (kg/m^3)
		3	7	28	90		
BOS80/PG15/BPD5	0.30	0.28	0.59	10.80	16.52	162	2540
BOS85/PG10/BPD5	0.30	0.21	0.46	10.10	15.70	162	2550
BOS77/PG20/BPD3	0.30	0.26	0.54	9.10	13.64	158	2370
BOS80/PG5/BPD15	0.30	0.35	0.68	9.40	16.10	140	2630
BOS80/PG10/BPD10	0.30	0.29	0.78	7.00	12.20	148	2570
BOS80/PG12/BPD8	0.30	0.28	0.76	9.60	11.80	154	2580
BOS80/PG2/BPD18	0.30	0.41	0.65	10.50	16.10	124	2700
BOS80/PG15/BPD5(semi-dry)	0.13	5.10	12.80	30.55	38.35	Semi-dry	2540
BOS30/ROSA50/PG15/BPD5(semi-dry)	0.19	0.98	2.60	26.60	42.10	Semi-dry	1830

As shown in Figure 59, the compressive strength of the paste mixes developed rapidly up to 28 days and then at a slower pace up to 90 days. In paste mixtures with a L/S ratio of 0.3, the highest strength was obtained with the mix incorporating 80% BOS, 15% PG and 5% BPD at both 28 and 90 days. But for semi-dry mixes, the mix incorporating ROSA showed a higher strength gain after 90 days. This result revealed the superior performance of combining ROSA and BOS, which is caused by faster reaction of ROSA to form pozzolanic calcium silicate hydrate (CSH) gel. It can also be postulated that the mix made without ROSA could reach the same level of strength after a longer period of curing. The rate of strength gain in all PG-BOS-BPD mixtures was almost similar (55% from 28 days to 90 days age).

Figure 59 Long-term compressive strength development of PG, BOS, ROSA and BPD mixtures

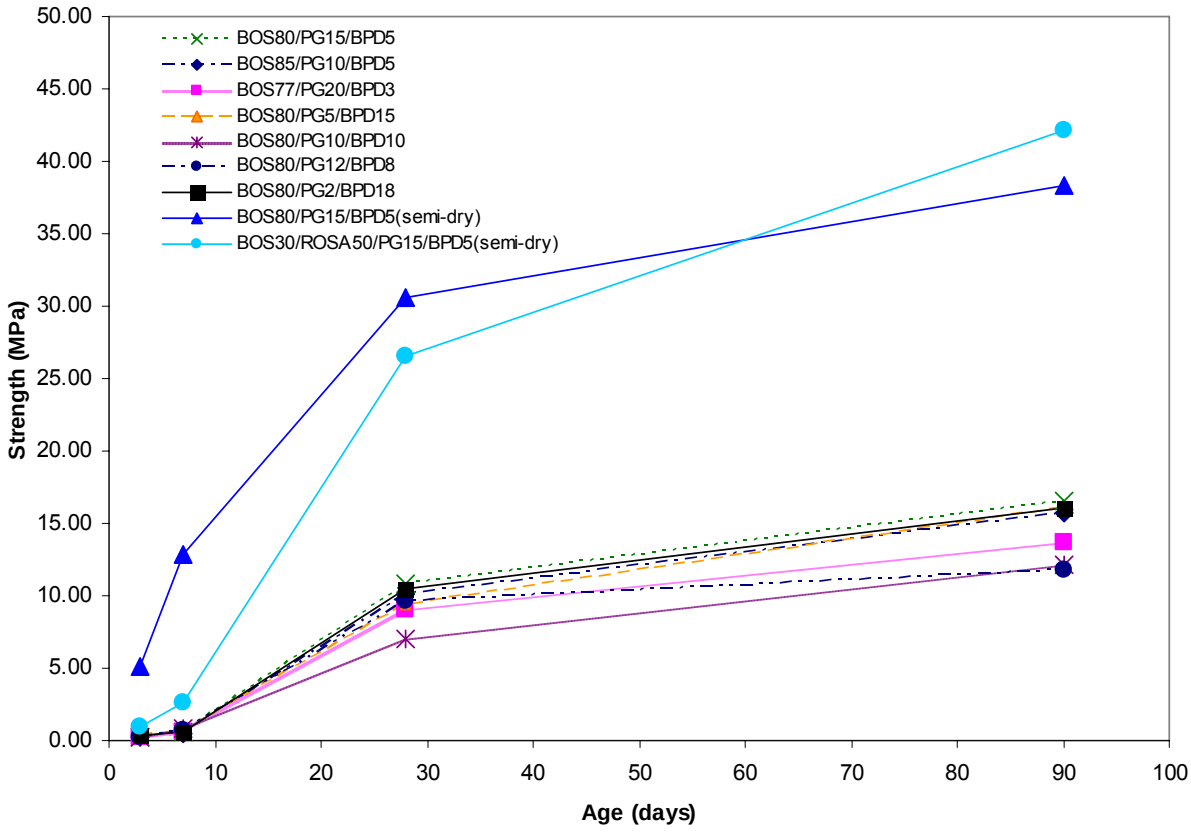

To evaluate the effect of longer periods of curing on the compressive strength of paste mixtures, a group of PG-CKD-BOS mixtures was tested at a curing age of 360 days under the standard curing conditions (Table 38).

Table 38 Long-term compressive strength of PG-CKD-BOS mixtures

Mix code	L/S	Strength at days (MPa)				Flow (mm)	Density (kg/m^3)
		3	7	28	360		
PG15/CKD5/BOS80-0.2	0.20	0.43	1.50	7.68	31.40	78	1970
PG15/CKD5/BOS80-0.25	0.25	0.37	1.10	5.65	30.27	145	2060
PG15/CKD5/BOS80-0.3	0.30	0.22	0.87	4.15	23.07	191	1890
PG15/CKD5/BOS80-0.4	0.40	0.15	0.39	2.49	12.15	High	1790

There was a four- to five-fold increase in the strength of paste mixtures at 360 days compared with the 28-day test results. This reveals the considerable potential of BOS to form a strong cementitious matrix as well as the slow reacting nature of this pozzolanic material even in presence of activators such as gypsum and alkalis.

The effect of L/S ratio on long-term compressive strength of PG-CKD-BOS mixes is shown in Figure 60. The rate of strength gain increased when the L/S ratio decreased from 0.4 to 0.2; in other words, the lower the water content in the mix, the higher pace of strength gain in the paste mixtures. This could be due to less voids forming in the cementitious structure of the samples available to be filled by the increasing amount of pozzolanic product in the longer period of curing. The highest strength in this group of mixes was for the mix made with a L/S ratio of 0.2.

Figure 60 Long-term compressive strength development of PG-CKD-BOS paste mixtures (50 mm cubes)

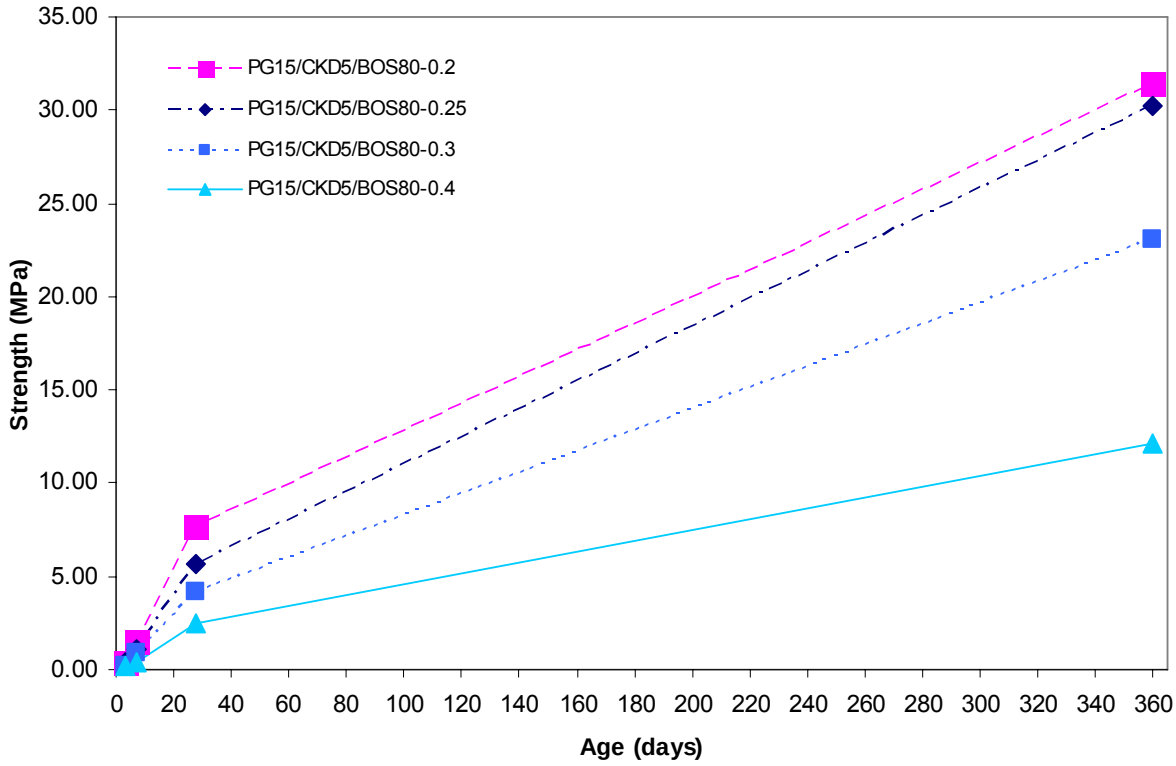

3.2 Concrete mixes

Concrete mixes were developed according to the optimised proportions obtained from paste mixtures described above. The effect of workability was investigated by employing two different types of superplasticisers.

As shown with the semi-dry paste mixtures, water content plays a major role in the strength of pastes and concretes. It was therefore proposed to use the minimum amount of water in the concrete mixes. The low proportion of water resulted in concrete with a very low or even zero slump.

The compressive strength of concrete is linked directly with the level of compaction. Therefore, concrete with zero slump should be compacted in different ways from conventional methods in which a vibrating table is used. These types of concretes are known as roller-compacted concrete (RCC) and usually contain low proportions of cement.

Due to the use of slow-reacting cementitious novel binder materials in this project, the 'binder content' was kept at a normal amount of 380 kg/m^3. Compaction for 150-mm cube moulds was carried out using a hammer drill and attached plate. The results of compressive strength testing of the various concrete mixes are presented in Table 39 (all results have been converted to the strength for 150-mm standard cubes).

Figure 61 shows the strength development of concrete mixes made using proportions obtained from candidate paste mixes incorporating PG, BPD and BOS. Using recycled aggregate (RA) resulted in considerably less compressive strength compared with those mixes made with natural aggregates and the same water content.

This suggests that the weakest link in the concrete that developed was the interface between the cementitious matrix and the aggregate. As the binder was made of slow-reacting pozzolanic materials (mainly BOS), the bond between the aggregate and the paste was not strong enough to resist the tension.

The amount and type of aggregate plays a major role in the ultimate compressive strength of a concrete mix. The recycled aggregate used contained some asphalt and fine clay or silt, which had a detrimental affect on the matrix aggregate interface, thereby reducing the ultimate strength of the concrete. To cope with the problem of concrete with low strength, increasing the workability of mixes using superplasticiser (SP) was considered.

Using superplasticiser to increase the flow of the concrete had a beneficial effect on compressive strength (Tables 39 and 40).

Two types of superplasticiser – sulphonate base and polymer base – were used in this study. The sulphonate chains of conventional superplasticisers carry a high anionic charge and are immediately adsorbed onto the surface of the cement particles, rendering them negatively charged. However, the adsorbed sulphonate chains are overlapped rapidly by crystals developed during the hydration of the cement; the consequence is early loss of the superplasticising action. In contrast, the new generation polymer superplasticisers have anionic carboxylic groups and long polyethylene chains. After the addition of the superplasticiser to concrete, its anionic main chain is adsorbed onto the positively charged surface of the cement particles whereas the side chains induce a steric repulsion effect between the cement particles. This repulsive force means that maximum dispersibility is attained and agglomeration can be avoided.

In this research the polymer superplasticiser (PSP) was found to be more efficient than ordinary superplasticiser (SP) in increasing the flow of the mix, but appeared to have a negative effect on the compressive strength of the concrete (Figures 61 and 62). This might be due to the retarding effect of this type of superplasticiser on the blended binder. Moreover, it would impose an extra cost when using this type of concrete made with waste materials.

Table 39 Compressive strength of PG/BPD/BOS concrete mixes developed

Mix code	Strength at days (MPa)*			Slump (mm)	Density (kg/m^3)	L/B
	3	7	28			
PG15/BPD5/BOS80 (SP)	1.19	1.67	7.65	10	2380	0.40
PG15/BPD34/BOS51	1.45	1.99	7.29	10	2300	0.40
PG15/BPD5/BOS80 (PSP)	0.76	1.08	6.60	180	2400	0.40
PG15/BPD5/BOS80 (RA-PSP)	1.02	1.89	5.67	20	2310	0.40
PG15/BPD5/BOS80 (PPG-PSP)	0.29	0.80	3.06	160	2400	0.40
PG15/BPD5/BOS80 (RA-PPG-PSP)	0.01	0.52	1.83	40	2270	0.40
PG15/BPD5/BOS80 (RA-RCC)	0.96	2.02	10.80	0	2390	0.25

* Highlighted cell indicates the highest or optimum compressive strength achieved in the group.
SP = superplasticiser
PSP = polymer superplasticiser
RA = recycled aggregate
PPG = processed plasterboard gypsum
RCC = roller-compacted concrete

Table 40 Compressive strength of PG/BPD/BOS/ROSA concrete mixes developed

Mix code	Strength at days (MPa)*			Slump (mm)	Density (kg/m^3)	L/B
	3	7	28			
PG15/BPD5/BOS60/ROSA20	0.61	1.03	5.49	0	2310	0.40
PG10/BPD5/BOS32/ROSA53 (SP)	0.79	1.62	10.98	120	2440	0.40
PG15/BPD5/BOS30/ROSA50 (RA-PSP)	0.58	1.28	9.27	30	2250	0.40
PG15/BPD5/BOS30/ROSA50 (RA-RCC)	1.23	2.20	12.30	0	2310	0.30

* Highlighted cell indicates the highest or optimum compressive strength achieved in the group.
SP = superplasticiser
PSP = polymer superplasticiser
RA = recycled aggregate
RCC = roller-compacted concrete

Figure 61 Compressive strength development of concrete mixes of PG-BPD-BOS

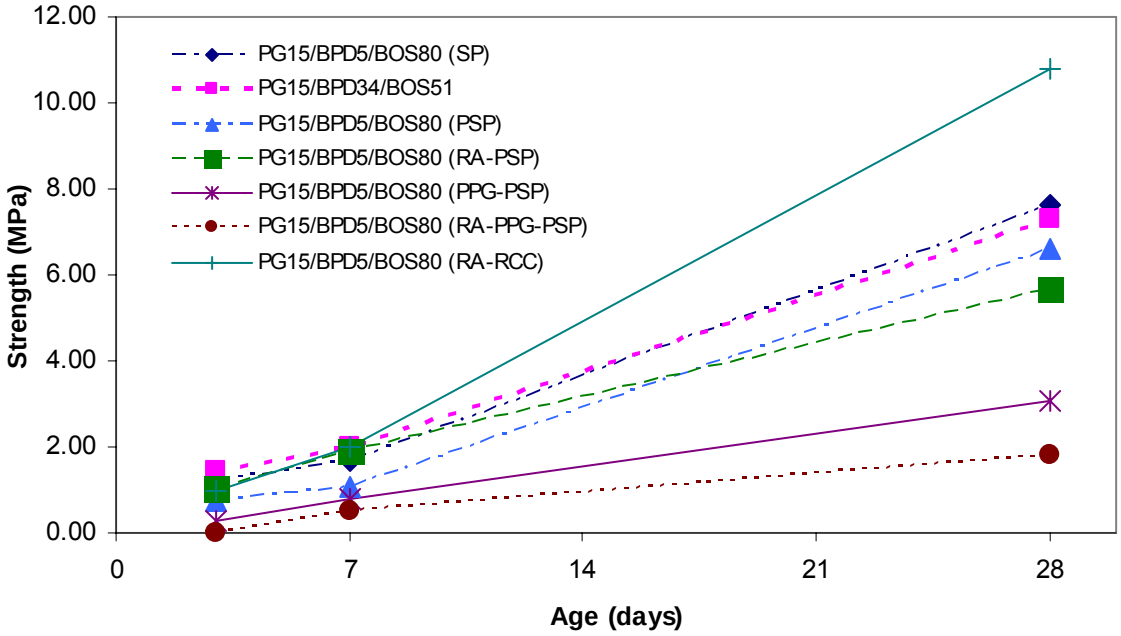

Use of roller-compacted concrete with a minimum amount of water was therefore proposed. Mixes with RCC gave the highest compressive strength; although the compressive strength at early ages was not high, an acceptable compressive strength was achieved in the long run. This mix was chosen for the site trial to be used as sub-base layer in the car park area (see section 4).

Figure 62 shows the results obtained for concrete mixes made with binder incorporating ROSA. The compressive strength development of concrete using plasterboard gypsum, BOS, ROSA and BPD shows clearly the slow-reacting nature of this type of binder. However, the ultimate compressive strength of the mix was acceptable and it was considered as an option for the site trial. But as described in section 3.1.6, the highest compressive strength of semi-dry paste was for the mixture of 15% PG, 5% BPD and 80% BOS (Table 27). In addition, limitations in materials preparation meant that the mixture with fewer different materials was preferred. This mixture is referred to as the Coventry Binder.

Figure 62 Compressive strength development of concrete mixes of PG-BPD-BOS-ROSA

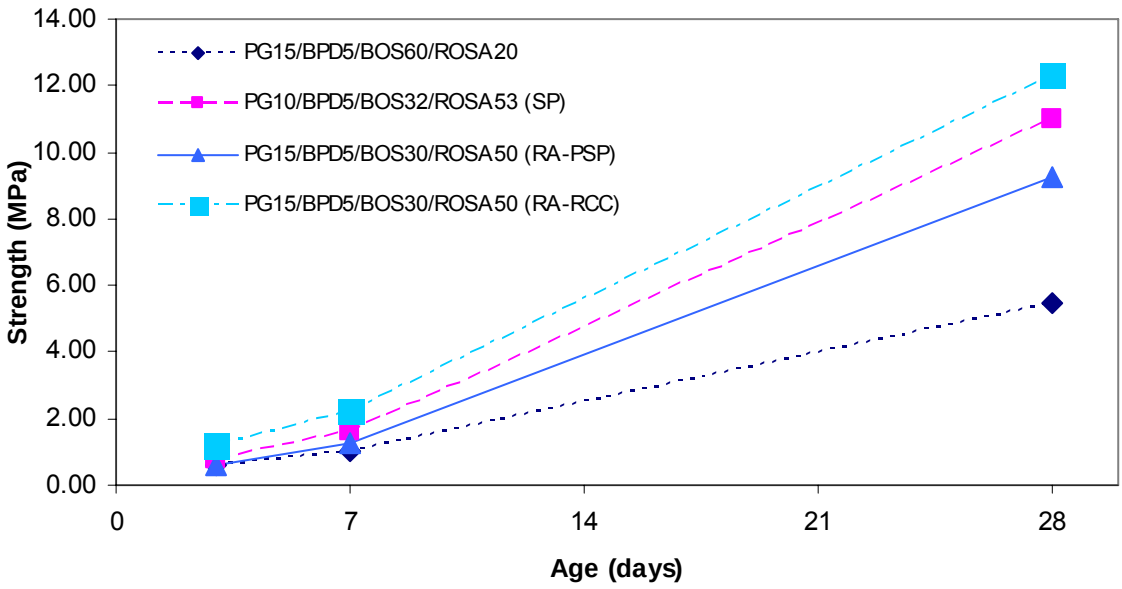

3.3 Soil stabilisation

The recommendations of the Transport Research Laboratory (TRL) Road Note 31 [18] for strength requirements of cement and lime stabilised sub-base and base materials are summarised in Table 41. The seven-day strength of stabilised soil using 50% by weight of the Coventry Binder is within the recommended range of strength for a sub-base layer. Furthermore, the seven-day strength of stabilised soil using 60% by weight of Binder-B is within the recommended range of strength for sub-base and base layers.

Table 41 Recommended strength of cement and lime stabilised sub-base and base materials [18]

Type	Soil unconfined compressive cube strength at 7 days (MPa)
Stabilised base (CB 1)	3.0–6.0
Stabilised base (CB 2)	1.5–3.0
Stabilised sub-base	0.75–1.5

Tables 42 and 43 present the compressive strength results of two different soils (Soil-A and Soil-B) stabilised with two types of novel binders (Binder-A and Binder-B).

Soil-A is sandy clay and Soil-B is silty sand (see section 2.4.2). Binder-A is mix PG15/BPD5/BOS80 (Coventry Binder) and Binder-B is mix PG15/BPD5/BOS50/ROSA30.

Table 42 Compressive strength of stabilised Soil-A with various amounts of Coventry Binder and Binder-B

Mix code	Strength at days (MPa)*		Dry density (kg/m^3)
	7	28	
Unstabilised Soil-A	0.19	0.11	1820
Soil-A 80/Binder-A 20	0.67	1.56	1900
Soil-A 60/Binder-A 40	0.82	1.86	1940
Soil-A 50/Binder-A 50	1.14	3.75	1970
Soil-A 40/Binder-A 60	1.22	4.45	2010
Soil-A 40/Binder-B 60	2.16	10.80	1890

* Highlighted cell indicates the highest or optimum compressive strength achieved in the group.

Table 43 Compressive strength of stabilised Soil-B using various amounts of Coventry Binder*

Mix code	Strength at days (MPa)*		Dry density (kg/m^3)
	7	28	
Unstabilised Soil-B	0.21	0.13	1800
Soil-B 80/Binder-A 20	1.07	2.80	1900
Soil-B 60/Binder-A 40	1.21	3.40	1950
Soil-B 50/Binder-A 50	1.43	5.98	1990

* Highlighted cell indicates the highest or optimum compressive strength achieved in the group.

Figures 63 and 64 show the strength development of the two stabilised soils at 7 and 28 days. The stabilised soil with 60% of binder incorporating ROSA (Binder-B) showed the highest strength (Figure 63), revealing the potential of ROSA for use in soil stabilisation. The mix with 50% by weight of Binder-A performed satisfactorily according to TRL recommendations. Comparison with the compressive strength of stabilised soil with no binder reveals the beneficial effect of the novel blended binders in stabilising these two types of soil.

Figure 63 Compressive strength development of Stabilised Soil-A blended with Binder-A and Binder-B

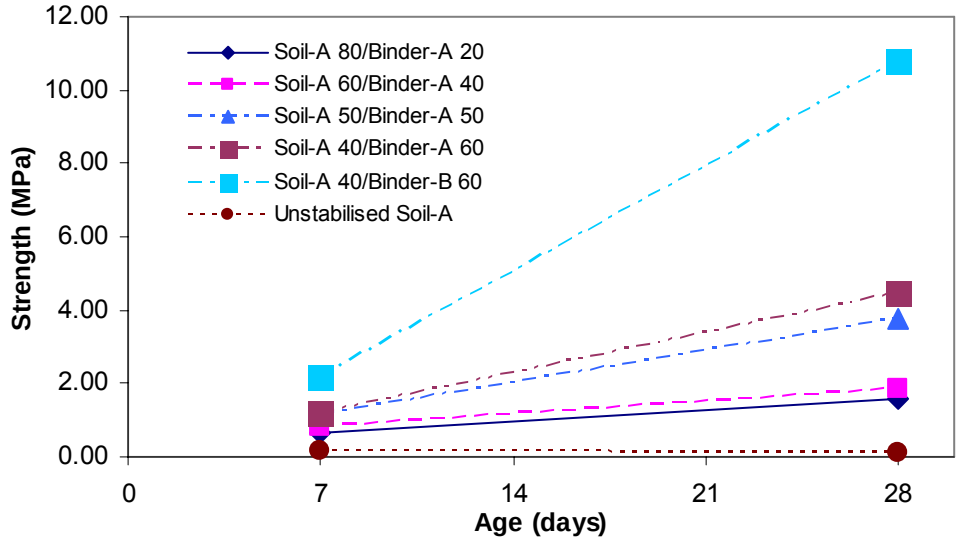

Figure 64 Compressive strength development of Stabilised Soil-B blended with Binder-A

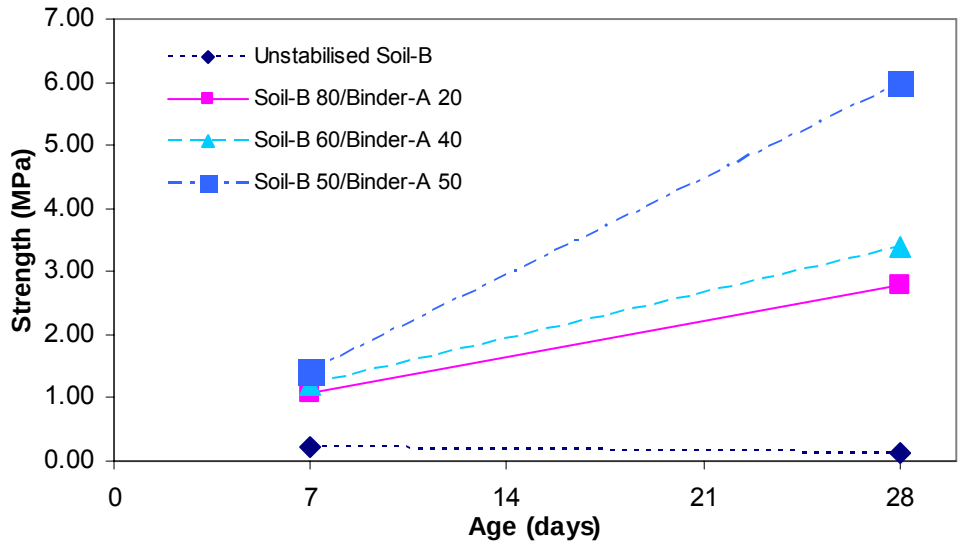

Binder-A (Coventry Binder) performed relatively better with Soil-B (Figure 63) than with Soil-A (Figure 64). Soil-A was taken from one of the trial sites (see section 4.3) long before the trial was due to begin out. But this soil was not available later and another source of soil (Soil-B) was provided from the same site for the site trial tests.

The effect of binder content is shown in Figures 65–67. Increasing the amount of binder mixed with the soil resulted in a higher compressive strength. The pattern was found to be similar for both soils. It can be postulated that the relationship between compressive strength and binder content is linear (Figures 65 and 66), although more investigation is needed to establish the precise relationship.

Figure 65 Compressive strength of Stabilised Soil-A versus binder content

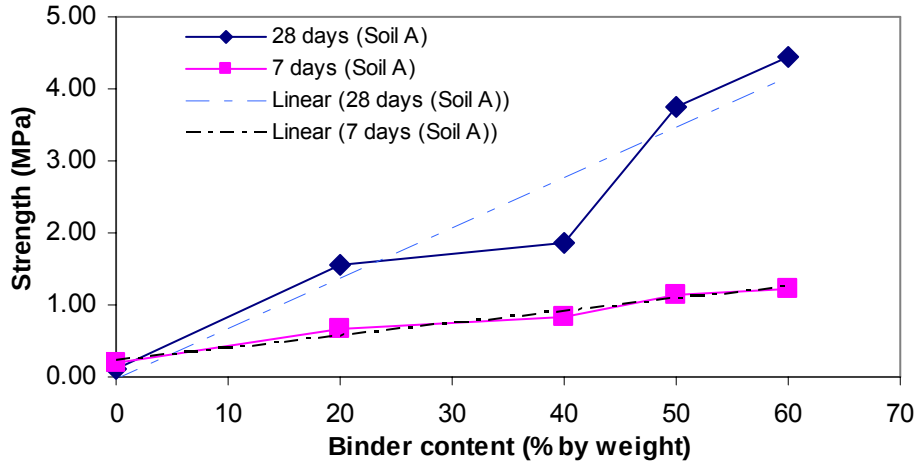

Figure 66 Compressive strength of Stabilised Soil-B versus binder content

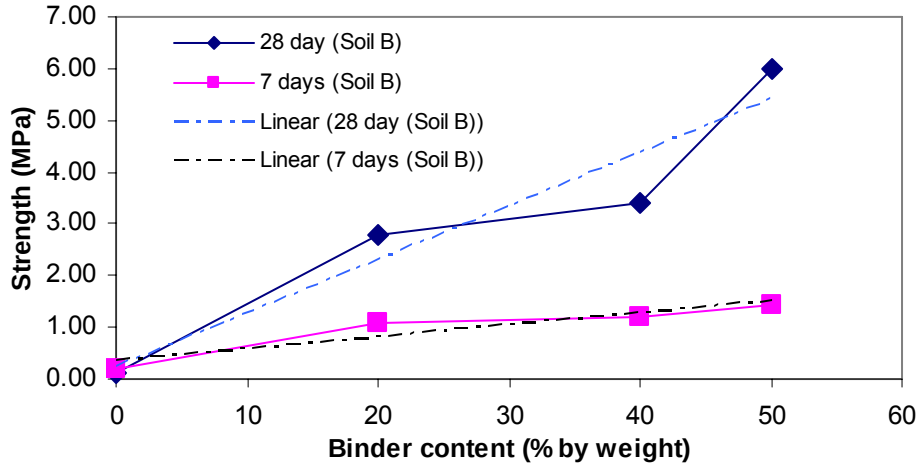

Figure 67 Comparison of compressive strength of Soil-A and Soil-B with blended mixture of PG-BPD-BOS (Binder-A)

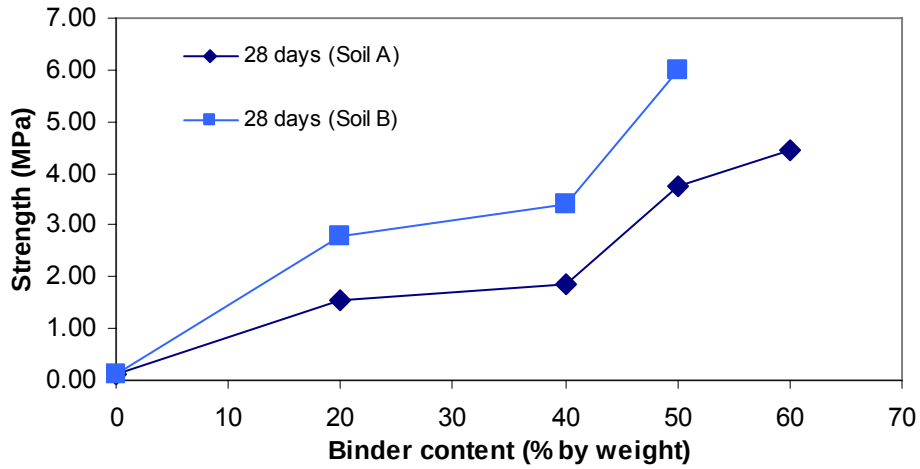

3.4 Hydrogen sulphide release

Under the anaerobic conditions in landfills, the gypsum in plasterboard can react with biodegradable waste (such as the paper backing of the plasterboard itself) to produce toxic hydrogen sulphide gas. By binding the sulphate content of the plasterboard into a low permeability matrix, the reaction with the paper leading to the release of hydrogen sulphide will not proceed.

During the life of a road, the surface layer and drainage systems will keep the foundation dry but end-of-life conditions also need to be considered. The ability to use plasterboard without paper removal is a key aspect of this work.

In order to confirm that hydrogen sulphide (H_2S) was not emitted from the developed blended powder, paste samples were prepared using the original blended powder with 10 and 20% (by weight) extra paper added to the mix. Specimens were kept in airtight plastic bottles to trap any hydrogen sulphide released (Figure 68). Samples were stored at 20° C in a similar manner to other paste specimens.

Figure 68 Plastic bottles containing paste specimens for H_2S check

The bottles were removed from the curing propagator after 28 days. The following methods were used to determine any H_2S released.

3.4.1 Infrared spectrometry

In this method, gas was extracted from the bottle using a gas-tight syringe and injected into a pre-vacuumed infrared (IR) gas cell. The spectrum obtained was then analysed according the standard pattern for hydrogen sulphide (Figure 69).

Figure 69 Different parts (A, B and C) of the infrared spectrum for H_2S [19]

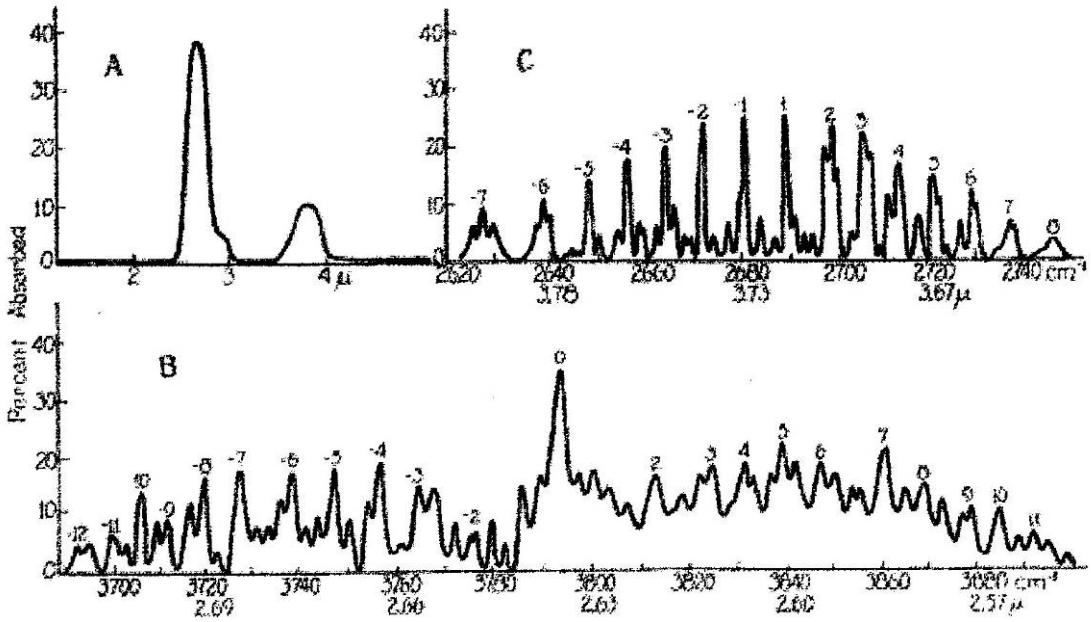

Figure 70 shows the IR spectra of the gas extracted from specimens containing 10 and 20% paper. No distinctive difference can be seen between the spectrum obtained with an empty cell and the one containing extracted gas.

The accuracy of this method depends on the level of vacuum of the empty cell and the method of injecting gas into the cell. It appeared that, although high pressure vacuum was applied to empty any gas from the IR cell, it still contained some gases such as carbon dioxide (CO_2) or carbon monoxide (CO).

Figure 70 IR spectra of gas extracted from paste samples with 10 and 20% paper

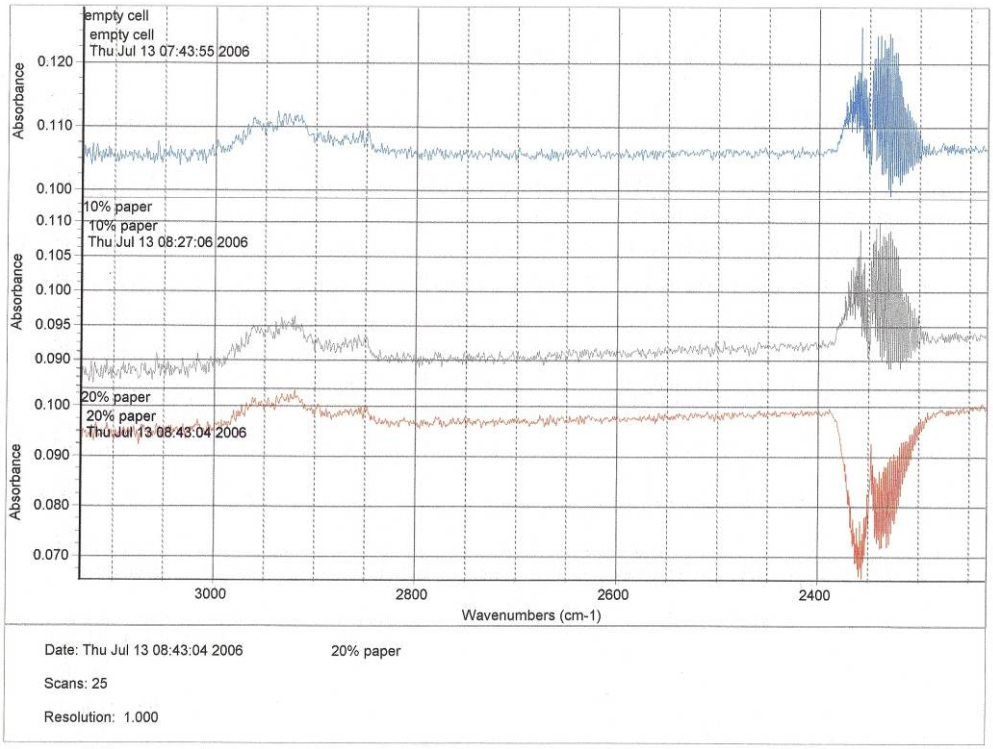

In order to validate more effectively, pure hydrogen sulphide gas was injected into the IR cell. Figure 71 shows a magnified part of the spectrum for pure H_2S. The magnified parts of the spectra for the samples with 10 and 20% paper shown in Figures 72 and 73 were compared with the spectrum for pure H_2S, but no similarity was

found between the pattern of gas injected and pure hydrogen sulphide. The initial conclusion from this investigation was that no hydrogen sulphide was released from the paste specimens.

Figure 71 Magnified IR spectrum of pure hydrogen sulphide (wavelength 2600–2800 cm^{-1})

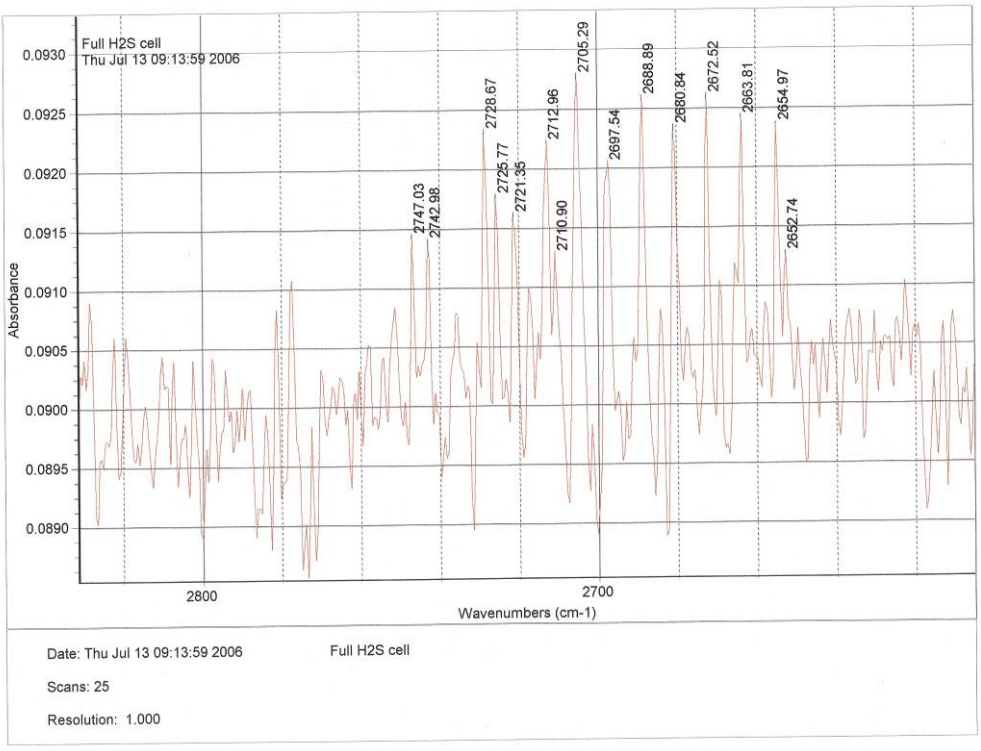

Figure 72 Magnified IR spectrum of sample with 10% paper (wavelength 2600–2800 cm^{-1})

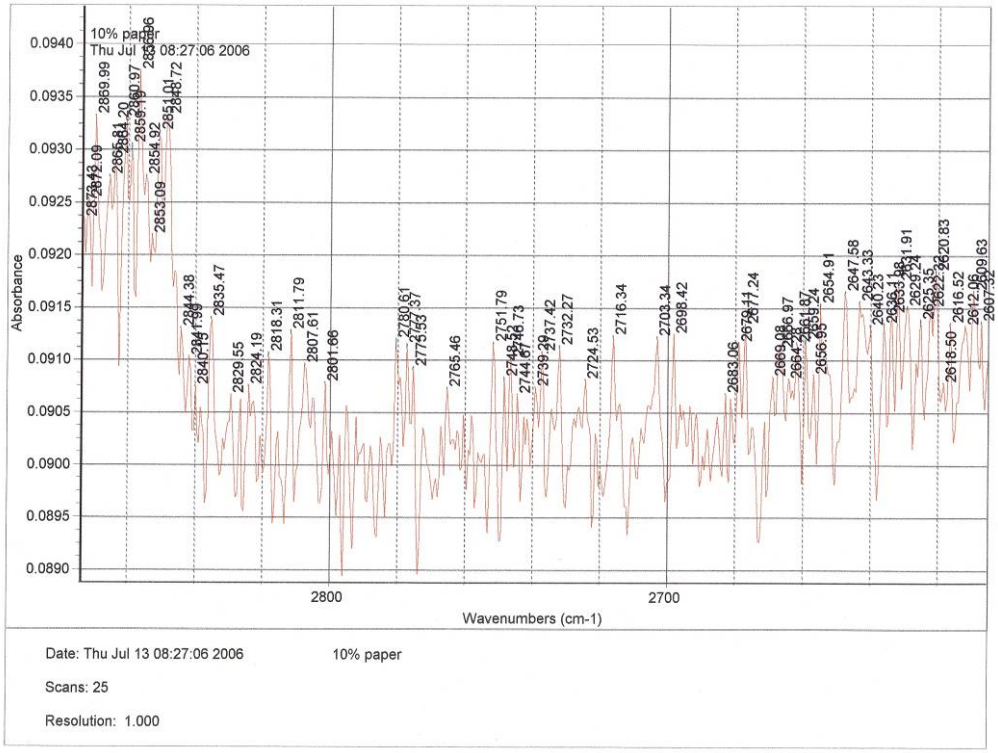

Figure 73 Magnified IR spectrum of sample with 20% paper (wavelength 2600–2800 cm^{-1})

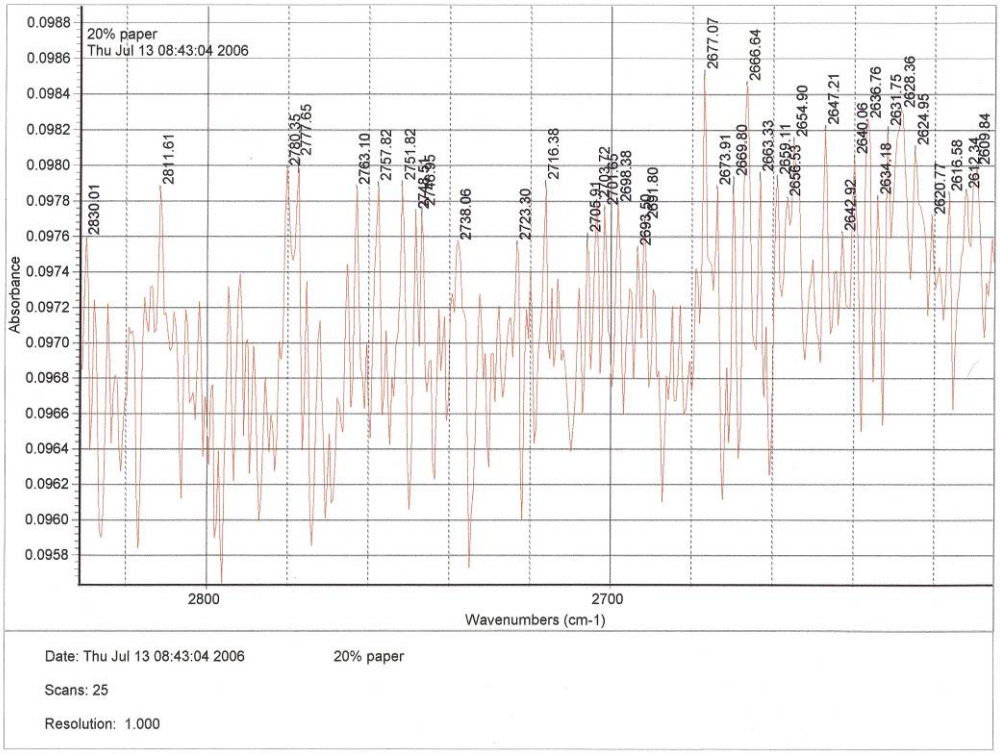

3.4.2 XRF analysis

In another approach, XRF analysis was carried out on a sample of original blended powder and paste samples prepared with 5, 10 and 20% extra paper at 1, 14 and 28 days after casting.

It was proposed that monitoring the comparative amounts of sulphate in the original blended powder and in paste samples over a period of time would give an indication of any loss or conversion of sulphur to other compounds such as hydrogen sulphide.

The results of XRF analysis of samples containing different percentage of paper are presented in Table 44. These indicate that the amount of sulphate (measured as SO_3) did not change considerably between samples tested at different ages. The variation in sulphate content was within ±4% and did not follow any distinctive pattern. However, comparison between samples with less than 0.5% by weight paper and those containing 5, 10 and 20% by weight paper indicated that the higher the amount of paper, the higher the amount of sulphate. This might be due to the presence of sulphate in the paper itself.

The results with samples containing 10 and 20% paper indicated that no conversion of sulphate to hydrogen sulphide gas had occurred by 28 days. Since most chemical reactions take place in presence of water, it can be postulated that hydrogen sulphide gas is more likely to be emitted when the samples are fresh, i.e. during early ages of paste mixtures. This implies that conversion of sulphate to hydrogen sulphide is more unlikely when the rate of reaction falls during the later stages of hydration.

Table 44 XRF analysis of mixtures containing various percentage of paper

Mix	Percentage											
	SiO_2	TiO_2	Al_2O_3	Fe_2O_3	MnO	MgO	CaO	Na_2O	K_2O	P_2O_5	SO_3	LOI
Paste <0.5% paper (1 day)	11.12	0.32	2.16	18.89	2.78	6.95	41.12	-0.01	0.36	1.09	8.97	7.14
Paste <0.5% paper (14 days)	11.02	0.33	1.98	19.13	2.88	6.90	41.12	-0.02	0.34	1.17	8.92	7.47
Paste <0.5% paper (28 days)	11.05	0.31	2.17	18.37	2.67	6.82	39.88	0.00	0.46	1.03	9.91	8.31
Paste + 5% paper (14 days)	10.77	0.31	2.27	18.35	2.66	7.20	40.26	-0.04	0.55	1.03	10.24	7.35
Paste + 10% paper (14 days)	10.99	0.32	2.30	18.74	2.74	7.41	40.12	-0.04	0.56	1.06	9.79	6.63
Paste + 20% paper (1 day)	10.74	0.34	2.27	18.62	2.61	7.17	39.21	-0.02	0.75	1.08	10.45	6.82
Paste + 20% paper (14 days)	10.91	0.31	2.30	18.43	2.68	7.27	40.21	-0.02	0.72	1.04	10.37	6.17
Paste + 20% paper (28 days)	10.62	0.30	2.28	17.80	2.60	7.04	39.58	-0.01	0.78	1.00	10.81	7.69
Binder powder	11.46	0.34	2.26	19.59	2.87	7.19	42.34	-0.02	0.63	1.12	9.68	2.08

3.4.3 H_2S detection tubes

To confirm the presence or absence of hydrogen sulphide from the paste mixture containing paper, a very accurate and sensitive device was used to detect the hydrogen sulphide gas. Figures 74 and 75 show the H_2S detection tube and the pump kit respectively. This device indicates the presence of trace amounts of hydrogen sulphide (accuracy 0.2–5 ppm) by a change in colour of chemicals in the tube.

Figure 74 Drager Accuro H_2S detection tube

Figure 75 Drager Accuro pump kit and H_2S detection tube

Paste samples containing 5, 10, 15, 20 and 50% extra paper was tested at 1, 14 and 28 days curing (Figure 76). No change in colour was observed during testing of different samples (Figure 77). This indicated the absence of hydrogen sulphide in the airtight containers and confirmed that hydrogen sulphide was not formed even when the binder contained a large amount of paper (50%).

Figure 76 Testing the paste samples using the H_2S detection tube

Figure 77 Comparison between new and used H_2S detection tube for mix containing 50% paper

3.5 High pressure through-flow test

Paste and concrete specimens of blended powder were made using a cylindrical mould for a high pressure through-flow test. This test was performed to:

- confirm the long-term stability of the mixes; and
- check the potential for leaching to the environment.

Figure 78 shows the modified Hoek cell in which distilled water is eluted through a column of proposed material under a pressure gradient [20, 21].

Figure 78 Hoek cells used for high pressure through-flow test

Figure 79 shows paste samples prepared for the high pressure through-flow test. Samples were cut from the cylindrical specimens and made with the two binders and two L/B ratios of 0.13 and 0.15. Paste and concrete samples from the site trials (see section 4) were also tested and compared with OPC paste. Sample solutions were collected from the specimens tested in the Hoek cell and analysed using an inductively coupled plasma (ICP) spectrometer in the chemistry department at Coventry University (Table 45).

Figure 79 Paste specimens prepared for high pressure through-flow test

Table 45 ICP analysis of high pressure through-flow test samples (ppm) at Department of Chemistry, Coventry University

Element	BOS80/PG15/BPD5 (0.15, Lab.)	BOS80/PG15/BPD5 (0.13, Lab.)	BOS30/ROSA50/PG15/BPD5 (0.19, Lab)	BOS80/PG15/BPD5 (0.13, Site)	BOS80/PG15/BPD5 (0.13, Site core)	RCC (Site)	OPC paste (0.3)
Na	182.8	178.9	172.9	16.75	706.7	116.4	43.3
Mg	<1	<1	<1	<1	<1	<1	0
Al	0	0	0	0	0	0	0
Ba	0	0	0	0	0	0	0
Ca	1101	1021	1558	1373	1664	403.8	154
K	3195	3611	2042	604.7	2155	1326	35.1
Cr	0	0	0	0	0	0	0
Ni	0	0	0	0	0	0	0
Pb	0	0	0	0	0	0	0
S	449.1	460.7	375.5	214.5	840.3	116.2	14.5
Si	78.7	51.62	35.53	2.96	1.64	9.94	0
Sr	0	0	0	0	0	0	0
P	<1	<1	<1	2.01	1.99	<1	<0.2

Table 46 Repeated ICP analysis of high pressure through-flow test samples (ppm) at Department of Geology, Leicester University

Element	BOS80/PG15/BPD5 (0.15, Lab.)	BOS80/PG15/BPD5 (0.13, Lab.)	BOS30/ROSA50/PG15/BPD5 (0.19, Lab)	BOS80/PG15/BPD5 (0.13, Site)	BOS80/PG15/BPD5 (0.13, Site core)	RCC (Site)
Na	264.78	286.47	201.85	27.49	775.66	143.55
Mg	0.02	0	30.64	0.02	0.03	0
Al	0	0	0.04	0	0.02	1.04
Ba	0	0	0	0	0	0
Ca	1065.80	1524.20	1630.25	1328.35	1518.23	239.50
K	4684.37	5181.02	2033.01	551.90	1742.45	1132.91
Cr	0	0	0	0	0	0
Ni	0	0	0	0	0	0
Pb	0	0	0	0	0	0
S	762.04	722.42	667.98	363.83	1320.33	198.75
Si	66.60	47.67	28.60	0.00	0.00	7.07
Fe	0	0	0.09	0	0.01	0
Sr	0	0	0	0	0	0
P	0	<1	0	0	2.07	1.87

The results indicated that no heavy metal elements had leached from the samples. The major ions dissolved in water were sodium, potassium, calcium, silicon and sulphur – all considered to typically exist in soil and rocks.

Comparison between samples made with the blended binder and with OPC indicated that the level of sulphur (as sulphate) and calcium leached from the samples made with the novel binders under high pressure water was more than from those made using OPC. This could be due to the lower hydration rate and reduced cementitious matrix available to bind the sulphates and calcium ions formed in samples made with novel cement. However, the conditions under which the high pressure through-flow test is carried out are much more accelerated than normal ground conditions. Thus, dissolution of a high level of sulphate ions is not expected using these novel binders.

Table 45 also shows that the amount of sulphate and calcium dissolved from the RCC mix used in the site trial was less than from the semi-dry paste mixes. This is because less cementitious material was used to make the concrete mix. However, the levels of sulphate and calcium dissolved from site core samples were much higher than those from samples made in the laboratory or taken during the site trial.

The high amount of potassium found in all the samples was not expected due to the low amount of potassium oxide (K_2O) in the binder used. To validate the ICP results, the analysis was repeated using an independent ICP machine at Leicester University's geology department (Table 46). The concentration of elements in this second set of results was in the same order as from the analysis carried out using the ICP machine at Coventry University. Slight changes in the concentration of ions might have been due to precipitation or internal reactions in the solutions during storage of the samples. The concentration of potassium remained high in all samples.

To determine the source of potassium in the binder, chemical analysis of the raw materials was repeated using XRF. The chemical compositions of BOS and PG found were similar to previous analyses, but the BPD used to make the Coventry Binder contained more potassium than the previous batch of BPD (Table 1 in section 2.3). This illustrates the variation in the chemical composition of BPD from one batch to another. As the potassium in BPD is in the soluble form of K_2O, the high concentrations of potassium in the solutions from the high pressure through-flow test probably arise from the BPD used in the blended binder.

The coefficient of permeability of laboratory and site paste and concrete samples was also measured in the high pressure through-flow test (Table 47). The semi-dry site paste [BOS80/PG15/BPD5 (0.13, Site)] had the highest permeability compared with the laboratory samples; this was due to the lower moisture content when compacting the sub-base layer in the site trial. However, the coefficient was only 10 times greater than that for OPC and, in real ground conditions, the effect will be less than with the high-pressure water conditions in the test. The permeability of concrete varies over four orders of magnitude, so a factor of 10 difference is not as significant for permeability as it would be for strength. The measured permeability of RCC used in the Lowdham Grange site trial (see section 6.2) was less than OPC paste, possibly due to the presence of aggregates in the concrete. Aggregates generally have a lower permeability than cement matrices, so the presence of large volume of aggregates in the RCC concrete resulted in a lower permeability than the OPC paste.

Table 47 Coefficient of permeability to water of laboratory and site samples

Mix	Coefficient of permeability to water (m/s)
BOS80/PG15/BPD5 (0.15, Lab.)	3.98E-11
BOS80/PG15/BPD5 (0.13, Lab.)	1.64E-10
BOS30/ROSA50/PG15/BPD5 (0.19, Lab)	1.29E-10
BOS80/PG15/BPD5 (0.13, Site)	4.11E-09
BOS80/PG15/BPD5 (0.13, Core)	3.57E-09
RCC (Site)	6.91E-11
OPC paste (0.3)	6.03E-10

3.6 X-ray diffraction of paste mixtures and hydration mechanism

The changes in mineralogy of BOS80/PG15-BPD5 (0.13) semi-dry paste mixture at different ages were investigated using X-ray diffraction (XRD). Figure 79 shows the XRD patterns of paste mixtures after 1, 3, 7, 28 and 180 days curing at 20° C and 98% RH.

Gypsum was the dominant crystalline phase, an observation related to the presence of plasterboard gypsum in the mixture. The initial setting and early age strength of the paste is associated with the formation of ettringite as a result of the reaction of sulphate from gypsum with aluminium and calcium dissolved from the BOS. The peak associated with ettringite was more evident after 3 days, corresponding to the lower strength of the paste than at 7 and 28 days. At the later ages, more ettringite was found in the mixture and higher strength was achieved.

The long-term strength of the mixture is related mainly to the formation of CSH within the cementitious matrix around slag particles, which it was not possible to determine using XRD due its amorphous structure. At 180 days, the presence of a strong peak of ettringite indicated the stability of this phase in the long-term curing of the samples in a moist condition.

Alkali-activated slag mixes are sensitive to carbonation [5] and this phenomenon was observed in XRD patterns of paste mixes at 180 days (Figures 80 and 81). The peak associated with calcite was identified at 28 and 180 days, indicating the formation of a considerable amount of calcium carbonate within the matrix. According to Bakharev [22], the main reasons for rapid carbonation of alkali-activated slag are the absence of portlandite as a hydration product (it normally acts as a carbonation buffer in cement systems) and the low pH of the pore solution. In OPC pastes, a near-surface layer of precipitated calcium carbonate acts as a seal and reduces the diffusion speed of CO_2 into the cementitious matrix. Furthermore, the low Ca/Si ratio of CSH could accelerate carbonation. The carbonation rate in hydrated slag and sulphate mixes is controlled only by the carbonation of CSH and ettringite. Thus the higher content of hydrates can reduce the rate of carbonation. This phenomenon was also observed in this investigation. The peak associated with calcite remained at the same intensity in samples at 28 and 180 days. The presence of a very low intensity peak of portlandite was in the line with the findings of Bakharev [22].

Figure 80 XRD of PG-BOS-BPD(0.13) semi-dry pastes at different ages: (1) 1 day; (2) 3 days; (3) 7 days; (4) 28 days; and (5) 180 days (An = anorthite, C = calcite, E = ettringite, G = gypsum, Mer = merwinite, P = Portlandite, Q = quartz)

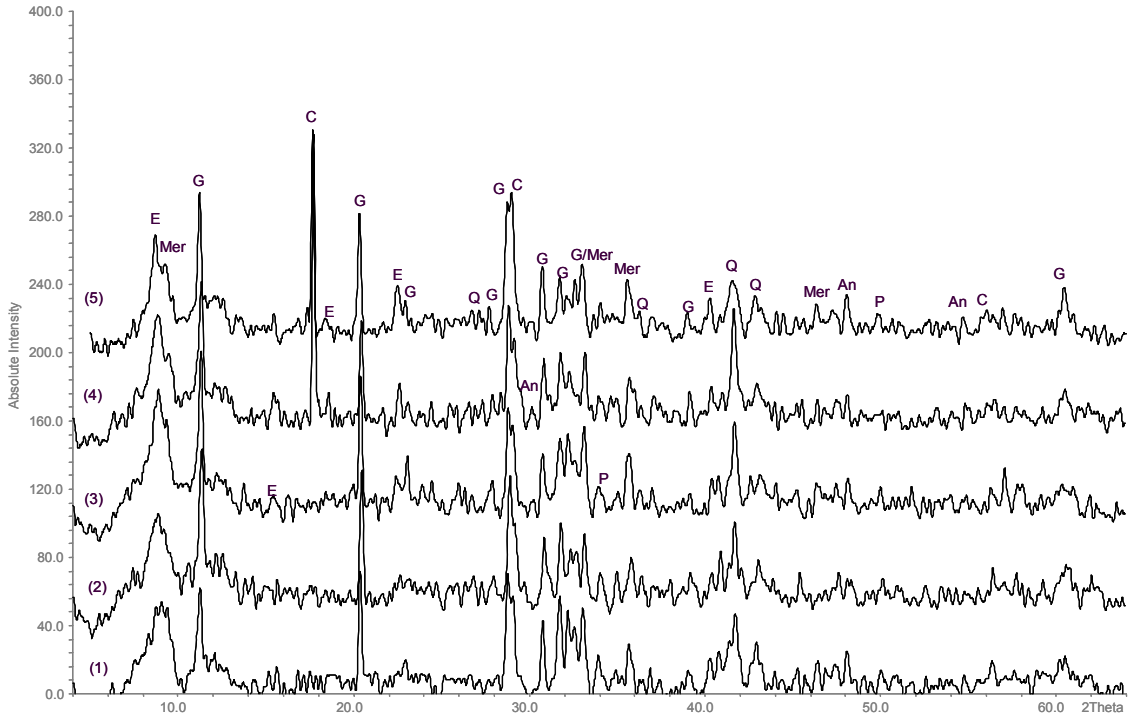

The phases related to slag (merwinite) were identified within the matrix, indicating the presence of unhydrated slag particles within the mixture (Figure 80). As the slag is a slow-reacting material, it may be that only a low percentage of the total slag fraction reacts at 28 and even 180 days.

Figure 81 shows the expanded XRD patterns of Coventry Binder (PF-BOS-BPD) semi-dry paste at values of 2Theta (2θ) of 6–20°. The growth of ettringite with time was observed in peaks at 9.096, 15.79 and 17.83°, though the strongest intensity appeared at 9.096°. In addition, the strong peak of calcite at 17.073° indicated the intensity of carbonation on the hydrated matrix of the mixture.

Figure 81 X-ray analysis of PG-BOS-BPD (0.13) semi-dry paste at different ages showing ettringite and calcite evolution

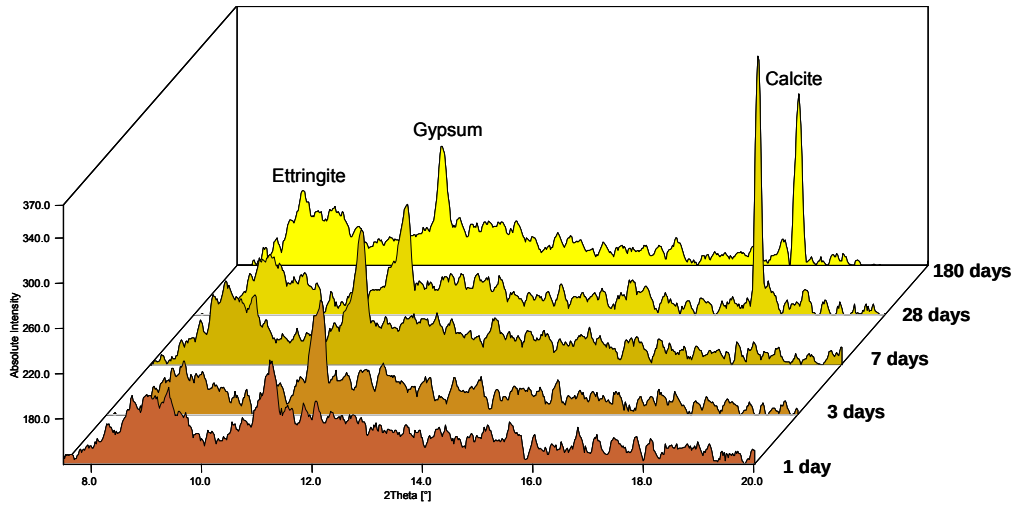

Figure 82 shows the XRD patterns of stabilised soil samples containing 20, 40 and 60% Coventry Binder after 28 days curing at standard condition. The intensity of the peak associated with gypsum was lower in the sample containing 60% binder, possibly due to the advanced reaction of binder within the clay and the inclusion of sulphates from gypsum in hydration products.

The presence of a peak associated with ettringite confirmed that part of the gypsum was present in the sulphate-bearing component of ettringite. Quartz was the predominant phase in stabilised soil samples; it was the main constituent of the sandy clay used in this investigation. The presence of a kaolinite peak in the pattern also indicated the mixture of siliceous gravel/sand and clay in the soil.

The formation of calcite in samples containing more binder was due to the carbonation of hardened binder within the clay; the more binder used to stabilise the clay, the higher the intensity of calcite in the XRD pattern.

it was not possible to determine the formation of CSH cementitious gel in the matrix of stabilised soil using XRD. However, the lower intensity of quartz in the sample made with 60% binder could be due to the reaction between silica and alumina in clay constituents with alkalis in the binder to form cementitious gel. The presence of a trace of portlandite confirmed the contribution of calcium hydroxide from BKD in the hydration reactions.

Figure 82 XRD of stabilised soil with different percentages of Coventry Binder: (1) 20%; (2) 40%; and (3) 60% (C = calcite, E = ettringite, G = gypsum, K = kaolinite, P = portlandite, Q = quartz)

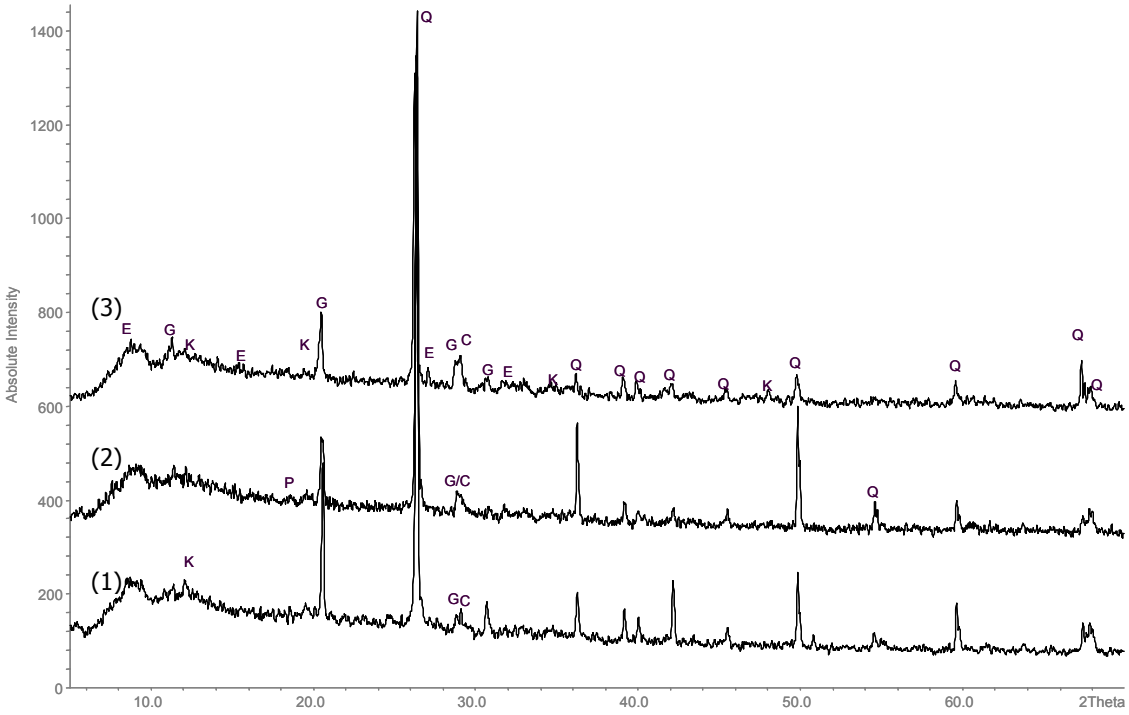

Figure 83 shows the hydration scheme of slag in the presence of gypsum and alkalis based on the results obtained in this project and previous experience. The sequence of the hydration reactions at different stages after mixing the binder with water can be explained as follows.

Directly after mixing with water, ions of readily soluble alkali compounds and free lime from the cement BPD – as well as released ions from the slag and gypsum – enter solution. Ca^{2+}, Al^{3+}, Si^{4+}, Mg^{2+}, SO_4^{2-}. Na^{+}, K^{+} and OH^{-} ions are available in the system after about 10 minutes of hydration [7]. The pH of the pore solution then increases to approximately 11.6. Alongside the rising calcium concentrations, the pH increases to 12.3 after 2 hours of hydration. A high saturation index was calculated for ettringite [23], with a maximum saturation index occurring between 2 and 4 hours. Scanning electron microscopy (SEM) micrographs of paste [24] showed ettringite needles (1–1.5 µm) loosely distributed in the hydrating structure and CSH formation beginning on the surface of slag grains after 4 hours (as shown schematically in Figure 82).

Figure 83 Hydration scheme for the hardening of alkali-sulphate activated slag

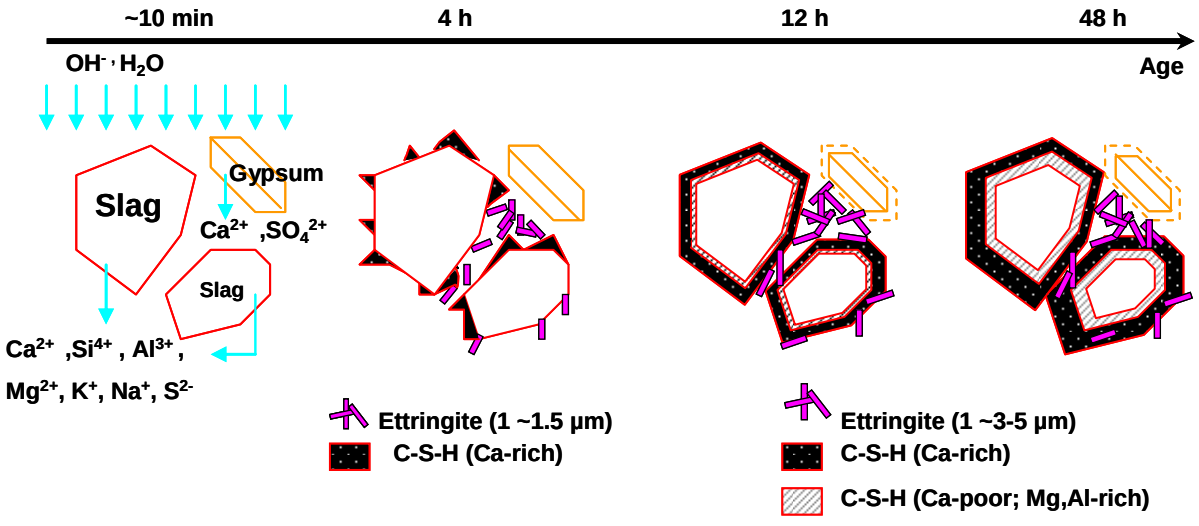

As a result of hydrate precipitation, Ca^{2+}, Al^{3+}, Si^{4+} and OH^- ions are partly removed from the pore solution. The sulphate content of the pore solution increases in order to balance the positive charges on the alkali metal (Group I: Na^+, K^+) and alkaline earth (Group II: Ca^{2+}, Mg^{2+}) ions created by the removal of the hydroxide ions. The hydration reactions accelerate the corrosion of the slag to reach an apparent chemical equilibrium between solid and liquid phases. The rising Group I, Group II and sulphate content indicates continuous hydration of the slag-gypsum-bypass dust paste. The additional positive ions are balanced with the sulphate ions in the pore solution, resulting in the pH of the pore solution remaining nearly constant at between 11.7 and 12.0 [24].

Richardson [25] reported finding two CSH reaction fronts around the hydrating slag grains; the inner layer showed a lower Ca/Si ratio (Ca/Si ~1.2) than the outer layer (Ca/Si ~1.4). However, it is possible that a homogenous Ca/Si ratio may be approached with progressing hydration time. The morphology of CSH observed by Richardson [25] was more foil-like than the fibrillar CSH of OPC with high Ca/Si ratios of ~1.8. Moreover, the low solubility of magnesium may cause the precipitation of magnesium-containing hydrates such as hydrotalcite. Thus, the inner hydrate layer could contain more aluminium and magnesium than the outer layer. Möser [26] showed an incorporation of magnesium and aluminium into the structure of the magnesium-calcium-silicate-aluminate-hydrate (M-C-S-A-H) identified as hydration products of slag. More recently Brews and Glasser [27] described the possibility of magnesium silicate hydrate (MSH) gel formation as an additional product of hydrated blast furnace slag.

Two separate spatial equilibria arise as a result of the accumulation at the slag surface of dense CSH. Hence further hydration reactions are controlled by diffusion. This causes a very slow reaction rate, which declines with the increased thickness of the CSH layer around the slag. The formation of this layer means that only about 26% (by weight) of the total slag fraction can react at 60 days [7].

Several researchers have reported the sensitivity of alkali-sulphate activated slag mixtures to imprecise dosages of alkaline activators [28, 29]. The results presented in section 5.1.2 also showed that the compressive strength fell as the CKD/BPD content of the binary and ternary paste mixtures increased. The lower strength due to a high alkali metal content in the pore solution can be attributed to the location of the ettringite precipitation [30].

Ettringite forms hexagonal-prismatic crystals based on columns of cations of the composition $\{Ca_3[Al(OH)_6].12H_2O\}^{3+}$ [31] in which the $Al(OH)_6^{3-}$ octahedra are bound up with the edge-sharing CaO_8 polyhedra. This means that each aluminium ion, bound into the crystal, is connected to Ca^{2+} ions with which they share OH^- ions. The intervening channels contain the SO_4^{2-} tetrahedra and remaining water molecules. The water molecules are partly bound very close into the ettringite structure. Figure 84 shows a structural model of ettringite [31].

Ettringite appears in many different forms and shapes, although the causes of this are not yet fully explained. According to investigations by Chartschenko and colleagues [32, 33], the length–thickness ratio of ettringite crystals is extremely dependent on the pH value of the reaction solution (Figure 85). Long, fibre-shaped crystals are formed at pH values between 10 and 12, but extremely microcrystalline ettringite is present at pH values above 13.0.

Mehta [34] described two modifications of ettringite which differ in habit and size. The long lath-like crystals, which can be 10–100 µm long and several µm thick, formed at low hydroxyl ion concentrations (i.e. with low pH values in the pore solution) and were designated by Mehta as Type I. If a hydrated binder contains significant amounts of these large ettringite crystals, this would lead to high strength but not to expansion effects. Mehta therefore proposed that Type I ettringite is not expansive. The rod-like crystals, which are only 1–2 µm long and 0.1–0.2 µm thick or even smaller, form at the high hydroxyl ion concentrations present during hydration of OPC or high alkaline-activated slag; these were called Type II ettringite by Mehta. According to Mehta, fairly large amounts of this microcrystalline ettringite can cause expansion effects through water adsorption. The expansion-related properties of the novel blended binder used in this project are discussed in section 3.7 and can be associated with the formation of the microcrystalline form of ettringite within the cementitious matrix.

Figure 84 Structural model of ettringite [31]

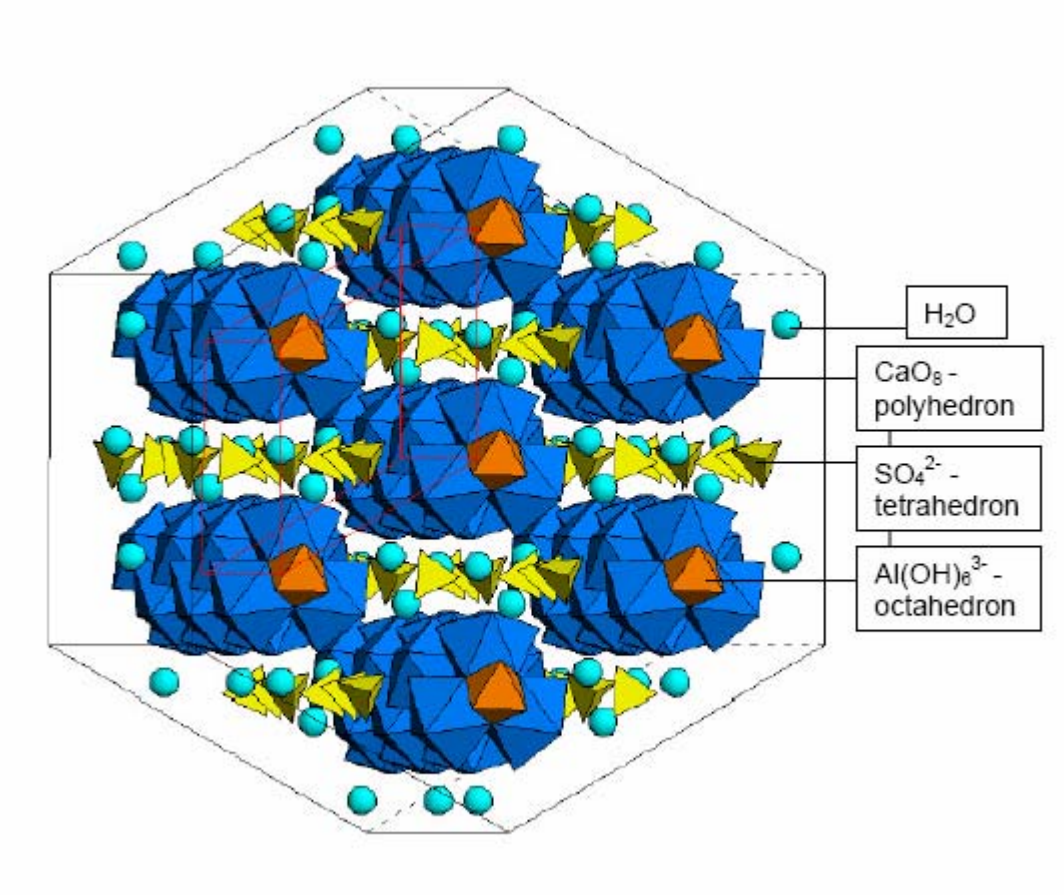

Figure 85 Change in length–thickness ratio of ettringite crystals [31]

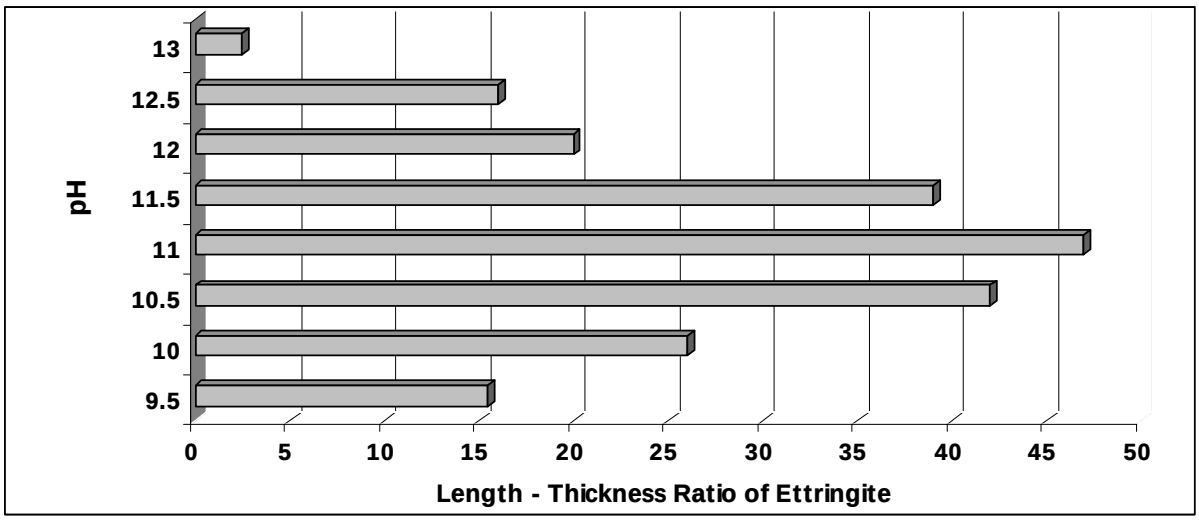

In alkali-sulphate activated slag systems with low alkali contents, ettringite is precipitated preferably in larger pores. Environmental SEM (ESEM) micrographs of alkali-sulphate activated slag paste with high alkali contents in the pore solution demonstrated a preferred growth of ettringite crystals on the surface of hydrated slag grains [35]. The addition of positive charges to the pore solution (Na^+, K^+, Ca^{2+}) leads to an increased sulphate concentration (negative charges) in order to obtain a charge-balanced pore solution.

A high local supersaturation for ettringite near the surface of the slag grains results from the enhanced content of sulphate and hydroxide in the pore fluid. The precipitation of ettringite impedes the migration of aluminium ions from slag grains into the pore solution and the concentration of aluminium ions is <0.1 mmol/l from the beginning. Taylor [31] described a similar mechanism for a high concentration of calcium in the pore solution. As a consequence, spatial isolation of the slag grains in conjunction with a coarsening of the pore structure leads to lower compressive strength.

The ettringite layer on the slag surface can be responsible for the lower reaction rates due to a lower diffusion rate of ions from the slag into the pore solution. Furthermore, the formation of microcrystalline ettringite at higher pH can result in a denser layer of ettringite around the slag grains, lowering the hydration rate of slag in the matrix.

3.7 Length change of PG-BOS-BPD paste and mortar mixtures

To provide information on the long-term durability and stability of the Coventry Binder, the length change of paste and mortar samples made using the novel binder was measured according to ASTM C151 [36]. The length change was also compared with a control OPC mortar sample.

Prism samples of 25×25×285 mm were made using gang prism moulds with steel inserts fitted at both ends of each sample. Figure 86 shows the apparatus used to determine the length change of hardened paste and mortars (ASTM C490) [37]. The length change of samples was measured at 3, 7, 14 and 28 days, with the results reported as the percentage change.

The maximum allowed expansion or shrinkage of any mix depends on the type of binder application. For example, for in expansion due to alkali-silica reactivity (ASR), ASTM C1260 [38] and ASTM C227 [39] indicate a 26-week test limit of 0.1%. BS 812-123: 1999 [40], which is also related to ASR expansion, sets the limit of 0.1% at 52 weeks. BS 2028: 1968 [41] recommended the maximum shrinkage of 500×10^{-6} to 600×10^{-6} (relative length change) for pre-cast construction blocks used for general applications.

Figure 86 Apparatus for determination of length change

Details of the paste (P) and mortar (M) mixes investigated are given in Table 48. Mortars were made using a sand to binder ratio of 2.7 with different L/S ratios. The semi-dry paste investigated was similar to the mix used in the site trial, i.e. Coventry Binder (COV). Samples were cured at 20° C and 98% RH, though the paste and mortar mixes made with the Coventry Binder were also placed at 40° C to investigate the effect of curing temperature on the expansion of this novel blended binder.

Table 48 Mix proportions of paste and mortars for length change test

Mix code	Binder (%)	Sand (%)	L/S	Temperature (° C)
COVP-20-0.13	100	–	0.13	20
COVM-20-0.13	27	73	0.13	20
COVM-20-0.3	27	73	0.30	20
COVM-20-0.5	27	73	0.50	20
OPCM-20-0.5	27	73	0.50	20
COVP-40-0.13	100	–	0.13	40
COVM-40-0.13	27	73	0.13	40

Figure 87 shows the results of the length change test for paste and mortar mixes made using Coventry Binder and OPC. The greatest expansion was observed in the paste mix (COVP-20-0.13) that had the lowest L/S ratio of 0.13.

Figure 87 Length change of paste and mortar mixes at different ages

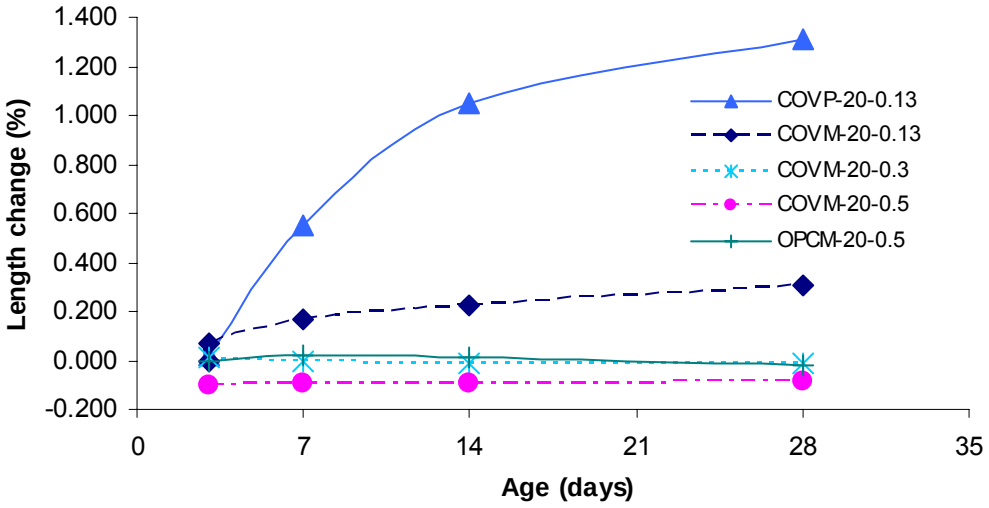

Incorporating aggregate in the mixture resulted in less expansion, mainly because less binder was used in the mix and the constraining effect of fine and coarse aggregate in the system. The expansion of mortar samples made with a similar water to binder ratio was only about 15% of that of the semi-dry paste. In addition, the lower L/S ratio led to greater expansion in the mortar samples.

A possible explanation for the lower expansion in samples made with a higher water to binder ratio could be the increased available space within the pore structure of the cementitious matrix that can be filled up by expansive hydration products as time progresses. Mortar samples made with a L/S ratio of 0.5 showed shrinkage from an early age of curing due to the evaporation of excess water immediately after casting. The length of the control OPC samples remained nearly the same, with slight shrinkage at 28 days. This was as reported by Neville [5].

The observed expansions for paste and mortar mixes made with Coventry Binder using a L/S ratio of 0.13 exceeded the recommended limit of expansion in BS 812-123: 1999 [40] for destructive ASR in concrete. It also exceeded the ASTM C227 [39] six-month test limit of 0.1% at only 7 days. This demonstrated the expansive nature of the Coventry Binder, which might be considered an advantage for use in certain applications in which

expansive cements are needed. In addition, no limit was suggested for cements used for backfilling or road foundations. Such an expansion can to, some extent, be restrained with steel reinforcement providing a protective layer is present to prevent corrosion of the steel due the chloride effect in a sulphate-bearing environment. The reason for the expansion of the novel blended binder is not yet clear, though formation of ettringite as a part of cementitious matrix and also the higher MgO content of BOS (as discussed above) might be responsible for progressive expansion of the hardened paste and mortars. The lower binder content in mortar and concrete mixtures results from less ettringite being formed within the matrix; less expansion was therefore observed in those samples.

With respect to the effect of temperature on the expansion of paste and mortars made using the Coventry Binder, Figure 88 shows the results of length change in samples cured at 20° and 40° C for 28 days. The expansion of paste and mortar mixes cured at higher temperature was lower than those cured at a standard temperature of 20° C and at a similar humidity (98% RH).

The expansion of the mortar sample made with the Coventry Binder cured at 40° C (COVM-40-0.13) remained almost constant and did not exceed the limit of 0.1% at 28 days. In addition, the expansion of the paste mixture cured at 40° C was about 30% of those cured at 20° C.

The lower expansion of paste and mortar mixes cured at the higher temperature might be due to faster hydration of slag at elevated temperatures, resulting in higher strength. This can provide more constraints within the cementitious matrix and therefore less expansion is observed. This implies that the Coventry Binder can be used in pre-cast concrete manufacture in which elevated and high pressure curing is used to produce concrete paving blocks. However, further investigations are needed to evaluate the effect of steam and high pressure curing on this novel blended binder.

Figure 88 Effect of temperature on length change of paste and mortar mixes

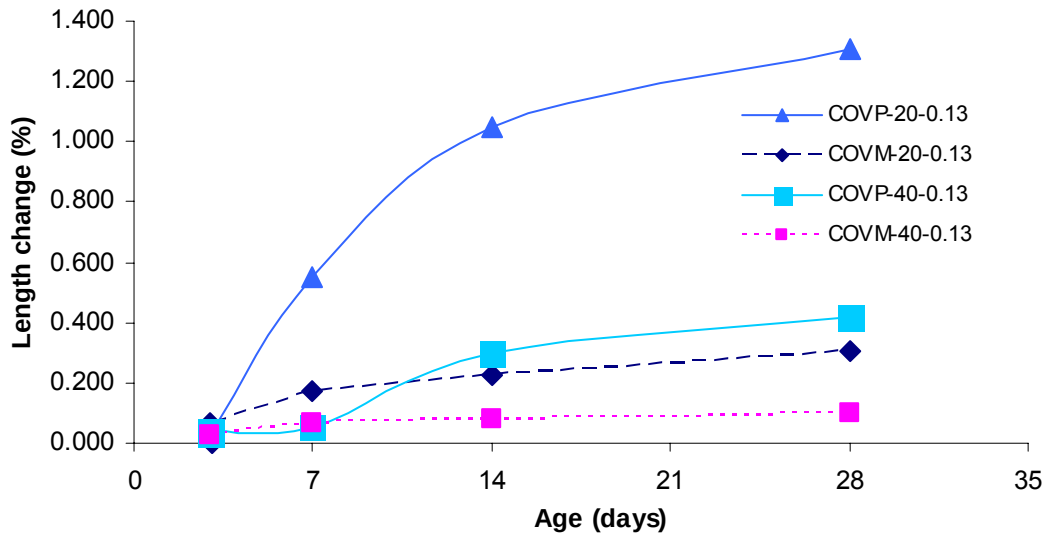

Figure 89 shows an overall comparison of the length change of the paste and mortar samples at 28 days. Among all the samples investigated, the semi-dry paste sample made using Coventry Binder with a L/S ratio of 0.13 showed the greatest expansion after 28 days curing at 20° C and 98% RH. The semi-dry paste sample cured at 40° C showed almost similar expansion to the mortar sample cured at 20° C with the same L/S ratio.

This highlights the significant effect of curing temperature on the long-term performance of the novel Coventry Binder. The lowest expansion in the semi-dry paste and mortar samples (L/S 0.13) was observed in the mortar sample that was cured at 40° C for 28 days. Mortar samples made with higher L/S ratios did not show any expansion up to 28 days, though shrinkage was observed similar to that obtained with the control OPC mortar at 20° C. Moreover, the higher the water content in the mixture, the greater is the drying shrinkage in the mortar samples.

Figure 89 Comparison of length change of paste and mortar mixes at 28 days

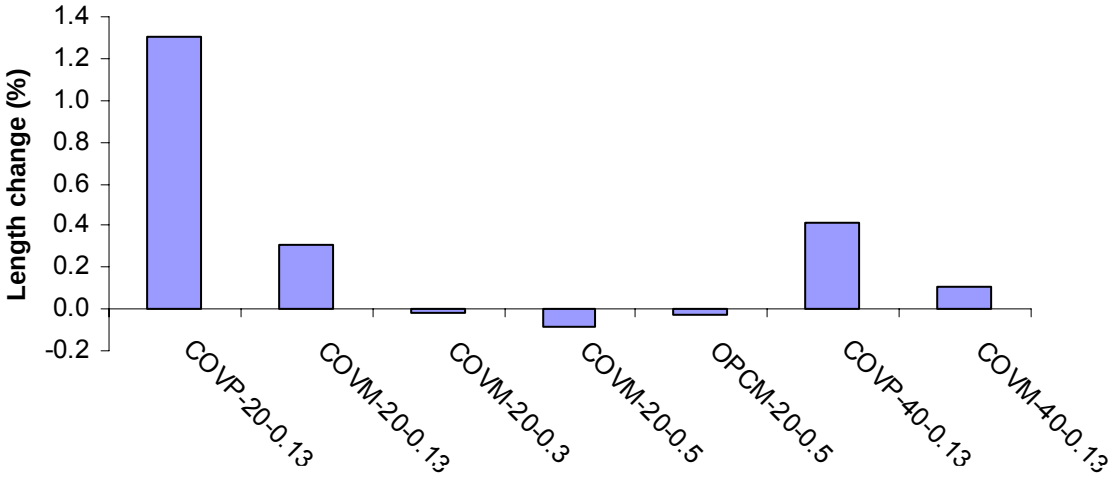

4.0 Site trials

Discussions with Skanska resulted in the selection of two construction sites to carry out the site trials:

- A car park at the Lowdham Grange prison construction site in Nottingham was selected to evaluate the use of roller-compacted concrete (RCC) as the sub-base layer using Coventry Binder.
- An area at the King's Mill Hospital construction site in Nottinghamshire was allocated to make a 22-metre access road using Coventry Binder stabilised soil and semi-dry paste (grout) as the sub-base and base course respectively.

The site trials were carried in July 2006 and the constructed layers evaluated until February 2007.

4.1 Material preparations

The final optimised proportions of the ternary mixture of PG, BPD and BOS as described in section 3 were chosen for the site trials.

In order to fulfil the requirements for concrete, stabilised soil and paste for the site trial, over 100 tonnes of blended powder was prepared at Ryder Point Processing in Matlock in Derbyshire (www.thebgs.co.uk/foundation-web/RyderPoint.html). The blended powder consisted of 80% ground BOS, 15% ground PG and 5% BPD supplied as blended powder.

The BOS was dried before grinding. Both the BOS and PG passed through a 500 µm mesh installed on the ball mill. The ground materials were then blended with BPD according to the designed proportions and bagged in 20-kg bags (Figure 90) and 1000-kg sling bags (Figures 91 and 92). The bags were shrink-wrapped before delivery.

Although the plasterboard supplied by Lafarge contained paper, the ground PG was sieved before blending and the major part of paper was removed. The BPD was expected to be in form of a fine powder, but it was found to contain big lumps of condensed material. To produce a fine blended powder, the lumps were removed as much as possible before blending the BPD with the other materials.

Pre-blending the material facilitates its use in ready-mix plants or with other types of mixing methods. The pre-blended powder was easy to use, like ordinary cement, with no further work or preparation required.

Figure 90 Blended powder delivered to the ready-mix plant in 20-kg bags

Figure 91 Blended powder delivered to the King's Mill Hospital site in 1000-kg sling bags

Figure 92 1000-kg bags of blended powder ready to use (King's Mill Hospital site)

4.2 Lowdham Grange site

A 6×17 m car park area at the Lowdham Grange prison construction site was allocated by Skanska for the sub-base trial for which the RCC designed in the laboratory experiments was used (see section 3.2).

Before work began the area was cordoned off using a pedestrian barrier. It was stripped of the existing hardcore to expose the sub-grade, which was hard clay, similar to that in the rest of the site. The sub-grade was trimmed to level, compacted and inspected by all parties (the contractor, WRAP and the technical group from Coventry University).

Figure 93 shows the layout of the construction layers designed for the site trial. This design was similar to that of the existing layers of constructed car park area in order to provide comparable data for the conventional sub-bases and the RCC layer.

Figure 93 Layout of trial construction layers at Lowdham Grange site

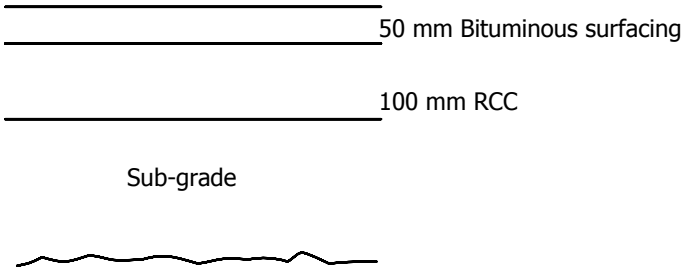

4.2.1 Ready-mix concrete

The RCC mix was prepared at a Lafarge ready-mix concrete plant at Lockington in Leicestershire (Figure 94). The concrete mix design used is presented in Table 49. The volume of the concrete required to construct the sub-base layer (in a loose condition) including wastage was estimated to be 16 m^3. It was therefore batched in three loads delivered by three truck mixers.

Table 49 Mix proportions of concrete mix used at the Lowdham Grange site trial

Mix code	Mix proportions (kg/m^3)			W/B	Slump (mm)
	Blended novel binder	Water	Recycled aggregate		
PG15/BPD5/BOS80 (RA-RCC)	400	100	1900	0.25	0

The moisture of the aggregates was measured in the laboratory and also by an automatic sensor installed in the aggregate stock of the ready-mix plant. All necessary adjustments to the proportions of the concrete mix were carried out before the materials were loaded into the truck mixers.

Figure 94 Lafarge ready-mix concrete batching plant

Aggregates and part of the water content were loaded first into the truck mixer (Figure 95) to allow the aggregates to absorb enough water and reach SSD condition.

Figure 95 Loading aggregates and water into the truck mixer

After mixing the aggregates and water thoroughly for about five minutes, the blended binder was loaded manually into the truck mixer. It had been planned to load the blended binder into the truck mixer using an auger system but a scheduling problem meant that the binder had to be loaded by hand (Figures 96 and 97).

Figure 96 Loading blended binder into the truck mixer

Figure 97 Loading blended binder bags into the truck mixer

The mixture of aggregates, water and blended binder was mixed thoroughly in the truck mixer for about 10 minutes before being delivered to the site.

The same procedure was carried out to load all three truck mixers (two 5-m^3 trucks and one 6-m^3 truck) used to batch the 16 m^3 of concrete.

4.2.2 Placing concrete and compaction

A layer of 160 mm of concrete was placed over the sub-grade layer using the truck mixer chute (Figure 98) before being spread and levelled manually (Figure 99). As the concrete was delivered in three truck loads, placing and compaction of the RCC layer was carried out in three segments of the allocated area. As a result, a slightly different moisture content and compaction level was expected for different sections. However, the workability of the mixes on-site was observed to be very consistent. The hot weather on the day was allowed for in all measurements.

The placed concrete layer was then compacted using a 3-tonne vibrating roller in accordance with the compaction requirements of the Specification for Highways Works [42] to form a 100-mm RCC layer as shown in Figures 99 and 100.

Figure 98 Placing concrete using the truck mixer chute

Figure 99 Placing and spreading the last batch of concrete

Figure 100 Spreading the concrete using a mechanical excavator

Figure 101 Concrete compaction using a 3-tonne vibrating roller

The completed layer of RRC is shown in Figure 102. The surface of the concrete was sprayed with a bituminous emulsion layer to prevent evaporation of water up to 28 days curing.

Figure 102 Completed 100-mm layer of RCC at the Lowdham Grange site

4.2.3 Concrete sampling

To evaluate the level of compaction of concrete in the site trial and compare it with laboratory experiments, 150-mm cubes samples were prepared from each batch of concrete delivered to the site. Concrete samples were compacted using a hammer drill and attached plate in three layers (Figure 103). These samples were kept under standard curing conditions in the laboratory; the results of compressive strength testing are presented in section 4.4.

Figure 103 Sampling of concrete using 150-mm cubes and hammer drill

4.3 King's Mill Hospital site

A 22-m length of the site access road (4 m wide) was allocated by Skanska within the stores area of the King's Mill Hospital construction site.

The trial included two major works undertaken to evaluate the feasibility and performance of the Coventry Binder for use in soil stabilisation and also as a binder itself. The construction layers of the 22 metres of temporary access road were designed to compare conventional cement stabilised soil and bituminous base course layers with Coventry Binder stabilised soil and semi-dry compacted paste (grout). Figure 104 shows the layout of the designed layers for each section of the trial access road.

Table 50 presents the proportions of materials used for soil stabilisation and the semi-dry paste. The volume of stabilised soil needed for the site trial was estimated at 72 m^3 (in a loose condition) including wastage. For the semi-dry paste, the volume of material needed was estimated to be 6 m^3 (in a loose condition) and including wastage. As shown in Figure 104, half the temporary access road was designed to be constructed using a conventional base course of the same thickness as the semi-dry compacted paste. Finally, the surface of the whole road was paved using 50 mm bituminous wearing surface.

Figure 104 Layout of the trial construction layers at the King's Mill Hospital site

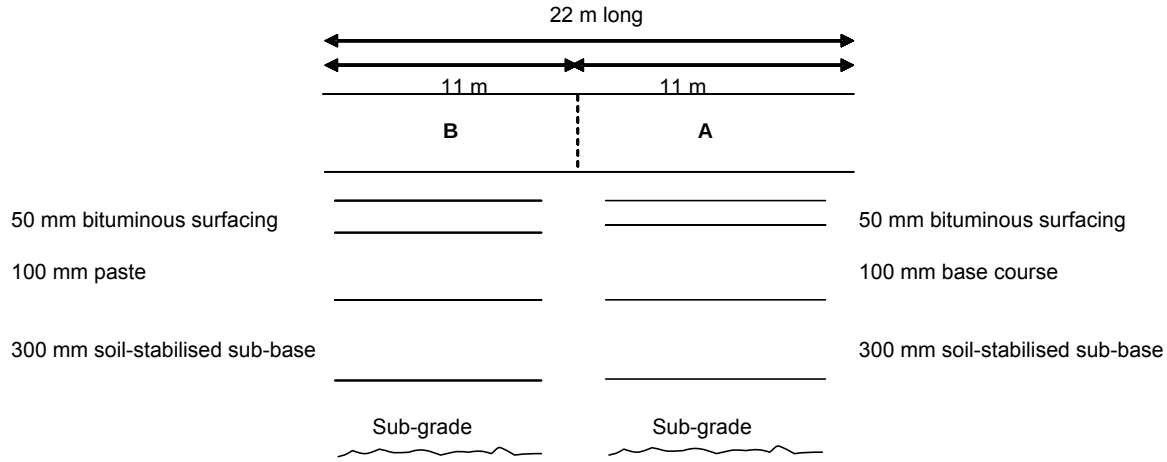

Table 50 Mix proportions of stabilised soil and semi-dry compacted paste (grout) mixes used

Mix code	Soil (%)	Binder (%)	Moisture content (%)
Stabilised soil (Soil50/Binder50)	50	50	14.2
Semi-dry paste (PG15/BPD5/BOS80-0.13)	–	100	13

4.3.1 Site preparation

The area identified in the stores area of the north field compound was stripped of existing hardcore to expose the sub-grade, which was sandy and similar to that in the rest of the north field. The area was trimmed to level, compacted and inspected by all parties (the contractor, WRAP and the technical group from Coventry University). Figures 105 and 106 show the preparation of the trial area using Skanska's heavy excavator.

Figure 105 Preparation of the trial area using an excavator

Figure 106 Trimming and levelling the trial area to expose the sub-grade

4.3.2 Soil stabilisation

A 300-mm layer of soil stabilised using Coventry Binder was placed on the prepared area. First, the soil was spread and levelled using a JCB machine (Figures 107 and 108). As the allocated area sloped, all efforts were made to spread the soil with the same thickness along the road (Figure 109).

Figure 107 Spreading and levelling the soil in the trial area

Figure 108 Levelling the spread soil using the JCB

Figure 109 Controlling the accuracy of the thickness of spread soil

The blended powder was then spread over the area using a volumetric method. To achieve the required amount of binder per cubic metre of the compacted soil, 150 mm of the blended powder was spread over the trial area manually and using the JCB. Figures 110 and 111 show the placing and levelling of the powder on top of the level soil.

Figure 110 Placing and spreading the powder on top of levelled soil

Figure 111 Levelled layer of powder on top of the soil

The mixture of soil and powder was blended using a rotavating blending machine as shown in Figures 112–114. The powerful and heavy blade of the machine provided a homogeneous blend of soil and binder along the road.

Figure 112 Blending the mixture of soil and binder using the rotavator (rotavator moving into position)

Figure 113 Rotavator in blending position

Figure 114 Inspecting the blended soil and powder before adding extra water

As the natural moisture of the soil used was not enough to provide the optimum compaction of stabilised soil, extra water was added to the mixture using a mobile sprinkler (Figure 115.). Then the mixture was blended again using the rotavating blender and levelled using the JCB. Visual control of the water content was challenging due to the hot weather and rapid evaporation. But despite this, the moisture content and compaction of the stabilised soil was satisfactory.

Figure 115 Watering the mixture of soil and the binder using the sprinkler

The blended soil and powder with sufficient moisture was levelled using the JCB and compacted using a 10-tonne vibrating roller. Figure 116 shows the levelled, stabilised soil and Figure 117 the compaction being carried out. The finished surface is shown in Figure 118. To protect the layer from rain and evaporation, a bituminous emulsion layer was sprayed on top of the finished surface.

Figure 116 Levelled blended soil and powder ready for compaction

Figure 117 Compacting the blended soil and the binder using the 10-tonne roller

Figure 118 Finished surface of the stabilised soil

Sampling
Sampling of the stabilised soil was performed in order to evaluate the moisture, level of compaction and compressive strength of the blended soil and binder. The results (see Tables 47 and 48) were compared with laboratory results for quality control purposes.

Two sets of 100 and 150 mm cubes were prepared using the standard method. For the 100-mm cubes, stabilised soil was compacted in three layers using a standard proctor rammer (25 drops). For 150-mm cubes, the blended soil and binder was compacted in five layers by 51 drops of the standard proctor rammer (Figure 119).

Figure 119 Sampling the stabilised soil

4.3.3 Semi-dry compacted paste
A layer of 100-mm semi-dry compacted paste using PG15/BPD5/BOS80 (Coventry Binder) was laid on top of the stabilised soil for half the length of the access road in order to compare it with the conventional base course laid on the other half of the trial road. Figure 120 shows the sprayed surface of the stabilised soil prior to constructing the paste layer.

Figure 120 Sprayed surface of stabilised soil before constructing the paste layer

As the water content of the semi-dry paste was limited to 13%, a volumetric mixer was used to mix the blended binder with water (Figure 121). The mixer contained a vessel to accommodate the binder and a 1600-litre tank of water. The binder was passed to a screw by means of a belt conveyer where the water was added, and was mixed in the extending arm.

The semi-dry paste (grout) was spread through the extended arm of the volumetric mixer and then levelled using the JCB machine. The only challenge was measuring the amount of water because the mixer was not equipped with any means of measuring the amount of water added to the mixture. Therefore, the required amount of water was adjusted based on visual inspection and past experience. Figures 121 and 122 show the mixing and spreading of the semi-dry paste.

Figure 121 Loading the mixer with blended powder

Figure 122 Spreading and levelling the semi-dry paste

After levelling the semi-dry paste, the layer was compacted using a 3-tonne vibrating roller. Figures 123 and 124 show the compacted and finished surfaces of the layer respectively.

Figure 123 Compacting the semi-dry paste layer using a 3-tonne roller

Figure 124 Finished surface of the compacted semi-dry paste

The surface of the compacted semi-dry paste was sprayed with bituminous emulsion for curing purposes.

The other half of the trial road was later laid using a 100-mm base course and then the whole length of the road was paved with 50 mm of bituminous surfacing.

Sampling

Sampling the semi-dry paste was performed in order to evaluate the level of compaction, moisture content and compressive strength. Two sets of 100 and 50 mm cubes were prepared using the standard method [44, 45]. For 100-mm cubes, semi-dry paste was compacted in three layers using a standard Proctor rammer (25 drops). For 50-mm cubes, paste was compacted using a small tamper in three layers (Figure 125).

Figure 125 Sampling the semi-dry paste using 100 and 50 mm cubes

4.4 Site trial evaluation

The site trial evaluation was conducted at 14, 28, 90 and 180 days after placing the semi-dry paste and RCC in order to monitor the performance of the different base and sub-base layers prepared using Coventry Binder.

The strength of the semi-dry paste and RCC layers was evaluated using in-situ core drilling. In addition, a visual inspection for any kind of damage such as large deflections or settlement was carried out and the state of the site was monitored by taking photographs of different sections.

The following sections detail the results of the site trial evaluation for the King's Mill Hospital and Lowdham Grange sites.

4.4.1 King's Mill Hospital site

The evaluation of the stabilised sub-grade and semi-dry sub-base at the King's Mill Hospital site was conducted in stages.

First, the moisture and compaction level of the stabilised soil using novel binder was measured using a nuclear density gauge. Table 51 shows the in-situ density and moisture content at four different points of the trial pavement.

The maximum dry density achieved in the laboratory was 2030 kg/m^3 and the optimum moisture content was about 13.9%. The stabilised soil layer was compacted at a slightly lower moisture content of 8.9% (Table 51). Although the amount of water added to the soil while mixed with the binder on-site was gauged by the look and feel of the mix, the results show that the variation in moisture content was within an acceptable range.

Table 51 In-situ density and moisture content of stabilised sub-grade

Location	Depth of test (mm)	Moisture (%)	Dry density (kg/m^3)	Compaction (%)
5 m from lowest	125	8.9	1790	88
10 m from lowest	125	8.9	1755	87
15 m from lowest	125	10.3	1789	88
20 m from lowest	125	8.9	1793	88

The compressive strength of the stabilised soil was evaluated by measuring the strength of cube samples taken on the day of the site trial; 100-mm cube specimens were taken from middle and end sections of the trial road. Table 52 summarises the results of compressive strength and density together with the in-situ test results.

Table 52 Compressive strength of stabilised sub-grade together with in-situ density and moisture

Mix code	Laboratory tests					In-situ tests	
	Strength at days (MPa)			Moisture (%)	Dry density (kg/m^3)	Moisture (%)	Dry density (kg/m^3)
	3	7	28				
Unstabilised Soil-B (Lab.)	0.08	0.21	0.13	13.40	1835.1	–	–
Soil-B 50/Binder 50 (Lab.)	0.94	1.43	5.98	13.90	2030.15	–	–
Soil 50/Binder 50 (Site-Mid)	0.78	1.11	5.80	8.02	2033.06	8.90	1755
Soil 50/Binder 50 (Site-End)	0.96	1.15	5.10	7.90	2027.55	8.90	1793

The compressive strengths of the cube specimens from the site trial were close to the results obtained with laboratory samples (Table 52). Despite the stabilised sub-grade being compacted with a lower moisture content than the optimum moisture content defined in laboratory tests, satisfactory compressive strength results were achieved from the site samples. Figure 126 shows the strength development of the site sample and laboratory-designed stabilised soil. The rate of the strength gain in laboratory and site mixes was almost similar. The slight difference in the strength of the site specimens taken from the middle and end sections of the trial road could be due to a variation in moisture content at different locations.

With respect to the density of the stabilised sub-grade, the in-situ density measured after 1 day was less than the maximum dry density achieved in the laboratory. This was due to the lower moisture content (8.9%) used to compact the soil. Control of the moisture content was not precise on the day of site trial because of the hot weather and, as mentioned above, the suitable moisture content was defined by eye based on previous experience.

Figure 126 Compressive strength development of stabilised sub-grade at the King's Mill Hospital site

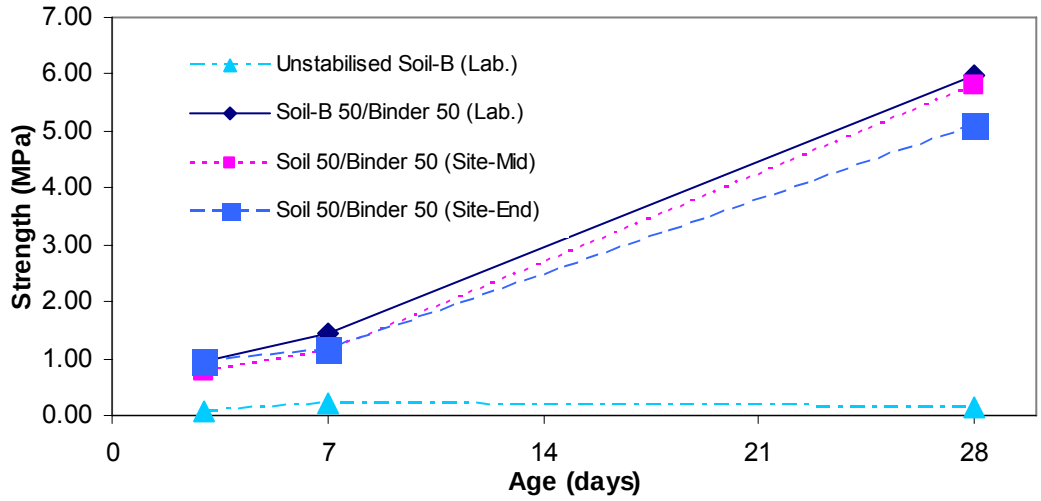

A general view of trial road is shown in Figure 127. The lower part of the trial road, which was constructed with a semi-dry paste sub-base layer, has been subject to frequent loads from heavy trucks and occasionally from heavy excavators. There was no sign of cracking or large deflections of the surface of the road, as shown in the close-up view of the road surface in Figure 128. In addition, a close inspection of the road found no sign of cracking at the interface of that part of the road made with bituminous sub-base and that made with semi-dry paste.

These observations demonstrated that the performance of both layers under heavy site traffic was similar after three months. Further inspections conducted at six months also found no evidence of cracks or large displacements in the part of the road constructed with a sub-base layer made with Coventry Binder. This confirmed the adequacy of the long-term performance of Coventry Binder when used in the construction of road foundations.

Figure 127 General visual evaluation of trial road at the King's Mill Hospital site

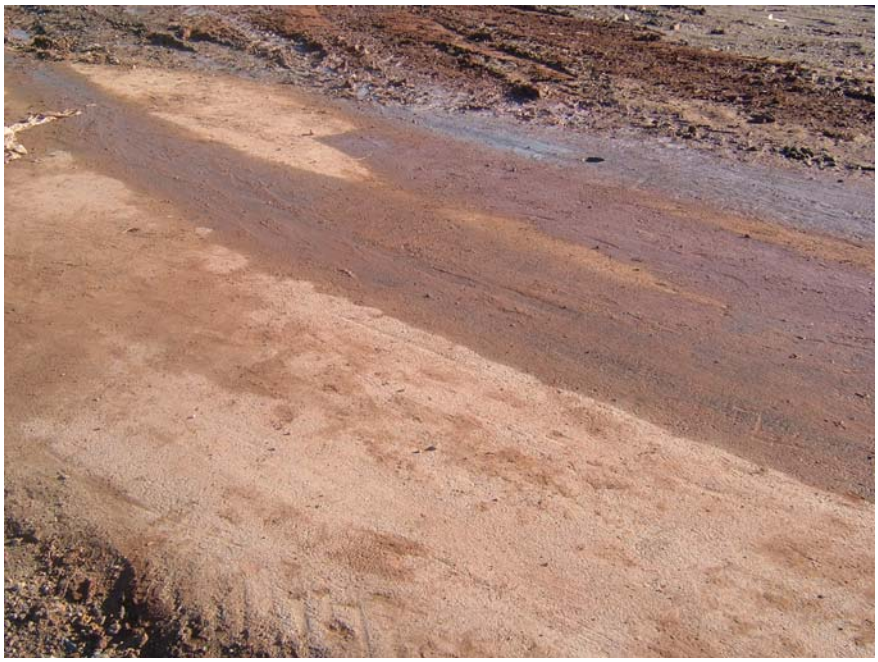

Figure 128 Close-up of the trial road at the King's Mill Hospital site

In order to evaluate the compressive strength of the semi-dry paste layer, 100-mm core samples were drilled from the lower, middle and upper sections of the trial road. Figure 129 shows the apparatus used to drill the cores.

Figure 129 Coring machine used to drill the cores at the King's Mill Hospital site

Figure 130 shows the drilled core from the lower section of trial road. The bituminous layer on top of the semi-dry paste was 50-mm wearing course laid 14 days after the semi-dry paste was placed. A 50-mm core sample was also taken in order to measure the permeability of the semi-dry paste.

Figure 130 Core sample taken from the lower part of trial road at the King's Mill Hospital site

A group of core samples drilled from different locations in the trial road is shown in Figure 131. The sample on the left-hand side was taken from upper part of the trial road, which was laid using a bituminous sub-base layer.

Figure 131 Core samples taken from different locations in the trial road at the King's Mill Hospital site

Table 53 gives the compressive strengths of the site samples and cores. The compressive strength of site samples measured on the day of the trial indicated that the strength of site trial semi-dry paste layer was 26% lower than that achieved in the laboratory mixes. This was due to the lower moisture content used in the site trial layer. However, the strength of the site cores taken at 14, 28, 90 and 180 days showed satisfactory performance for the placed semi-dry paste. The strength of the site cores was almost similar to that of the designed laboratory mixes at 28 days. Moreover, the long-term compressive strength of the site cores at 90 and 180 days was about 50% higher than the 28-day laboratory strength.

The strength development of the semi-dry site pastes in comparison with the laboratory mix is shown in Figure 132. The rate of strength gain in the site core samples declined at later ages in line with the laboratory results discussed in section 3.1.8. The strength continued to increase even at later ages. This was because the presence of the bituminous layer prevented the evaporation of moisture from the base layer and its drying out.

Figure 132 Compressive strength development of semi-dry site paste at the King's Mill Hospital site

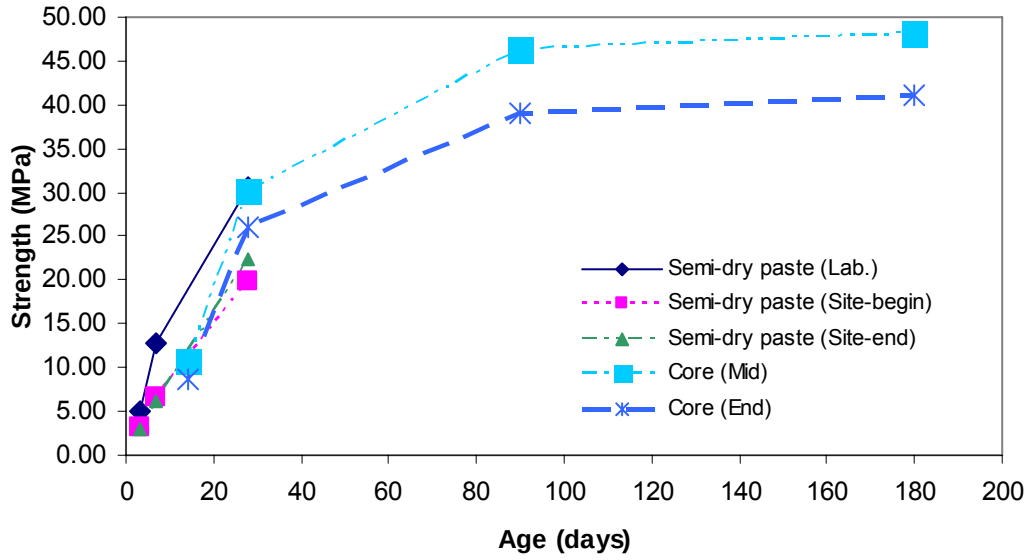

Table 53 Compressive strength of laboratory and site semi-dry paste layer

Mix code	Laboratory tests					In situ tests				
	Strength at days (MPa)			Moisture (%)	Density (kg/m^3)	Strength at days (MPa)				Density (kg/m^3)
	3	7	28			14	28	90	180	
Semi-dry paste (Lab.)	5.10	12.80	30.55	13.00	2540	–	–	–	–	–
Semi-dry paste (Site-Begin)	3.20	6.64	19.90	8.55	2487	–	–	–	–	–
Semi-dry paste (Site-End)	2.95	6.20	22.40	7.76	2492	–	–	–	–	–
Core (mid)	–	–	–	–	–	10.75	30.1	46.41	48.2	2381
Core (end)	–	–	–	–	–	8.64	26.1	38.98	41.1	2011

Table 54 Compressive strength of laboratory and site RCC layer

Mix code	Laboratory tests				In situ tests				
	Strength at days (MPa)			Density (kg/m^3)	Strength at days (MPa)				Density (kg/m^3)
	3	7	28		14	28	90	180	
RCC (Lab.)	0.96	2.02	10.80	2390	–	–	–	–	–
RCC (Site-Truck 1)	0.70	1.20	5.47	2350	–	–	–	–	–
RCC (Site-Truck 2)	0.68	1.29	4.70	2232	–	–	–	–	–
RCC (Site-Truck 3)	0.99	1.42	7.10	2293	–	–	–	–	–
Core (Location 1)	–	–	–	–	Soft	8.70	13.41	16.40	2257
Core (Location 2)	–	–	–	–	Soft	10.11	15.43	17.30	2226

4.4.2 Lowdham Grange site

Figure 133 shows a general view of the trial car park at the Lowdham Grange site. The car park was not covered with wearing surface as the strength of RCC layer was not sufficient when tested after 14 days. However, the area of the site trial was sprayed with a bitumen protective layer at 28 days and used for site access and storage. At 28 days and 90 days, the RCC layer was quite hard and even the leftover concrete at the sides of the area could not be removed easily. Although the surface of the RCC layer had irregularities due to the placing of the concrete in three segments, no signs of major deflection were observed in the trial car park.

Two core samples were drilled from the middle and end sections of the car park at 28, 90 and 180 days (Figure 134). The samples represented two different segments of the trial car park and corresponded to two different truck mixers delivering the concrete to the site. Cores taken from the site were cut at both ends using a lathe and tested for compressive strength. Figure 135 shows the prepared concrete core samples prior to compressive strength testing. Results for the site cores together with those from cube samples taken on the day of the site trial are presented in Table 54.

Figure 133 General view of trial car park site at Lowdham Grange

Figure 134 Core sample taken from middle and end part of the trial car park at the Lowdham Grange site

Figure 135 RCC core samples taken from different locations of the trial car park at the Lowdham Grange site

The results obtained with the concrete cubes samples from each truck indicated that the compressive strength was much lower than the laboratory strength of 10.8 MPa. However, the cube samples were compacted using a vibrating table attached to a hammer drill and therefore, due to the size of the aggregates and the nature of the roller-compacted concrete, compaction was different in each set of moulds. As a result, these samples were less compacted than the RCC layer which was laid and compacted using a 3-tonne vibrating roller.

Although the strength of the concrete at the early age of 14 days was not enough to be cored (Table 52), a satisfactory strength was obtained at 28 days. Moreover, the long-term compressive strength of the concrete at 90 and 180 days demonstrated the excellent performance of this type of binder when used in roller-compacted concrete. This is due the energy of the compaction applied by the heavy vibrating roller to achieve a fully compacted layer of concrete.

Figure 136 shows the strength development of the site cubes and core samples. The slower rate of strength gain is obvious in the concrete samples and is similar to the paste mixtures at the King's Mill Hospital site trial. The rate of strength gain fell as time progressed. The slower rate of strength development from 90 to 180 days is associated with the slower hydration rate of slag in the mixes. The mechanism of the hydration of slag in the Coventry Binder is discussed in section 3.6. The formation of hydrated products around slag grains results in reduced diffusion of ions from the slag particles into the solution to allow the further formation of the CSH gel responsible for the compressive strength of the concrete.

The results indicated that an even higher compressive strength than the desired strength for the car park base layer was achievable using Coventry Binder. Moreover, it may be possible to improve the strength further with the use of chemical agents such as sodium silicate and sodium carbonate.

Figure 136 Compressive strength development of site RCC samples at the Lowdham Grange site

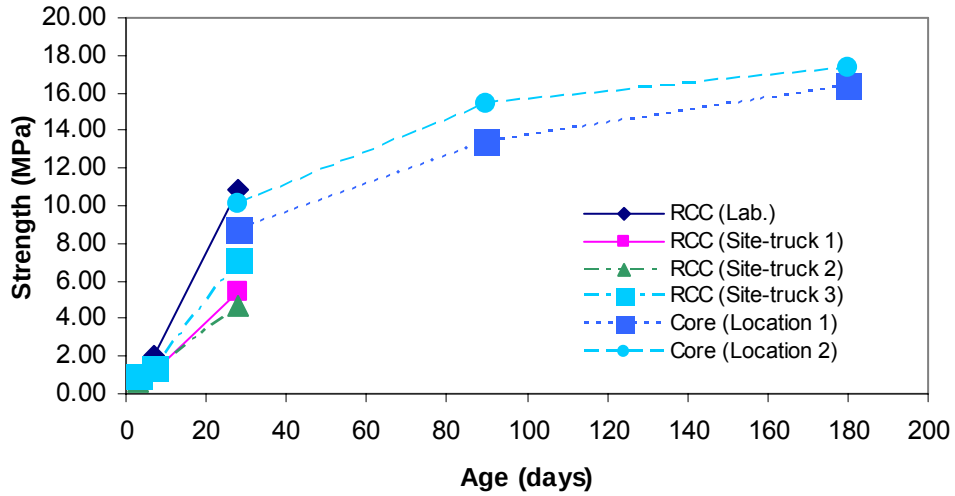

5.0 Conclusions

The following conclusions can be drawn from the results:

- Crushed plasterboard gypsum (PG) can be used as a source of sulphate together with slag (BOS) and cement kiln dust/bypass dust (CKD/BPD) to form a sulphate-activated pozzolan. The optimum proportions of gypsum depend on the chemical properties of the slag and cement kiln dust/bypass dust. Laboratory experiments showed that a ternary combination of PG-BPD-BOS containing 15% crushed plasterboard gypsum resulted in the highest compressive strength.
- Optimisation of the proportions in ternary and four-component combinations is not a linear task. Results showed that the optimum proportions obtained from the three combinations of PG-BPD-BOS, BPD-BOS-BPD and BOS-PG-BPD are different. Fine tuning is needed to give the proportions of materials for maximum compressive strength.
- The mix with 15% PG, 5% BPD and 80% BOS was identified as the optimum ternary combination of PG, BPD and BOS.
- Run-of-station ash (ROSA) showed satisfactory pozzolanic potential for use with slag and plasterboard gypsum. Using 30% ROSA and 50% BOS with 10% PG and 5% BPD resulted in a relatively higher compressive strength than with other proportions of these materials.
- Increasing the content of bypass dust in ternary combinations of PG, BOS and BPD resulted in a lower compressive strength. This was due to the location and orientation of ettringite formed around slag particles; XRD analysis confirmed the formation of ettringite within the matrix at later ages.
- Replacement of the BPD with commercial hydrated lime or Maerz kiln dust (MKD) resulted in up to 50% less compressive strength at 28 days. The efficiency of MKD was found to be less than hydrated lime.
- As with ordinary Portland cement (OPC) concrete, water content plays a major role in compressive strength development – the lower the water content, the higher the compressive strength.
- Use of superplasticiser is an effective way of increasing the flow of the paste and concrete mixes with a lower water content. The mixes incorporating water-reducing agent showed the highest compressive strength. Polymer base superplasticiser was found to be very efficient, but concrete made with the novel binder could suffer from a retarding effect.
- Slag requires less water than ROSA in order to achieve the same workability level. For a given L/S ratio, the higher the amount of slag, the higher the flow of the mix. Mixes incorporating ROSA need more water to achieve the same workability, though increasing the mixing time improves the workability of the mixes due to the ball bearing effect of the carbon particles in this ash.
- Semi-dry compacted paste made with 80% BOS, 15% PG and 5% BPD with 13% water (the so-called Coventry Binder) achieved the highest compressive strength at 28 days. Therefore, roller-compacted semi-dry paste was used for the base course in the road site trial. But at 90 days age, the paste mixture incorporating ROSA (BOS30/ROSA50/PG15/BPD5) achieved a higher compressive strength than the BOS80/PG15/BPD5 paste mixture.
- Roller-compacted concrete (RCC) made with optimum proportions of BOS, PG and BPD showed higher compressive strength than mixes with superplasticiser. An RCC mix with a water to binder ratio of 0.25 was used as the sub-base layer in the car park site trial.
- Evaluation of the site trials at 28, 90 and 180 days indicated satisfactory performance of the semi-dry paste and roller-compacted concrete. Despite the inability to measure the water content during the site trials mixes, the strength of sub-bases made with Coventry Binder was similar to the designed laboratory strength.
- The novel blended binder developed in this project can be used to stabilise soil containing clay and/or sand. Using 50% binder resulted in an acceptable compressive strength according to standard recommendations – the higher the binder content, the higher the compressive strength. XRD analysis indicated the formation of hydration products such ettringite after 28 days standard curing.
- Concrete mixes incorporating slag and gypsum developed strength at a slower rate than OPC mixes. Sufficient time must be allowed for the setting and curing of such mixes.

- The long-term compressive strength results of paste mixtures made with PG15/CKD5/BOS80 showed an increase of up to four-fold after 360 days standard curing compared with the strength at 28 days.
- Semi-dry paste made with PG15/BOS80/BPD5 showed a 25% increase in strength at 90 days compared with that at 28 days. Mixes incorporating ROSA showed a greater rate of strength gain (58%) than BOS mixes.
- No heavy metal or any other hazardous elements leached from the paste made with Coventry Binder. However, the amounts of sulphate and calcium that leached were more than from OPC paste.
- Incorporating up to 50% extra paper in the paste mixtures had no adverse effect on the emission of hydrogen sulphide from paste or concrete made with Coventry Binder. No trace of hydrogen sulphide was found with any of the developed mixtures.
- As expected, the permeability of roller-compacted concrete made with Coventry Binder was lower than OPC paste due to the presence of aggregates. Semi-dry paste in the site trial showed higher permeability compared with the same laboratory paste mixture.
- Investigations on the length change of paste and mortar samples indicated that semi-dry Coventry Binder paste showed the largest progressive expansion at 28 days age at 20° C. Incorporation of aggregates resulted in less expansion in mortar samples. Increasing the storage temperature to 40° C also resulted in reduced expansion for all paste and mortar mixes.

5.1 Future work

The results presented in this report are being analysed using artificial neural networks to provide information to allow the prediction of the compressive strengths of a series of cementitious mixtures based on existing data and without the need for extensive experimental work.

The mechanism of the hydration reactions of the binary and ternary blended binders will be investigated further by means of electron microscopy (SEM) to provide a more accurate model of the interactions of the chemical components and admixtures.

6.0 References

[1] Waste and Resources Action Programme (www.wrap.org.uk/construction/plasterboard/background.html)

[2] AEA Technology Plc. 2006. Review of plasterboard material flows and barriers to greater use of recycled plasterboard. Technical report for WRAP. Available from: www.wrap.org.uk/construction/plasterboard/report_review.html [Accessed 19 April 2007].

[3] American Concrete Institute (ACI). 1989. Ground granulated blast furnace slag as cementitious constituent in concrete. In: ACI Manual of Concrete Practice Part 1: Materials and General Properties of Concrete, ACI 226.1R, pp. 1-16.

[4] Hakkinen, T. 1993. The influence of slag content on the microstructure, permeability and mechanical properties of concrete. Part 1 Microstructural studies and basic mechanical properties. *Cement and Concrete Research Journal*, 23, 407-421.

[5] Neville, A.M. 1995. Properties of Concrete (4th and final edn.). Prentice Hall, London.

[6] British Standards Institution (BSI). 2004. BS 4248: 2004. Supersulfated cement. BSI, London.

[7] Hewlett, P.C. (ed.). 1998. Lea's Chemistry of Cement and Concrete (4th edn.). Butterworth-Heinemann, Oxford.

[8] Al-Jabri, K.S., Taha, R.A., Al-Hashmi, A. and Al-Harthy, A.S. 2006. Effect of copper slag and cement bypass dust addition on mechanical properties of concrete. *Construction and Building Materials,* 20, 322-331.

[9] Al-Harthy, A.S., Taha, R. and Al-Maamay, F. 2003. Effect of cement kiln dust (CKD) on mortar and concrete mixtures. *Construction and Building Materials*, 17, 353-360.

[10] Jones, M. and McCarthy, A. 2003. Moving fly ash utilisation in concrete forward: a UK perspective. Presentation to International Ash Utilisation Symposium, Centre for Applied Energy Research, University of Kentucky, held 20–22 October 2003.

[11] British Standards Institution (BSI). 2001. BS EN 459-1: 2001. Building lime. Definitions, specifications and conformity criteria. BSI, London.

[12] British Standards Institution (BSI). 1992. BS 882: 1992. Specification for aggregates from natural sources for concrete. BSI, London. [Superseded by BS EN 12620: 2002. Aggregates for concrete].

[13] British Standards Institution (BSI). 1990. BS 1377-4: 1990. Methods of test for soils for civil engineering purposes. Compaction-related tests. BSI, London.

[14] British Standards Institution (BSI). 1986. BS 1881-125: 1986. Testing concrete. Methods for mixing and sampling fresh concrete in the laboratory. BSI, London.

[15] British Standards Institution (BSI). 2000. BS EN 12350-5: 2000. Testing fresh concrete. Flow table test. BSI, London.

[16] British Standards Institution (BSI). 1998. BS 4555-1: 1998. Methods of testing mortars, screeds and plasters. Physical testing. BSI, London. [Superseded by BS 4555: 2005. Mortar. Methods of test for mortar. Chemical analysis and physical testing].

[17] ASTM International. 2003. C230/C230M-03 Standard specification for flow table for use in tests of hydraulic cement. ASTM International, West Conshohocken (PA).

[18] Transport Research Laboratory. 1993. A guide to the structural design of bitumen surfaced road in tropical and sub tropical countries. Road Note No. 31. Department of Transport, London.

[19] Nielsen, H.H. and Barker, E.F. 1988. Infrared absorption bands in hydrogen sulphide. *Physical Review*, 37, 727-732.

[20] Anon. 1994. Technical literature on Hoek cell and drainage platens produced by Robertson Geologging, Conwy, Gwynedd LL31 9PX [www.geologging.com].

[21] Claisse, P.A. and Unsworth, H.P. 1995. The engineering of a cementitious barrier. In: Engineering Geology of Waste Disposal, Geological Society Engineering Geology Special Publication No. 11, pp. 267-272. Geological Society, London.

[22] Bakharev, T. 2001. Resistance of alkali-activated slag concrete to carbonation. *Cement and Concrete Research*, 31, 1277–1283.

[23] Warren, C.J. and Reardon, E.J. 1994. The solubility of ettringite at 258C. *Cement and Concrete Research*, 24, 1515–1524.

[24] Odler, I. and Yan, P. 1994. Investigations on ettringite cements. *Advances in Cement Research*, 6, 165–171.

[25] Richardson, I. G. 2000. The nature of the hydration products in hardened cement pastes. *Cement and Concrete Composites*, 22(2), 97–113.

[26] Möser, B. 2003. Nano-Charakterisierung von Hydratphasen mittels Rasterelektronenmikroskopie. In: Proceedings of the 15th International Conference on Building Materials [Internationale Baustofftagung (Ibausil)], held Weimar 2003 (ed. H.B. Fisher), pp. 1-0589 to 1-0607. Finger-Institut für Baustoffkunde, Weimar.

[27] Brews, D.M. and Glasser, F.P. 2005. The magnesia–silica gel phase in slag cements: alkali (K, Cs) sorption potential of synthetic gels. *Cement and Concrete Research*, 35 (1), 77–83.

[28] Stark, J., Frohburg, U. and Mielke, I. 2001. Supersulfated cement with and without cement clinker. In: Proceedings of the International Symposium on Non-Traditional Cement and Concrete, held Brno (Czech Republic), 2001 (ed. V. Bílek and Z. Kerner), pp. 125-138.

[29] Ottemann, J. 1951. 'Die Bedeutung der Wasserstoffionenkonzentration für die hydraulische Erhaertung von Braunkohlenaschen und Gipsschlackenzement. *Silikattechnik*, 2(5), 143–149.

[30] Scrivener, K.L. and Taylor, H.F.W. 1993. Delayed ettringite formation: a microstructural and microanalytical study. *Advances in Cement Research*, 5(20), 139-146.

[31] Taylor, H.F.W. 1997. Cement Chemistry (2nd. edn.). Reedwood Books, Trowbridge.

[32] Chartschenko, I., Volke, K. and Stark, J. 1993. Untersuchungen über den Einfluß des pH-Wertes auf die Ettringitbildung. *Wissenschaftliche Zeitschrift der Hochschule für Architektur und Bauwesen Weimar*, 39(3), 171-176.

[33] Chartschenko, I. 1995. Theoretische Grundlagen zur Anwendung von Quellzementen in der Baupraxis. Habilitationsschrift [Professorial dissertation]. Weimar, Hochschule für Architektur und Bauwesen Weimar (HAB Weimar).

[34] Mehta, P.K. 1983. Mechanism of sulfate attack on Portland cement concrete – another look. *Cement and Concrete Research*, 13, 401-406.

[35] Puertas, F., Fernandez, A. and Blanco-Varela, M.T. 2004. Pore solution in alkali-activated slag cement pastes. Relation to the composition and structure of calcium silicate hydrate. *Cement and Concrete Research*, 34, 139-148.

[36] ASTM International. 2005. C151-05. Standard test method for autoclave expansion of hydraulic cement. ASTM International, West Conshohocken (PA).

[37] ASTM International. 2004. C490-04. Standard practice for use of apparatus for the determination of length change of hardened cement paste, mortar and concrete. ASTM International, West Conshohocken (PA)

[38] ASTM International. 2005. C1260-05a. Standard test method for potential alkali reactivity of aggregates (mortar-bar method). ASTM International, West Conshohocken (PA).

[39] ASTM International. 2003. C227- 03 Standard test method for potential alkali reactivity of cement-aggregate combinations (mortar-bar method). ASTM International, West Conshohocken (PA).

[40] British Standards Institution (BSI). 1999. BS 812-123: 1999. Testing aggregates. Method for determination of alkali-silica reactivity. Concrete prism method. BSI, London.

[41] British Standards Institution (BSI). 1968. BS 2028: 1968. Pre-cast concrete masonry units. Specification for pre-cast concrete masonry units. BSI, London.

[42] Highways Agency. 2006. Manual of Contract Documents for Highway Works: Volume 1 Specification for Highway Works. The Stationery Office, London.

[43] British Standards Institution (BSI). 2000. BS EN 12350-2: 2000. Testing fresh concrete. Slump test. BSI, London.

[44] British Standards Institution (BSI). 2000. BS EN 12390-1: 2000. Testing fresh concrete. Sampling. BSI, London.

[45] British Standards Institution (BSI). 2000. BS EN 12390-3: 2000. Testing fresh concrete. Vebe test. BSI, London.

Acronyms

ASR	alkali-silica reactivity
BOS	basic oxygen slag
BPD	bypass dust
CKD	cement kiln dust
CSH	calcium silicate hydrate
ESEM	environmental scanning electron microscopy
GGBS	ground granulated blast furnace slag
ICP	inductively coupled plasma
L/B	liquid to binder [ratio]
L/S	liquid to solid [ratio]
LOI	loss on ignition
MKD	Maerz kiln dust
OMC	optimum moisture content
OPC	ordinary Portland cement
PFA	pulverised fuel ash
PG	plasterboard gypsum
PPG	processed plasterboard gypsum
PSP	polymer superplasticiser
RA	recycled aggregate
RCC	roller-compacted concrete
RH	relative humidity
ROSA	run-of-station ash
SEM	scanning electron microscopy
SP	superplasticiser
SSC	supersulphated cement
SSD	saturated surface dry
TGA	thermogravimetric analysis
TRL	Transport Research Laboratory
XRD	X-ray diffraction
XRF	X-ray fluorescence

Appendix A Miscellaneous trial mixes

Table A1 gives the proportions of the various waste materials present in the preliminary cup mixes and primary trial mixes. Different properties of fresh and hardened mixes were measured and used in the main laboratory study.

Figures A1–A3 show the strength development of the primary trial mixes. Although the results of compressive strength were not all satisfactory, these data were used to design the main trial paste and concrete mixes.

Figure A1 Compressive strength trial mixes at testing age of 3 days

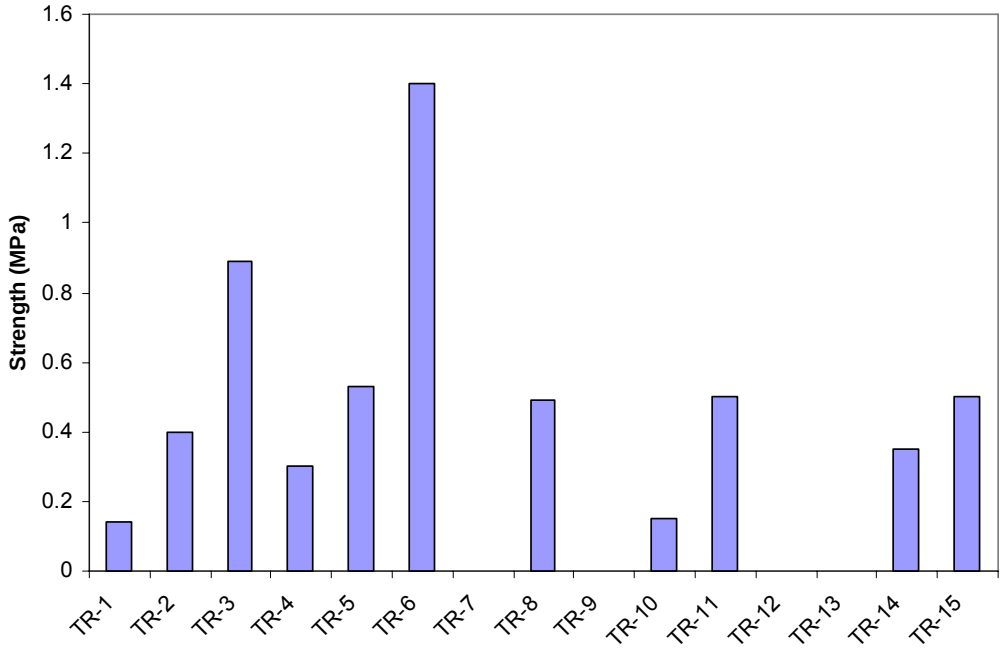

Table A1 Mix proportions of cup mixes and trial mixes

Mix code	PG (%)	CKD (%)	BPD (%)	W–BOS (%)	ROSA (%)	Incinerated ash (%)	Lime (%)	Pure $Ca(OH)_2$ (%)	NaOH (%)	Na_2CO_3 (%)	Na_2SO_4 (%)	Plasticiser (%)	L/S
Cup mix 1	34	–	–	60	–	–	–	–	–	6	–	–	0.3
Cup mix 2	34	6	–	60	–	–	–	–	–	–	–	–	0.3
Cup mix 3	38	–	–	60	–	–	–	–	2	–	–	–	0.3
Cup mix 4	34	–	–	60	–	–	–	–	–	6	–	–	0.2
Cup mix 5	15	–	–	80	–	–	–	–	5	–	–	–	0.3
Cup mix 6	20	–	–	80	–	–	0.4	–	–	–	0.4	–	0.3
Cup mix 7	20	–	–	80	–	–	0.3 slurry	–	–	–	–	–	
Cup mix 8	20	–	–	80	–	–	0.5	–	–	–	0.4	–	0.3
Cup mix 9	20	–	–	80	–	–	0.5 slurry	–	–	–	0.4	–	0.3
Cup mix 10	20	–	–	–	80	–	0.5	–	–	–	0.5	–	0.3
Cup mix 11	20	–	–	80	–	–	0.5	–	–	–	0.4	–	0.3
Cup mix 12	20	–	–	–	–	80	–	–	–	–		–	0.3
Cup mix 13	20	–	–	80	–	–	–	0.5	–	–	0.4	–	0.3
Cup mix 14	20	–	–	–	80	–	0.5	–	–	–	0.4	–	0.3
Cup mix 15	15	–	–	85	–	–	0.4	–	–	–	0.4	–	0.3
Cup mix 16	15	5	–	80	–	–	–	–	–	–	0.4	–	0.3
Cup mix 17	15	–	–	75	–	–	10	–	–	–	0.2	–	0.25
TR-1	15	3	–	80	–	–	–	–	–	2	–	–	0.3
TR-2	15	–	–	–	85	–	1	–	–	–	0.7	–	0.35
TR-3	15	–	–	85	–	–	0.8	–	–	–	0.5	–	0.3
TR-4	15	–	–	85	–	–	1.2	–	–	–	0.6	–	0.3
TR-5	15	–	–	85	–	–	0.7	–	–	–	0.6	–	0.3
TR-6	15	5	–	80	–	–		–	–	–	–	1.5	0.2
TR-7	15	0.81N solution*	–	85	–	–		–	–	–	0.5	–	0.27
TR-8	15	–	–	85	–	–	2	–	–	–	0.45	–	0.26
TR-9	15	–	–	85	–	–	5	–	–	–	0.4	–	0.25
TR-10	21.13 IG†	5	–	73.86 IG†	–	–		–	–	–	0.6	1.5	0.2
TR-11	15	–	–	75	–	–	10	–	–	–	–	–	0.25
TR-12	15	5	–	–	80	–	–	–	–	–	–	2	0.27
TR-13	15	–	5	80		–	–	–	–	–	–	2	0.2
TR-14	15	5	–	50	30	–	–	–	–	–	–	2	0.2
TR-15	15	–	5	50	30	–	–	–	–	–	–	2	0.2

* CKD was dissolved in water to form a 0.81N alkaline solution. † PG and BOS were interground (IG) and then added to the rest of the materials.

Figure A2 Compressive strength trial mixes at testing age of 7 days

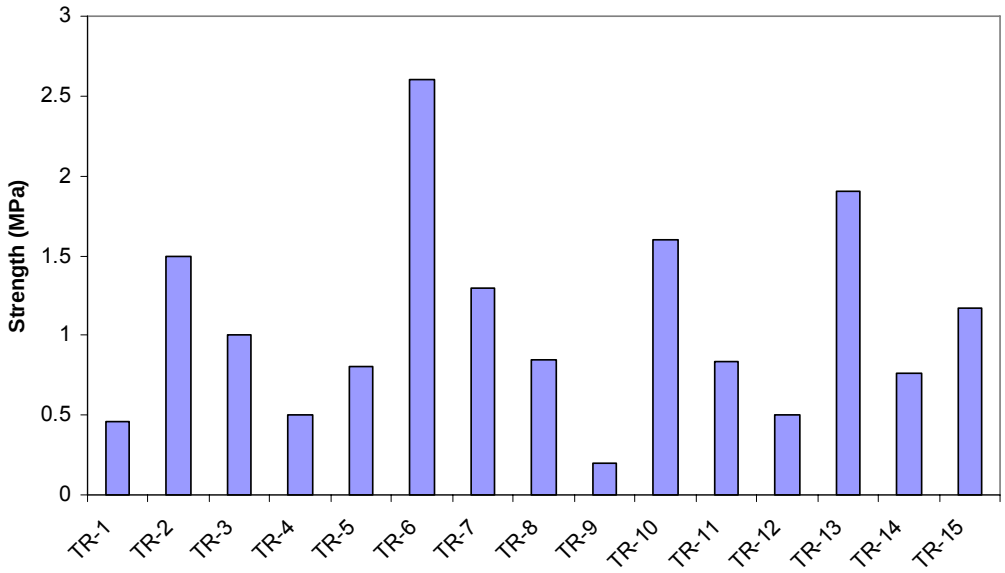

Figure A3 Compressive strength trial mixes at testing age of 28 days

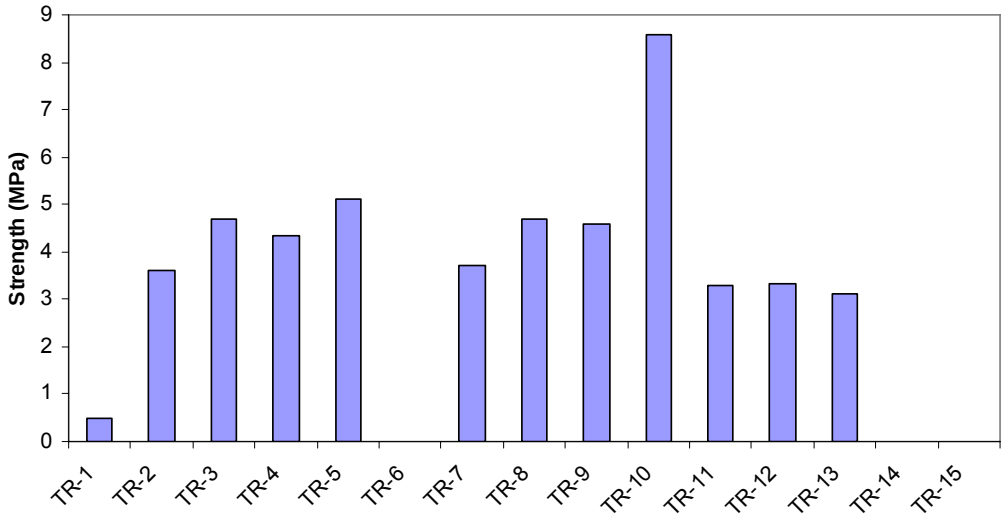

Appendix B Laboratory equipment

The 2-litre mechanical mixer with different rotating speeds used to make the paste mixes in shown in the right-hand side of Figure B1. The high shear mixer on the left-hand side of Figure B1 was used to make cup mixes. Figure B2 shows the horizontal 10-litre pan mixer used to make concrete mixes.

Figure B1 Small mixers used to make 'cup' mixes and main paste mixes

Figure B2 Pan mixer used to make concrete mixes

The small modified flow table used in this study is shown in Figure B3. Paste was poured into the cylinder (78 mm diameter) in two layers and compacted by tamping ten times using a small rod. After placing the cylinder, the table was jolted five times using the handle and the flow was measured in mm.

Figure B3 Modified flow table

Figure B4 shows the slump test equipment. More details of the test can be found in BS EN 12350-2 [43].

Figure B4 Slump test truncate cone and base

Figure B5 shows the laboratory ball mill used to grind the slag. This consists of a cylindrical shell rotating about a horizontal axis, partially filled with a grinding medium of metallic balls. The material to be ground is added so that it slightly more than fills the voids between the media. The shell is rotated at a speed that causes the media to cascade, thus reducing particle sizes by impact. The balls used in the grinder were of different sizes (Figure B6).

Figure B5 The laboratory ball mill

Figure B6 Metallic balls of different sizes used in the ball mill to grind the slag

Figure B7 shows the 50-mm and 100-mm cube moulds. The former were used to cast paste mixes and the latter to cast concrete samples. Moulds were filled with paste or concrete in three layers and compacted using a mechanical vibrating table to remove the air and to reach the maximum compaction.

Figure B7 100 mm and 50 mm cube moulds, places and mechanical vibrator table

Paste specimens stored in curing containers are shown in Figure B8. The containers were filled partially with water and samples were covered with a plastic lid. The humidity in the containers was measured to about 98% RH. All containers were kept at 20±2° C.

Figure B8 Paste samples stored in a container at 20±2° C and 98% RH

The concrete specimens were stored in a tank partially filled with water (Figure B9) and covered with lid to provide a curing condition of 98% RH at 20±2° C.

Figure B9 Concrete samples stored in a tank at 20±2° C and 98% RH

Paste samples were tested for compressive strength using the Lloyd computerised testing machine shown in Figure B10. The loading rate was kept constant at 10 mm/minute and the results were reported as MPa or N/mm^2.

Figure B10 Computerised compressive strength testing machine for paste specimens

Figures B11 and B12 show the paste specimens before and after crushing with the Lloyd compressive strength testing machine. The slight green colour of the crushed samples faded away gradually after being left in air. The colour is attributed to the presence of calcium sulphide in the slag and its slow disappearance is due to oxidation of sulphides in air.

Figure B11 A paste sample before crushing

Figure B12 A paste sample after crushing

Figures B13 and B14 show the crushing machine for testing concrete cubes. As the early strength of concrete samples was not high enough to use the normal concrete testing machine, a more accurate machine with a lower capacity of 100 KN was used to test the concrete samples. The results were obtained as MPa after dividing the load in N by the surface area in mm^2.

Figure B15 shows the machine built from a lathe to cut the concrete samples.

Figure B13 The 100 KN compressive strength testing machine for concrete specimens at early ages

Figure B14 A concrete sample after crushing

Figure B15 Special cutting machine for concrete samples (built from lathe)

Written by: Dr Essie Ganjian, Dr Peter Claisse and Homayoon Sadeghi Pouya, The University of Coventry

Published by
Waste & Resources Action Programme

The Old Academy
21 Horse Fair
Banbury, Oxon
OX16 0AH

Tel: 01295 819 900
Fax: 01295 819 911
E-mail: info@wrap.org.uk

Helpline freephone
0808 100 2040

www.wrap.org.uk